https://ntrs.nasa.gov/search.jsp?R=19740024672 2020-03-23T05:23:36+00:00Z

X-923-74-200
PREPRINT

AN ANALYSIS OF FRACTURE TRACE PATTERNS IN AREAS OF FLAT-LYING SEDIMENTARY ROCKS FOR THE DETECTION OF BURIED GEOLOGIC STRUCTURE

(NASA-TM-X-70742) AN ANALYSIS OF FRACTURE TRACE PATTERNS IN AREAS OF FLAT-LYING SEDIMENTARY ROCKS FOR THE DETECTION OF BURIED GEOLOGIC STRUCTURE (NASA) CSCL 08G G3/13 N74-32785 Unclas 48012

MELVIN H. PODWYSOCKI

JUNE 1974

GSFC — GODDARD SPACE FLIGHT CENTER
GREENBELT, MARYLAND

Reproduced by
NATIONAL TECHNICAL INFORMATION SERVICE
US Department of Commerce
Springfield, VA. 22151

PRICES SUBJECT TO CHANGE

X-923-74-200

AN ANALYSIS OF FRACTURE TRACE PATTERNS IN AREAS OF FLAT-LYING SEDIMENTARY ROCKS FOR THE DETECTION OF BURIED GEOLOGIC STRUCTURE

by

Melvin H. Podwysocki

June 1974

GODDARD SPACE FLIGHT CENTER
Greenbelt, Maryland

/

AN ANALYSIS OF FRACTURE TRACE PATTERNS
IN AREAS OF FLAT-LYING SEDIMENTARY ROCKS
FOR THE DETECTION OF BURIED GEOLOGIC STRUCTURE

by

Melvin H. Podwysocki

ABSTRACT

Two study areas in a cratonic platform underlain by flat-lying sedimentary rocks were analyzed to determine if a quantitative relationship exists between fracture trace patterns and their frequency distributions and subsurface structural closures which might contain petroleum. Fracture trace lengths and frequency (number of fracture traces per unit area) were analyzed by trend surface analysis and length frequency distributions also were compared to a standard Gaussian distribution. Composite rose diagrams of fracture traces were analyzed using a multivariate analysis method which grouped or "clustered" the rose diagrams and their respective areas on the basis of the behavior of the rays of the rose diagram.

Analysis indicates that the lengths of fracture traces are log-normally distributed according to the mapping technique used in this paper. Deviations from log-normality may be associated with both reef (passive) structures whose "closure" is caused by differential compaction of sediments over the reefs and with basement uplift (active) anticlinal structures. The primary control of fracture trace frequency and log-mean lengths is associated with variations in surficial lithology. This variation may be extracted using trend surfaces and the residuals may be analyzed. Fracture trace frequency appeared higher on the flanks of active structures and lower around passive reef structures. Fracture trace log-mean lengths were shorter over several types of structures, perhaps due to increased fracturing and subsequent erosion.

Analysis of rose diagrams using a multivariate technique indicated lithology as the primary control for the lower grouping levels. Groupings at higher levels indicated that areas overlying active structures may be isolated from their neighbors by this technique while passive structures showed no differences which could be isolated.

Preceding page blank

CONTENTS

PRECEDING PAGE BLANK NOT FILMED

ILLUSTRATIONS

ILLUSTRATIONS (Continued)

TABLES

AN ANALYSIS OF FRACTURE TRACE PATTERNS IN AREAS OF FLAT-LYING SEDIMENTARY ROCKS FOR THE DETECTION OF BURIED GEOLOGIC STRUCTURE

INTRODUCTION

Although linear features on the earth's surface had long been mapped solely on topographic and geologic criteria (Hobbs, 1911; Brock, 1957), more of these subtle features became apparent as aerial photographic coverage became available (Rich, 1928). Since then, airphoto linears have been applied to a wide range of topics such as groundwater studies (Lattman and Parizek, 1964; Siddiqui and Parizek, 1971), mineralization (Keim, 1962; Kutina, 1969) and engineering studies (Parizek and Voight, 1970; Parizek, 1971; Alpay, 1973; Benedict and Thompson, 1973). Linears observable on various scales of aerial photographs and topographic maps have been utilized extensively in regional tectonic studies (Plafker, 1964; Gol'braikh et al., 1968a; Gold et al., 1974). Although several investigators claim that analysis of airphoto linears will allow exploration for geologic structures which may bear petroleum (Permyakov, 1949, 1954; Blanchet, 1957; Mollard, 1957), few exploration techniques have been divulged due to their proprietary nature. This paper will discuss some parameters which can be extracted from an airphoto linear study for the purposes of exploration for several types of oil and gas traps.

NOMENCLATURE

The terms "airphoto linears" or "linears" were used above in order to circumvent the variety of names and non-systematic nomenclature for these topographic and photographic expressions. Barton (1933) used the term "topographic lines" and Gross (1951) used "topographic linears." Although their maps showed they did limit the size of the observed features, no comment was made concerning the distribution of their individual lengths. Only recently has attention been paid to the scale of observations and size of the features (Nemec, 1970; Gold et al., 1974) and until the advent of satellite imagery, there was no convenient format for direct observations of the large features.

Blanchet (1957) categorized his observations on linears observed on aerial photographs as "micro- and macrofractures," dividing the two categories at 2.5 miles (4 km). He claimed, but offered no proof, that microfractures (0.5 - 2.5 miles (0.8 - 4 km)) in length are intrinsic to the sediments themselves whereas macrofractures (greater than 2.5 miles (4 km)) are related to deep seated basement features. Because similar orientations prevailed in different parts of the world, he claimed that the fractures were related to a worldwide tectonic pattern.

Mollard (1957) used the term "lineament" to classify aerial photographic linears. His classification allowed the use of both continuous and discontinuous features ranging from 0. 2 - 5 miles (0. 3 - 8 km) in length. He too considered them related to global tectonics.

Gol'braikh et al. (1968 a,b) use the term "megajoint," which they adopted because of its relationship in hierarchy to other scales of jointing (i. e. micro- and macrojointing) and to the analytical techniques which could be applied regardless of scale. The term megajoint is based on the scale of maps or aerial photographs used and the minimum length (1 cm) which they believe can be precisely measured to determine the bearing of a megajoint. Their published works indicate a range of 1 to 6 km with a peak around 3 km (Mirkin, 1973, pers. comm.). Unfortunately, this scheme is dependent upon the scale of maps or photographs used. Other Russian terms used to describe the same phenomena are "lineamental jointing," "rectilinear elements of topography and stream networks" (Gol'braikh et al., 1968a) and "lineaments" (Shul'ts, 1969).

Lattman (1958) subdivides airphoto linears into "lineaments" and fracture traces," based on their length. He defines fracture traces as naturally occurring linear features observed on aerial photographs as alignments of stream segments, topographic features and soil and vegetational tonals which are expressed continuously for less than one mile in length. He relates them either to small faults or zones of joint concentration which are usually vertical or nearly vertical in cross-section (Lattman and Matzke, 1961). Excluded from the definition are bedding planes, compositional layering, and foliations. Lineaments are defined as consisting of the same morphological landscape elements as fracture traces, except that they are expressed discontinuously in the landscape and are greater than one mile (1. 6 km) and up to several tens or hundreds of miles (km) in length. They may consist of zones of increased fracture trace concentrations, transgressing structural, temporal and physiographic provinces and because of their great lengths, they are thought to be recurrent effects associated with basement faults or zones of tectonic adjustment between major crustal blocks (Wise, 1968; Gold et al., 1973, 1974). A plot of aerial photographic linears combining both of Lattman's categories indicates a bimodal distribution, with a minimum occurring at about the one mile length (Lattman, 1969, pers. comm.). Mirkin (1973, pers. comm.) indicates a similar bimodal distribution with his break occurring at the 3-4 km interval.

The present study will use the terminology of Lattman (1958) and will examine whether his definitions agree with observations made during this study.

MEASUREMENT PARAMETERS

Griffiths (1967) characterizes the measurable properties of an object by the following mathematical equation:

$$P = f\ (\text{material, size, shape, orientation, packing}) \quad (1)$$

Size (length) and orientation (bearing) are the most readily measured properties of fracture traces. Shape can be variously defined. Griffiths (1967) characterizes the shape of quartz grains or pebbles as the ratio of their long, intermediate and short axes. In this sense, the ratio of fracture trace width to its length might be a measurable parameter. However, measurement of fracture trace widths is a highly subjective study because of possible erosional and seasonal vegetal enhancement, and until more is known of their character with depth, no consistent classification can be attempted. In addition, since fracture traces are defined as lines, their width can be defined as infinitely small and unmeasurable. A radius of curvature can also be defined as a shape parameter, however, the scarcity of these features would preclude their use as a commonly measured and quantified parameter (Gol'braikh et al., 1968a). The possible significance of these curved and arcuate features has often been overlooked (Podwysocki and Gold, 1974); they may represent the surface expression of periclinal structures, listric faults and intrusive bodies.

The two remaining factors which can be studied are materials and packing. In this study, materials will refer to surficial geologic materials (formations) present in the mapping area. Packing (density or number of fracture traces per unit area) will be one of the parameters calculated as a result of this investigation.

STUDY AREAS

Two study areas were chosen representing different types of "structural traps" for the accumulation of petroleum. Both are located in the relatively stable cratonic platform areas of the central USA. A study area in south-central Kansas was chosen because it was regarded as typical of vertical uplift controlled by basement faulting. The other area was located in west Texas and is underlain by a series of reef structures with overlying sediments draping over them (differential compaction). No basement tectonic control is evident in the latter area.

The Kansas study area, covering approximately 150 square miles (270 sq. km), occupies the southern portion of Pratt and the northern part of Barber Counties (Figure 1). It overlies a portion of the southward plunging nose of the Pratt Anticline, a southerly extension of the Central Kansas Uplift (Merriam, 1963).

KANSAS STUDY AREA

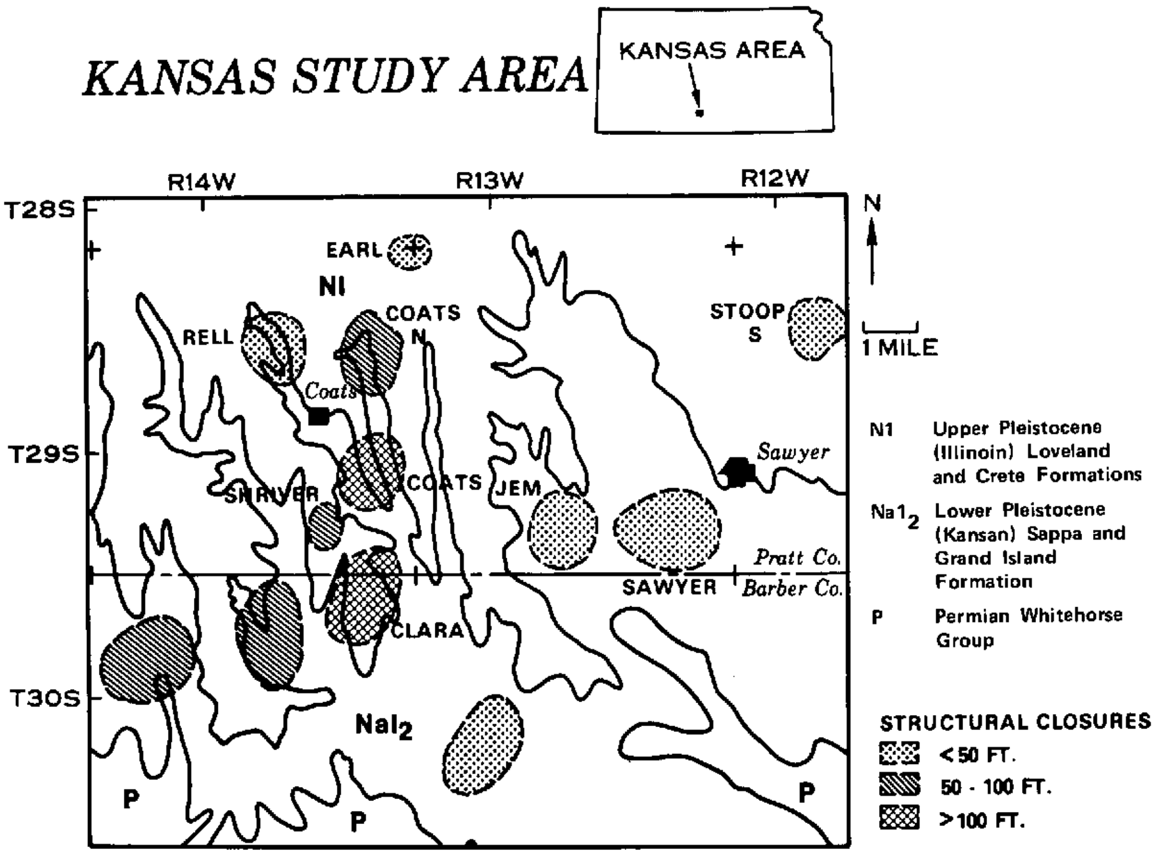

Figure 1. Schematic Geologic Map Showing Anticlinal Structures and If Productive, the Name of the Associated Oil Fields. The Outlines of the Fields Are Based on the Lowest Structure Contour Which Indicates Closure, and Structural Closure is the Difference Between the Structural Crest and the Lowest Contour of Structural Closure.

Although deformation occurred as early as Cambrian time (Williams, 1968), the major pulse is Mid-Pennsylvanian (Merriam, 1963), and produced an unconformity between pre-Mississippian and late Pennsylvanian rocks. Structural and structural-stratigraphic traps suitable for the entrapment of petroleum were created by "crenulations" of 2-3 km diameter on the Pratt Anticline. A northeast trending fault underlines the Coats Oil Field, cutting the Precambrian basement (Cole, 1962). No documentation exists for this fault in higher stratigraphic horizons (Williams, 1968). Figure 1 contains a schematic representation of the oil fields in the area and the amount of structural closure as determined by structure contours on top of the Late Pennsylvanian Lansing Group (Williams, 1968). According to cross-sections by Curtis (1956), minor reactivation of some of the structures may have occurred as late as Permian time. Average depth to the top of the producing horizons is approximately 3500 feet (1065 m) below the surface and depth to basement averages about 5200 feet (1585 m).

Figure 1 also contains a surface geologic map. Glacial outwash gravels, sands, silts and some clays of the Pleistocene Kansan and Illinoian Stages predominate. The Illinoian materials are found on the upland surfaces in the northern portions of the study areas whereas Kansan materials are usually found in the southern part and the major stream valleys of the central portion (Layton and Berry, 1973). Thickness of these deposits reaches a maximum of 200 feet (61 m) in the northern part of the study area and gradually tapers to a zero edge where the Permian rocks of the Whitehorse Group crop out in the southern extremity of the study area. The latter consist of reddish-brown siltstones, shales and sandstones with lesser amounts of gypsum, salt, anhydrite and limestone (Layton and Berry, 1973).

The Texas study area, covering approximately 180 square miles (324 sq. km), is situated in the northwestern portion of Nolan and southwestern part of Fisher Counties (Figure 2). It lies on the eastern shelf of the Midland Basin, the site of the Pennsylvanian and pre-Pennsylvanian Concho Arch and Platform (Hope, 1956). Two major unconformities exist with a hiatus from Late Ordovician through the Mississippian and another from Triassic through the Cretaceous ages (Hope, 1956; Shamburger, 1967). During Pennsylvanian time the area was the site of extensive reef-building, caused by repetitive advances and retreats of the seas across this shallow platform area (Van Siclen, 1958). Subsequent deposition commonly covered the reefs with fine-grained clastic sediments, eventually draping over them, due to differential compaction, to create "structural highs" (Conselman, 1959). In addition, stratigraphic traps associated with the updip pinchout of fore-reef detritus are common. No documentation exists for faulting in the study area (Hope, 1956). Depth to "Canyon Reef" production horizons averages about 6000 feet (1830 m).

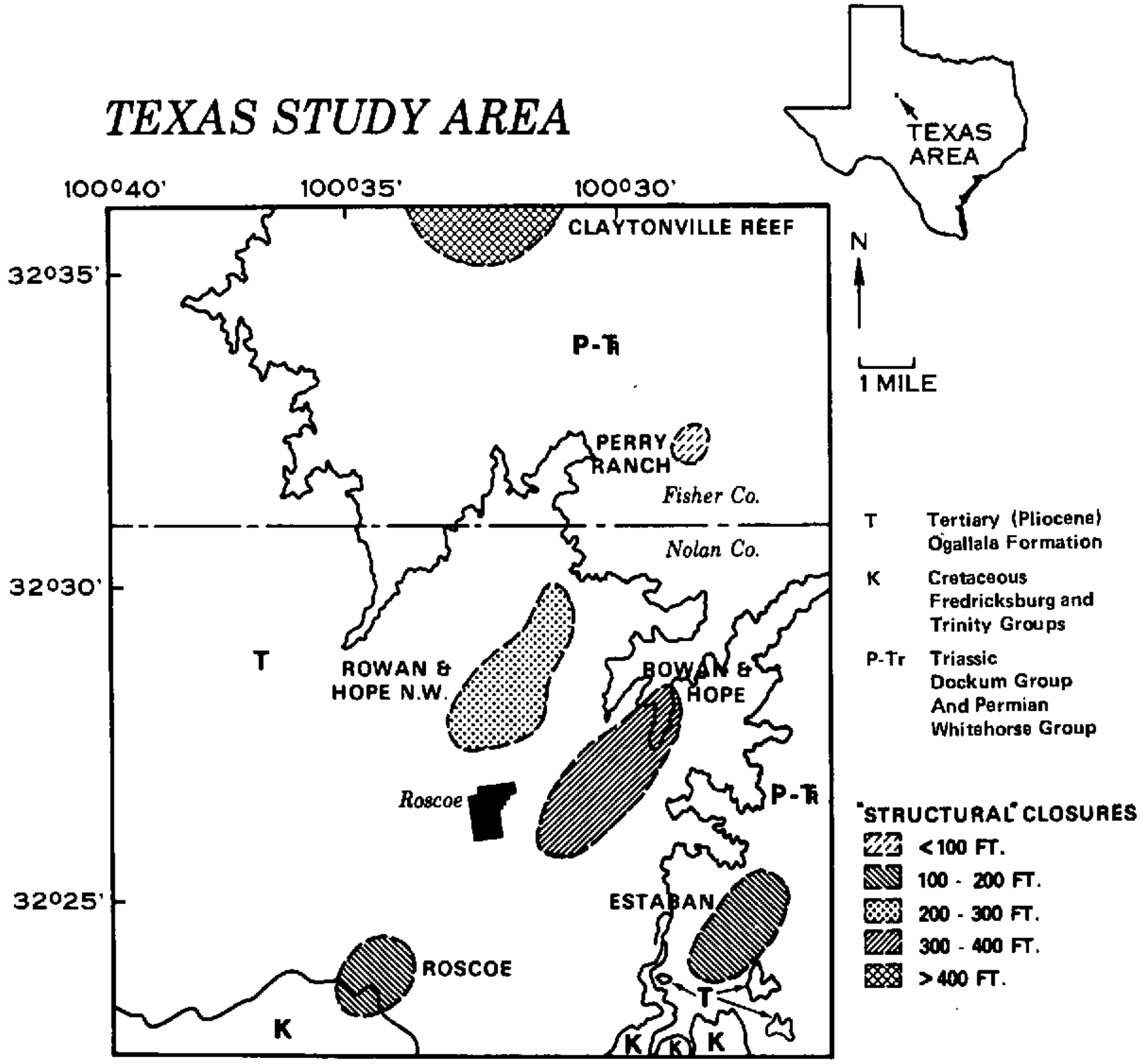

Figure 2. Schematic Geologic Map Showing Known Reef "Structures" and the Name of the Associated Productive Oil Fields. The Outlines of the Fields Are Based on the Lowest Structural Contour Which Indicates Closure, and Structural Closure is the Difference Between the Structural Crest and the Lowest Contour of Structural Closure.

Figure 2 contains a schematic representation of reef production with a minimum "structural closure" indicated for each reef and excludes stratigraphic traps such as the "Canyon Sands."

The surface geology is also portrayed in Figure 2. The Permian Whitehorse Group consists of sandstone, siltstone and shale redbeds with some interspersed gypsum beds. It crops out in the northern and extreme eastern portion of the study area. The Triassic Dockum Group crops out sporadically in the northern and eastern parts of the study area because of its cover by the Cretaceous and Tertiary units and its erosion during a later hiatus (Conselman, 1959; Shamburger, 1967). This unit consists mainly of red and tan conglomerates, sandstones and shales. Because of its small extent and similarity in lithology to the Permian, the two units have been grouped together. Dips on the Permo-Triassic and older subsurface units is about 0.5 - 1 degree to the west. The Cretaceous Trinity Group occupies the extreme southern part of the study area and consists of medium to coarse-grained quartz sands up to 80 feet thick which vary in color (Shamburger, 1967). Directly above is the Fredricksburg Group, consisting of thin to thick bedded arenaceous and fossiliferous limestones. Maximum thickness approaches 200 feet (61 m) in the Edwards Plateau directly to the south of the area, but it is considerably thinner locally. Karst features such as broad, shallow, poorly defined sinkholes are also found. Although these limestones underlie most of the central and western portion of the area, they are masked by a relatively thin cover of Tertiary Ogallala deposits. The Cretaceous units have been consolidated into one map unit because of the small lateral extent of the Trinity Group. Regional dips on these units usually do not exceed 1 degree to the southeast. The Pliocene Ogallala Formation consists of caliche, sands, gravels and some light colored clays; it forms a thin mantle over the central and western parts of the field area and, where exposed in cross-section in limestone quarries, it does not exceed 8 feet in thickness.

MAPPING METHOD

U.S. Department of Agriculture aerial photographs at a scale of 1:20,000 taken in the early 1960's were used as a basis for mapping the fracture traces. A pocket stereoscope was used in areas of moderate relief (up to 150 feet (46 m)), and for low relief areas (5 - 20 feet (1.5 - 6 m)), individual photographs were viewed at low oblique angles while the photos were rotated to view all possible "look directions." Mapping was done in flightlines, spending about 1/2 hour per stereo pair. Trainer (1967) showed that 84-89% of the fracture traces could be found in the first 20 minutes of observation.

As a check to determine if this operator was consistent in the selection of fracture traces, parts of the sidelap between adjacent flightlines were mapped and compared. A minimum of 83% of fracture traces were mapped consistently between several pairs of flightlines.

As a test of variations in the recognition of fracture traces, several experienced operators were compared to determine if the same general trends were mapped amongst the operators. Four sets of airphoto stereo pairs representing different types of topography in the study were mapped by two additional operators. Freidman Two-Way Analysis of Variance (Siegal, 1956) indicated that each operator mapped a different number of fracture traces on the four examples, based on a 0.05 level of rejection. However, the relative ranking by the operators of fracture trace direction indicated that in three out of four cases, there was no reason to reject the hypothesis that the operators were choosing the same directions. Thus, even though absolute numbers of fracture traces varied between operators, the same patterns of orientation and the same relative magnitude remained when the data were plotted in rose diagram plots. Gol'braikh et al. (1968a) achieves the same end by converting the absolute number or length of megajoints to percent rose diagrams in order to eliminate variation due to different operators and to more clearly discern the signal pattern.

Fracture traces were mapped directly onto aerial photographs by marking their endpoints with a soft colored pencil. In order to minimize planimetric errors, the fractures were mapped only within a three inch radius of the photograph centerpoint. These data were then transferred using a Saltzman projector to standard U.S. Geological Survey 1:24,000 scale topographic maps which were used as a base map. Figures 3 and 4 represent the fracture maps of the two areas. The grid on the left and top margins will be discussed later.

Cultural features such as pipelines and fencerows were usually readily distinguishable on aerial photographs. Subsequent field examinations verified and eliminated these features. Difficulty was encountered in differentiating some cultural features from fracture traces, notably relict plow patterns. This manifested itself in two fashions: 1) Plow patterns which paralleled some fracture traces would most likely cause the operator to overlook these fractures. This would eliminate north-south and east-west oriented fractures in the Kansas area. In west Texas, due to the orientation of the cultural pattern, those fractures oriented within several degrees of N12W and N78E could be easily overlooked. Conversely, old plowing practices did not heed the "lay of the land," and plowing was done normal to local slope. Those plow furrows normal to the slope would enhance and concentrate runoff in this direction, creating a series of parallel first and second order stream channels. Contour plowing practices alleviated this problem, however, they may have additionally obscured some of the original fracture pattern. Figures 5 and 6 are obvious examples of some

FRACTURE TRACE MAP
S. PRATT AND N BARBER COS., KS.

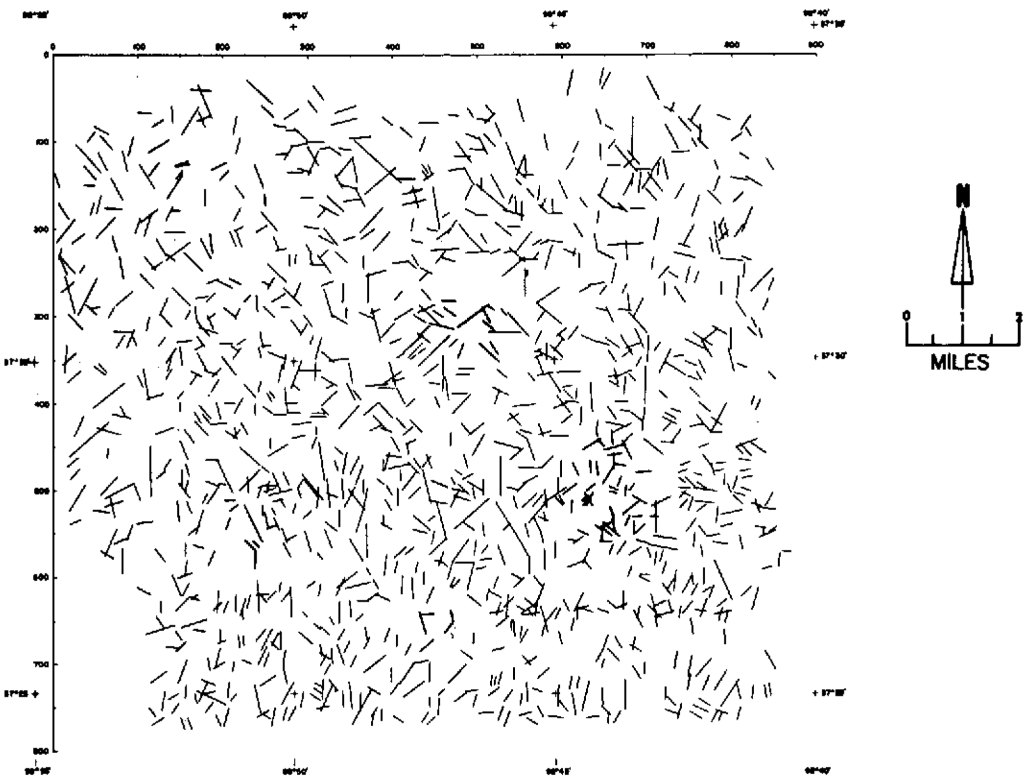

Figure 3. Fracture Trace Map of Kansas Study Area. The Upper and Left Margins Correspond to the Same Margins of Figure 1 and All Later Maps Using the Same Base.

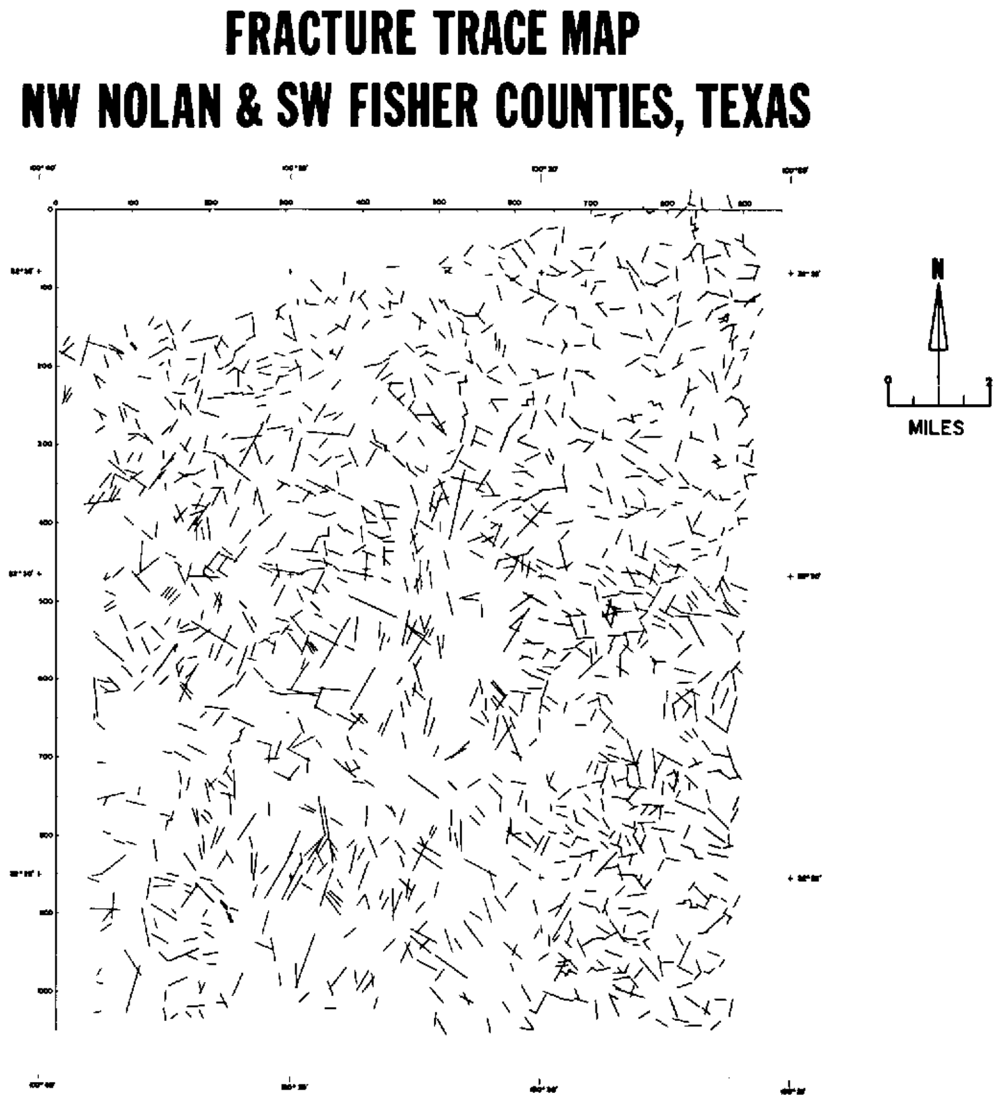

Figure 4. Fracture Trace Map of Texas Study Area. The Upper and Left Margins Correspond to the Same Margins of Figure 2 and All Later Maps Using the Same Base.

REPRODUCIBILITY OF THE
ORIGINAL PAGE IS POOR

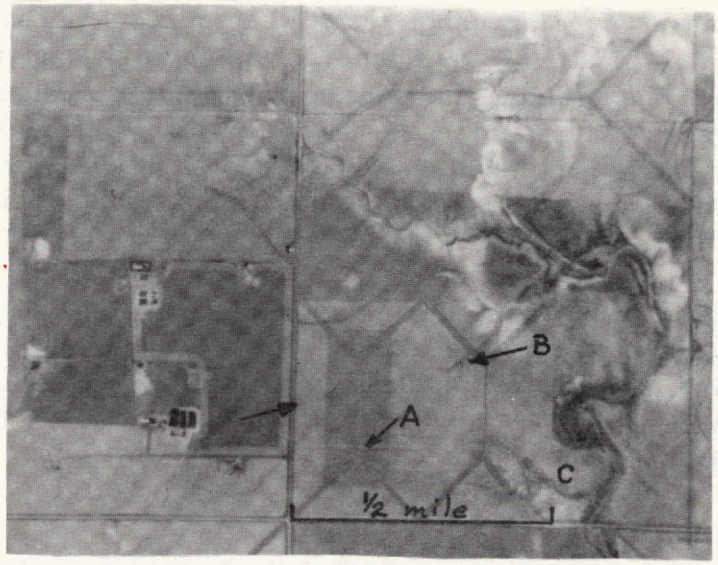

Figure 5. Vertical Aerial Photograph of a Portion of Pratt County, Kansas, Taken in 1950. Note the Finishing Passes in the Plow Pattern (A), the Fracture Trace (B) and Areal Extent of Exposed Carbonate-Rich "B" Soil Horizon at C. Compare with Figure 6.

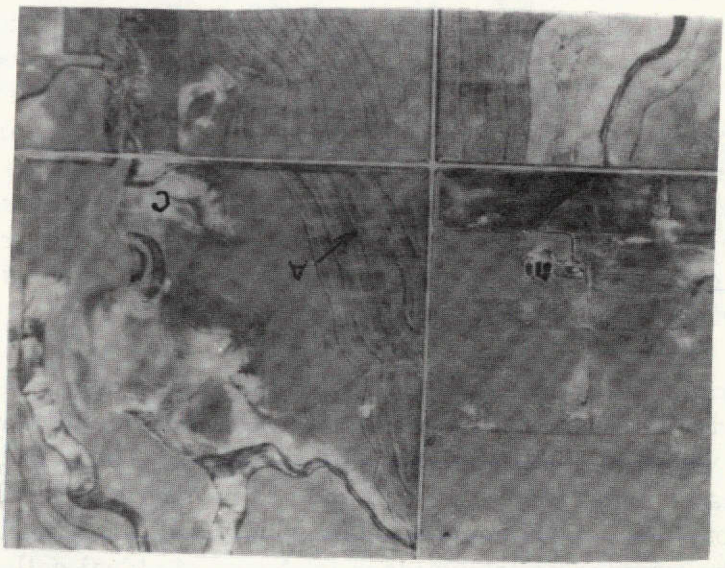

Figure 6. Vertical Aerial Photograph of a Portion of Pratt County, Kansas, Taken in 1963. Finishing Plow Patterns (A) Might be Mistaken for Fracture Traces. Fracture Trace (B in Figure 5) Has Been Obliterated by Land Contouring. Poor Agricultural Practices Have Caused Erosion and Exposed More Carbonate-Rich "B" Horizon (C).

of these phenomena. Many others exist where a decision concerning their origin is more difficult. 2) Plow patterns with their characteristic finishing passes through the field diagonals create linear patterns which later show through as relict patterns through a newer plowing pattern. Because most of these lines pass through field or section corners, they were regarded with suspicion and their significance downgraded. Gol'braikh et al. (1968a) noted similar problems in the USSR.

For the purpose of this study and to eliminate some of the subjectivity of the mapping, only continuous features were mapped as individual fracture traces. Thus, if a linear feature of 4 cm length on an aerial photograph appeared to have a break in its length, dividing it into two individual fractures, it would be mapped as such.

DATA HANDLING

Due to the large amount of information obtained, a computer-based data handling system was devised. A cartesian coordinate system was established with its origin in the upper left corner of each of the map areas. The X axis was chosen as latitudinal and positive to the right and the Y axis meridional and positive downward. The beginning and end points of each fracture trace could now be referenced with respect to this system which is illustrated in Figures 3 and 4. The map data were digitized onto standard 80 column Hollerith computer cards and preliminary treatment performed by a FORTRAN IV program TRANSFORM. Program listings and additional detail are described in Podwysocki (1974). The punched card output of this program contained the beginning, end and midpoints of each fracture trace as well as its length in millimeters on the map, azimuth and several other parameters which were then used in additional computer programs. Subsequent programs utilized the established cartesian base, dividing the map area into various grid cell sizes, and summarized the data in several fashions.

These programs were designed so that not only could data be summarized within a grid cell specified by the user, but the increment by which this grid cell was moved across the map could be specified. Thus, 1) the whole map could be treated as a single grid cell and all information would be summarized within that one cell, 2) the map could be subdivided into a series of smaller cells with the summaries taking place in those individual cells or 3) the map could be subdivided as in 2 above and the summary cell size could be incremented at a value less than the grid cell size, creating a "running average" or smoothing effect (see Podwysocki, 1974). Gol'braikh et al. (1968a) used the latter technique to look for changes in the number of megajoints and their orientation which might be associated with the presence of structural complications (i. e. structural closures, faults).

ANALYSIS OF FRACTURE TRACE LENGTHS

Treating the whole map of each area as a single grid cell, and classifying the fracture traces into 0. 05 mile (0. 08 km) class intervals, produced the results shown in Figures 7 and 8. VECLEN, the computer program for this classification, which is described in Appendix A, summarizes a fracture trace by its length if its midpoint falls within a grid cell. In both study areas the distributions of fracture trace lengths are highly skewed towards the shorter lengths. Gol'braikh and Mirkin (1973, pers. comm.) showed similar results for their studies of the Vilyuisk Syneclise and the Preverkhoyansk Downwarp. Although no conscientious effort was made by the operator to discriminate against linear features greater than one mile (1. 6 km) in length, it should be noted that all but a few fracture traces mapped were less than the maximum defined length of one mile as defined by Lattman (1958).

Because of the marked similarity between the observed distribution of fracture trace lengths and plots of sediment grain size distribution from sieve analysis, a variation of Krumbein's Phi scale transformation (1938) was applied to the data as follows:

$$z = \log_2 x + 6 \tag{2}$$

where x is the original length of the fracture trace in miles, z is the transformed value of the fracture trace length and 6 is a constant added to each value so that all resultant values in this work would be positive. Repeated analysis using the same techniques listed above produced the results illustrated in Figures 9 and 10. The histograms look like Gaussian distributions, however, the summary statistics in the figures do not bear this out. The following discussion of fracture trace lengths will utilize the transformed data.

It was thought that mixing of geologically different populations might cause the deviations from log-normality in the transformed data. The study areas were divided into quarters and each analyzed independently. Results indicated that only some areas showed normal distributions. It was noted that the log-mean fracture length was different for each of the 4 quarters of each of the two study areas.

To isolate those areas which were anomalous, the study areas were again quartered, producing a 1/16th unit of the total map area and the analysis performed on each unit. In addition, the summary unit cell was incremented by 1/2 cell intervals in both the X and Y directions, creating a running average as described earlier. The summaries produced cells which were approximately 3. 5 by 3. 9 miles (5. 6 by 6. 2 km) in the west Texas area and 3. 6 by 2. 9 miles

TEST OF FRACTURE TRACE DISTRIBUTION TO NORMALITY BY CHI SQUARE

KANSAS STUDY AREA; WHOLE AREA TREATED AS ONE CELL

CLASS INTERVAL = 0.05 MILES

ROW 1 ,COLUMN 1 (0 < X < 920 ; 0 < Y < 800)

CLASS	LOWER CLASS LIMIT	UPPER CLASS LIMIT	EXPECTED FREQUENCY	CHI SQUARE CONTRIB.	OBSERVED FREQUENCY	OBSERVED FREQUENCY HISTOGRAM
2	0.06	0.10	84.49	80.53	2.00	>
3	0.11	0.15	87.83	19.70	46.00	>XXXXXXXXX
4	0.16	0.20	134.22	106.88	254.00	>XXXXXXXXXXXXXXXXXXXXXXXXXXXXXXXXXXXXXXXXXXXXXXXXXXX
5	0.21	0.25	174.61	77.88	291.00	>XXXXXXXXXXXXXXXXXXXXXXXXXXXXXXXXXXXXXXXXXXXXXXXXXXXXXXXXXX
6	0.26	0.30	192.73	3.06	217.00	>XXXXXXXXXXXXXXXXXXXXXXXXXXXXXXXXXXXXXXXXXXX
7	0.31	0.35	180.61	9.55	139.00	>XXXXXXXXXXXXXXXXXXXXXXXXXXXX
8	0.36	0.40	143.48	19.93	90.00	>XXXXXXXXXXXXXXXXXX
9	0.41	0.45	96.73	14.72	59.00	>XXXXXXXXXXXX
10	0.46	0.50	55.36	7.49	35.00	>XXXXXXX
11	0.51	0.55	26.89	0.89	22.00	>XXXX
12	0.56	0.60	11.07	0.08	12.00	>XX
13	0.60	0.65	3.86	6.85	9.00	>X
14	0.66	0.70	1.14	41.07	8.00	>X
15	0.71	0.75	0.29	1.72	1.00	>
16	0.76	0.80	0.07	13.42	1.00	>
17	0.81	0.85	0.01	686.65	3.00	>
18	0.86	0.90	0.00	418.22	1.00	>
19	0.91	0.95	0.00	2435.68	1.00	>
20	0.96	1.00	0.00	0.00	0.0	>
21	1.01	1.05	0.00	0.00	0.0	>
22	1.06	1.10	0.00	547097.38	1.00	>
23	1.11	1.15	0.00	0.00	0.0	>
24	1.16	1.20	0.00	0.00	0.0	>
25	1.21	1.25	0.00	0.00	0.0	>
26	1.26	1.30	0.00	0.00	0.0	>
27	1.31	1.35	0.00	0.00	0.0	>
28	1.36	1.40	0.00	0.00	0.0	>
29	1.41	1.45	0.00	0.00	0.0	>
30	1.46	1.50	0.00	0.00	0.0	>
31	1.51	1.55	0.00	0.00	0.0	>
32	1.56	1.60	0.00	0.00	0.0	>
33	1.60	1.65	0.00	0.00	0.0	>
34	1.66	1.70	0.00	***********	1.00	>
	TOTALS		1193.00	551043.30*	1193.00	EACH "X" = 5.000 VECTOR(S)

DEGREES OF FREEDOM = 30

NON-FOLDED DISTRIBUTION CHI SQUARE PROBABILITY = 0.0

MODAL STATISTICS

CLASS	MIDPOINT	OBS. FREQUENCY
5	0.225	291.00

STATISTICAL MOMENTS

AVERAGE	VARIANCE	STANDARD DEVIATION	ROOT B1	B2
0.280	0.015	0.123	2.680	20.417

*CHI SQUARE TOTAL EXCLUSIVE OF CLASS 34

Figure 7. Plot of the Distribution of Fracture Trace Frequency versus Linear Length for the Kansas Study Area and the Test for Normality of the Distribution

REPRODUCIBILITY OF THE ORIGINAL PAGE IS POOR

TEST OF FRACTURE TRACE DISTRIBUTION TO NORMALITY BY CHI SQUARE

TEXAS STUDY AREA; WHOLE AREA TREATED AS ONE CELL

CLASS INTERVAL = 0.05 MILES

ROW 1 ,COLUMN 1 (0 < X < 960 ; 0 < Y < 1050)

CLASS	LOWER CLASS LIMIT	UPPER CLASS LIMIT	EXPECTED FREQUENCY	CHI SQUARE CONTRIB.	OBSERVED FREQUENCY	OBSERVED FREQUENCY HISTOGRAM
2	0.05	0.10	145.54	110.41	19.00	>XXX
3	0.10	0.15	112.71	0.16	117.00	>XXXXXXXXXXXXXXXXXXXXXXX
4	0.15	0.20	156.51	103.85	284.00	>XXXXXXXXXXXXXXXXXXXXXXXXXXXXXXXXXXXXXXXXXXXXXXXXXXXXXXXX
5	0.20	0.25	191.94	66.60	305.00	>XXXXXXXXXXXXXXXXXXXXXXXXXXXXXXXXXXXXXXXXXXXXXXXXXXXXXXXXXXXXX
6	0.25	0.30	207.98	32.35	290.00	>XXXXXXXXXXXXXXXXXXXXXXXXXXXXXXXXXXXXXXXXXXXXXXXXXXXXXXXXXX
7	0.30	0.35	199.07	9.76	155.00	>XXXXXXXXXXXXXXXXXXXXXXXXXXXXXXX
8	0.35	0.40	168.40	17.57	114.00	>XXXXXXXXXXXXXXXXXXXXXX
9	0.40	0.45	125.80	39.84	55.00	>XXXXXXXXXXX
10	0.45	0.50	83.03	27.78	35.00	>XXXXXXX
11	0.50	0.55	48.44	7.80	29.00	>XXXXX
12	0.55	0.60	24.96	0.15	23.00	>XXXX
13	0.60	0.65	11.35	6.60	20.00	>XXXX
14	0.65	0.70	4.55	2.61	8.00	>X
15	0.70	0.75	1.62	43.48	10.00	>XX
16	0.75	0.80	0.51	39.43	5.00	>X
17	0.80	0.85	0.15	0.15	0.0	>
18	0.85	0.90	0.04	232.79	3.00	>
19	0.90	0.95	0.01	1758.22	4.00	>
20	0.95	1.00	0.00	0.00	0.0	>
21	1.00	1.05	0.00	20209.82	3.00	>
22	1.05	1.10	0.00	10633.61	1.00	>
23	1.10	1.15	0.00	204163.44	2.00	>
24	1.15	1.20	0.00	0.00	0.0	>
25	1.20	1.25	0.00	0.00	0.0	>
26	1.25	1.30	0.00	0.00	0.0	>
27	1.30	1.35	0.00	25333696.00	1.00	>
	TOTALS		1483.00	25571200.00	1483.00	EACH "X" = 5.000 VECTOR(S)

DEGREES OF FREEDOM = 23

NON-FOLDED DISTRIBUTION CHI SQUARE PROBABILITY = 0.0

MODAL STATISTICS

CLASS	MIDPOINT	OBS.FREQUENCY
5	0.225	305.00

STATISTICAL MOMENTS

AVERAGE	VARIANCE	STANDARD DEVIATION	ROOT B1	B2
0.282	0.020	0.141	2.142	10.469

Figure 8. Plot of the Distribution of Fracture Trace Frequency versus Linear Length for the Texas Study Area and the Test for Normality of the Distribution

REPRODUCIBILITY OF THE ORIGINAL PAGE IS POOR

TEST OF FRACTURE TRACE DISTRIBUTION TO LOG-NORMALITY BY CHI SQUARE

KANSAS STUDY AREA; WHOLE AREA TREATED AS ONE CELL

MILEAGE CONVERTED TO LOG SCALE; Z=(1/LOG10(2))*LOG10(X)+6

ROW 1 ,COLUMN 1 (0 < X < 920 ; 0 < Y < 800)

CLASS	LOWER CLASS LIMIT	UPPER CLASS LIMIT	EXPECTED FREQUENCY	CHI SQUARE CONTRIB.	OBSERVED FREQUENCY	OBSERVED FREQUENCY HISTOGRAM
10	2.25	2.50	2.21	0.02	2.	>
11	2.50	2.75	6.62	6.62	0.	>
12	2.75	3.00	20.20	7.37	6.	>X
13	3.00	3.25	49.75	5.64	33.	>XXXXXX
14	3.25	3.50	99.00	1.98	113.	>XXXXXXXXXXXXXXXXXXXXXX
15	3.50	3.75	159.33	21.60	218.	>XXXXXXXXXXXXXXXXXXXXXXXXXXXXXXXXXXXXXXXXXXX
16	3.75	4.00	207.22	0.67	219.	>XXXXXXXXXXXXXXXXXXXXXXXXXXXXXXXXXXXXXXXXXXX
17	4.00	4.25	217.89	0.36	209.	>XXXXXXXXXXXXXXXXXXXXXXXXXXXXXXXXXXXXXXXXX
18	4.25	4.50	185.23	4.93	155.	>XXXXXXXXXXXXXXXXXXXXXXXXXXXXXXX
19	4.50	4.75	127.25	4.62	103.	>XXXXXXXXXXXXXXXXXXXX
20	4.75	5.00	70.68	0.08	73.	>XXXXXXXXXXXXXX
21	5.00	5.25	31.75	0.05	33.	>XXXXXX
22	5.25	5.50	11.51	3.66	18.	>XXX
23	5.50	5.75	3.37	0.12	4.	>
24	5.75	6.00	0.80(0.99)	6.04(16.27)	3.(5.)	>
25	6.00	6.25	0.16	4.50	1.	>
26	6.25	6.50	0.03	0.03	0.	>
27	6.50	6.75	0.00	252.83	1.	>
TOTALS			1193.00	321.12 (74.00)	1193.	EACH "X" = 5.00 VECTOR(S)

DEGREES OF FREEDOM (NON-FOLDED) = 15; CHI SQUARE PROBABILITY = 0.2249E-58

DEGREES OF FREEDOM (FOLDED) = 12; CHI SQUARE PROBABILITY = 0.5680E-10

MODAL STATISTICS

CLASS	MIDPOINT	OBS.FREQUENCY
16	3.875	219.00

STATISTICAL MOMENTS

AVERAGE	VARIANCE	STANDARD DEVIATION	ROOT B1	B2
4.059	0.289	0.537	0.531	3.513

Figure 9. Plot of Fracture Trace Frequency versus Log-Length for the Kansas Study Area and the Test for Log-Normality of the Distribution. Numbers Within Parentheses Represent Values When Distribution Tails Were Folded So That Expected Frequency > 0.95.

REPRODUCIBILITY OF THE ORIGINAL PAGE IS POOR

TEST OF FRACTURE TRACE DISTRIBUTION TO LOG-NORMALITY BY CHI SQUARE

TEXAS STUDY AREA: WHOLE AREA TREATED AS ONE CELL

MILEAGE CONVERTED TO LOG SCALE: Z=(1/LOG10(2))*LOG10(X)+6

ROW 1 ,COLUMN 1 (0 < X < 960 : 0 < Y < 1050)

CLASS	LOWER CLASS LIMIT	UPPER CLASS LIMIT	EXPECTED FREQUENCY	CHI SQUARE CONTRIB.	OBSERVED FREQUENCY	OBSERVED FREQUENCY HISTOGRAM
9	2.00	2.25	3.07	0.37	2.	>
10	2.25	2.50	7.02	2.26	11.	>XX
11	2.50	2.75	16.65	4.01	10.	>XX
12	2.75	3.00	42.24	5.50	27.	>XXXXX
13	3.00	3.25	81.57	0.00	81.	>XXXXXXXXXXXXXXXX
14	3.25	3.50	134.51	1.56	120.	>XXXXXXXXXXXXXXXXXXXXXXXX
15	3.50	3.75	189.37	11.48	236.	>XXXXXXXXXXXXXXXXXXXXXXXXXXXXXXXXXXXXXXXXXXXXXXX
16	3.75	4.00	227.45	0.49	238.	>XXXXXXXXXXXXXXXXXXXXXXXXXXXXXXXXXXXXXXXXXXXXXXX
17	4.00	4.25	233.26	7.11	274.	>XXXXXXXXXXXXXXXXXXXXXXXXXXXXXXXXXXXXXXXXXXXXXXXXXXXXXX
18	4.25	4.50	204.20	2.00	184.	>XXXXXXXXXXXXXXXXXXXXXXXXXXXXXXXXXXXX
19	4.50	4.75	152.54	4.97	125.	>XXXXXXXXXXXXXXXXXXXXXXXXX
20	4.75	5.00	97.26	10.05	66.	>XXXXXXXXXXXXX
21	5.00	5.25	52.96	0.17	50.	>XXXXXXXXXX
22	5.25	5.50	24.61	2.22	32.	>XXXXXX
23	5.50	5.75	9.74	1.09	13.	>XX
24	5.75	6.00	3.29	4.19	7.	>X
25	6.00	6.25	0.95(1.19)	26.74(28.29)	6.(7.)	>X
26	6.25	6.50	0.24	2.41	1.	>
TOTALS			1482.93	86.63 (85.77)	1483.	EACH "X" = 5.00 VECTOR(S)

DEGREES OF FREEDOM (NON-FOLDED) = 15; CHI SQUARE PROBABILITY = 0.4196E-11

DEGREES OF FREEDOM (FOLDED) = 14; CHI SQUARE PROBABILITY = 0.2375E-11

MODAL STATISTICS

CLASS	MIDPOINT	OBS.FREQUENCY
17	4.125	274.00

STATISTICAL MOMENTS

AVERAGE	VARIANCE	STANDARD DEVIATION	ROOT B1	B2
4.040	0.389	0.624	0.339	3.616

Figure 10. Plot of Fracture Trace Frequency versus Log-Length for the Texas Study Area and the Test for Log-Normality of the Distribution. Numbers Within Parentheses Represent Values When Distribution Tails Were Folded So That Expected Frequency > 0.95.

REPRODUCIBILITY OF THE ORIGINAL PAGE IS POOR

(5.8 by 4.6 km) in the Kansas area for a total of 64 cells (8 by 8 in each area). Summary statistics such as the log-mean fracture trace length, standard deviation, skewness ($\sqrt{\beta_1}$) and kurtosis (β_2) of each cell's frequency distribution as well as the number of fracture traces for each unit cell were produced for use in additional analyses.

The summary statistics produced in the above mentioned compilations of the data were analyzed using linear regression analysis. Due to the paucity of fracture traces in the southernmost tier of cells (less than 5 in each) in the Texas study area, these cells were eliminated from the analysis.

The significance test for correlations between the statistical moments for the Kansas data (Table 1) indicates a significant correlation for 1) log-mean fracture trace length and skewness, 2) number of fracture traces per unit cell and standard deviation and 3) skewness versus kurtosis. Figure 11 represents the plot of the standard deviation versus number of fracture traces per unit cell. The plot indicates low standard deviations associated with cells containing few fracture traces (lower left part of diagram). Because the reliability of the statistical moments for such small sample sizes is highly questionable, the offending samples (all cells containing less than 45 samples), which occurred along the eastern and southern margins of the map area, and were due to incomplete mapping coverage, were eliminated from consideration in further tests. Repeated regression analysis on the data exclusive of the mentioned marginal cells indicated no significant correlation between two of the three previously determined associations. However, it should be noted that a significant correlation did remain between the skewness and kurtosis measures; Figure 12, based on the original analysis of 64 samples, serves to illustrate the results. A small group of samples located near the right margin of the plot contains kurtosis values which are highly leptokurtic* (8-10). These cells contain several very long fractures (greater than the accepted length for a fracture trace) that were inadvertently included, and will be discussed later in the log-normality analysis. A removal of these four anomalous cells and repeated regression analysis indicated no significant correlation between the two moments. Removal of these correlations, or attributing them to some sampling inconsistencies, indicates the samples are homogeneous, that is, several discrete and very distinct populations do not exist in the data.

* More peaked than normal

Table 1

Results of Linear Regression Analysis
On Log-Mean Fracture Trace Moments

Kansas Data - 64 Samples

	Log-Mean Length	Standard Deviation	Skewness	Kurtosis
Standard Deviation	NS			
Skewness	S*	NS		
Kurtosis	NS	NS	S**	
No. of Fracture Traces per Unit Cell	NS	S**	NS	NS

Table 2

Results of Linear Regression Analysis
On Log-Mean Fracture Trace Moments

Texas Data - 56 Samples

	Log-Mean Length	Standard Deviation	Skewness	Kurtosis
Standard Deviation	S**			
Skewness	S**	NS		
Kurtosis	NS	S*	NS	
No. of Fracture Traces per Unit Cell	NS	NS	NS	S**

NS = non significant
S* = significant at 0.05 level
S** = significant at 0.01 level

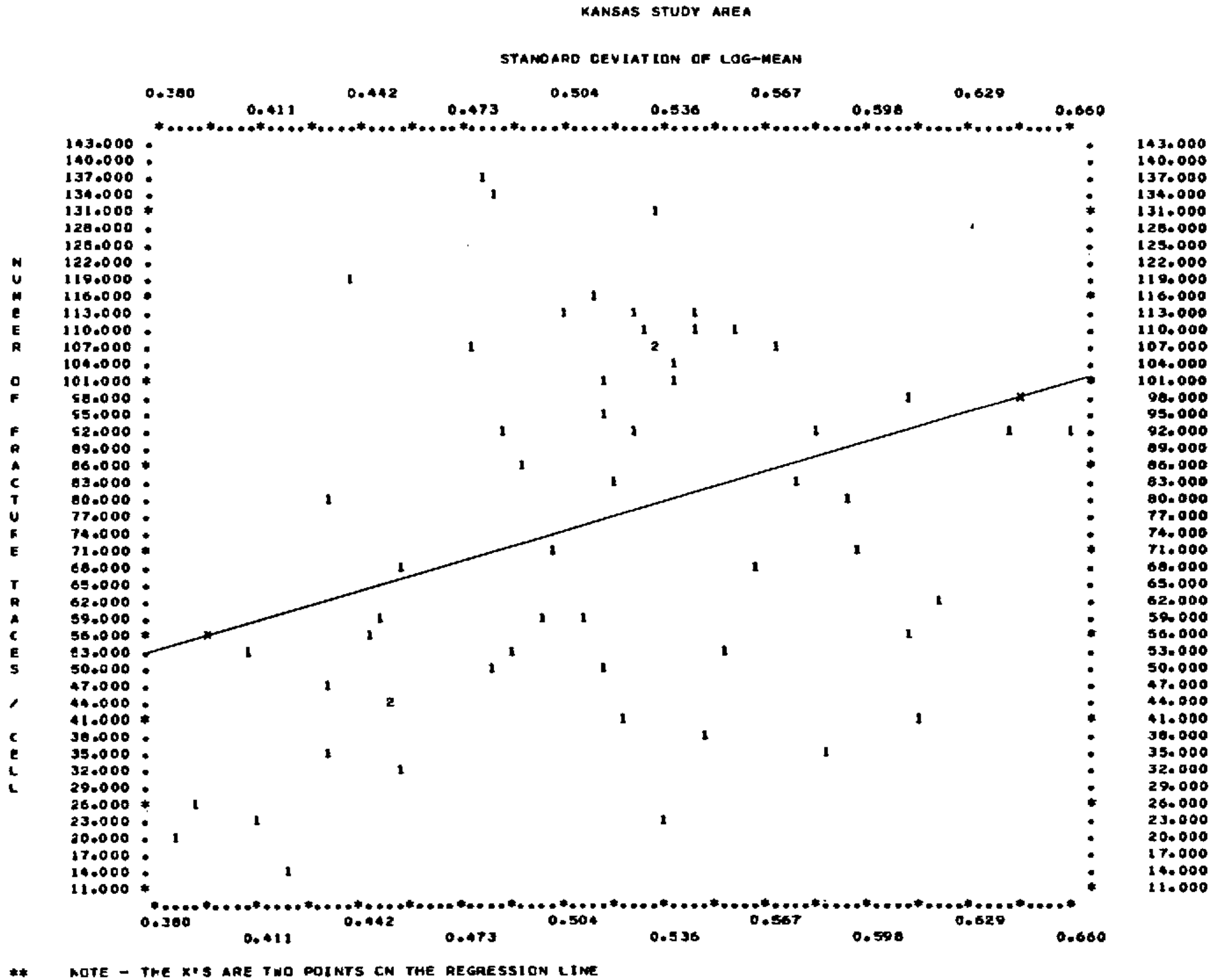

Figure 11. Regression Analysis Plot of Standard Deviation versus the Number of Fracture Traces Per Unit Cell for the Kansas Data. Numbers Within the Plot Indicate the Number of Data Points Located in that Position.

REPRODUCIBILITY OF THE ORIGINAL PAGE IS POOR

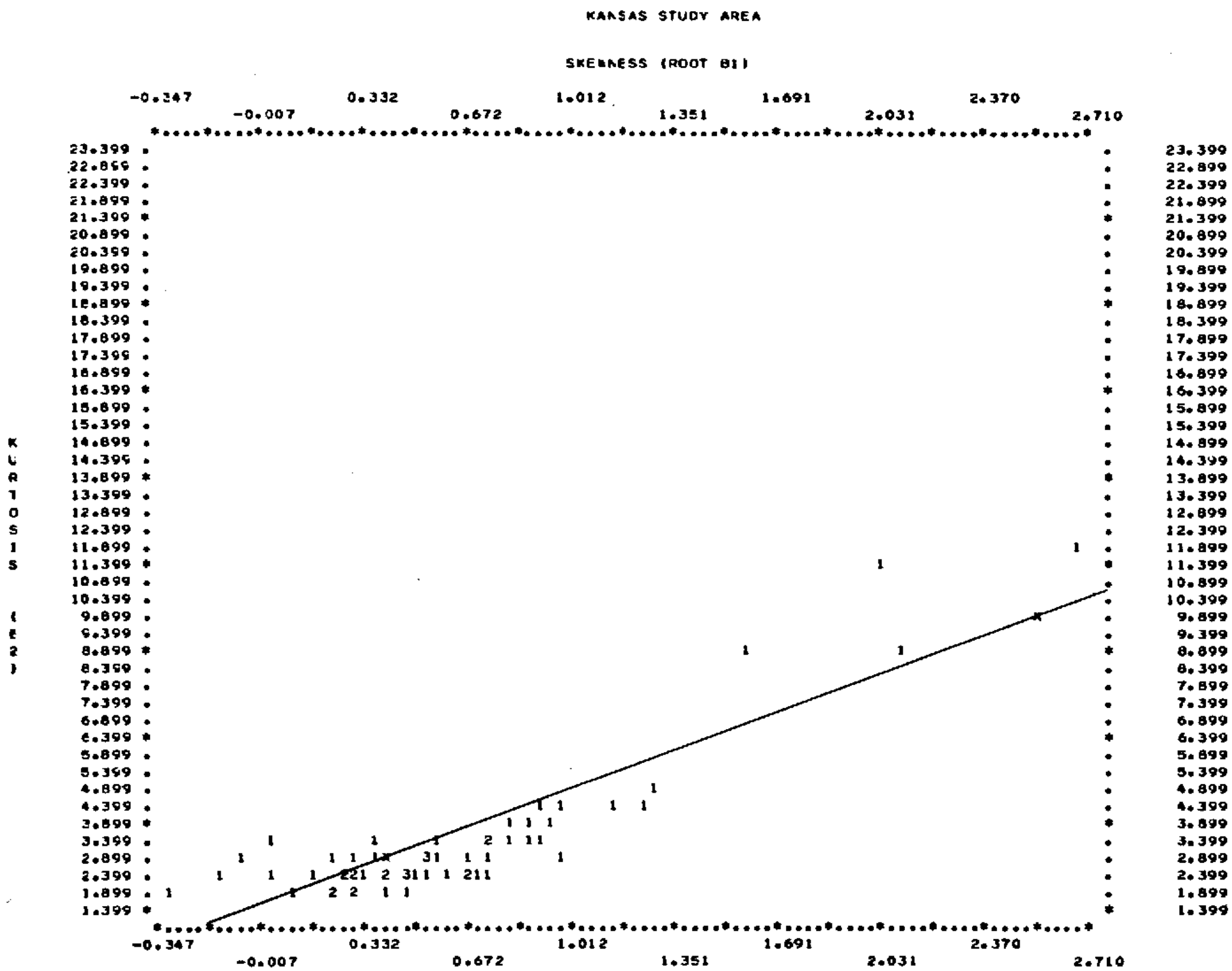

Figure 12. Regression Analysis Plot of Skewness versus Kurtosis for the Kansas Data.

REPRODUCIBILITY OF THE ORIGINAL PAGE IS POOR

The regression analyses on the Texas data are given in Table 2. Significant correlations exist between:

1) log-mean fracture trace length and standard deviation (Figure 13), which indicates increasing standard deviation with increasing mean fracture trace length;

2) log-mean fracture trace length and skewness (Figure 14), which illustrates an increasing positive skewness (mode displaced towards smaller values with respect to the mean of the distribution) with increasing fracture trace length;

3) standard deviation and kurtosis, (Figure 15); and

4) kurtosis and the number of fracture traces per unit cell (Figure 16).

Figures 13-15 can be interpreted together to indicate one of two possible causes. If the assumption is made that the samples were taken from a single homogeneous population, then the sampling technique indicates a bias. Conversely, the population may not be homogeneous, and the tests may indicate the sampling of two or more discrete and distinct populations of fracture traces. The second of the two hypotheses will be proven and more clearly illustrated by the use of trend surface analysis which will be discussed later.

The last significant correlation occurs between kurtosis and the number of fracture traces per unit cell (Figure 16). These high values are associated with large sample populations and are anomalous, perhaps suggesting some mixing of several populations of fracture traces.

Tests were performed using the Chi Square, skewness and kurtosis criteria (Griffiths and Ondrick, 1968), comparing the observed against a hypothetical Gaussian distribution. Deviations of each of the criteria were ranked, assigning values to those populations which significantly differed from normality at the 0. 05 and 0. 01 levels. Rankings were assigned as illustrated in Table 3.

If a criterion value was non-significant, it was assigned a zero value. The rankings of the three criteria for each cell were then summed to create an index value characteristic of the population distribution in each cell. High ranking values indicate strong deviations from log-normality as illustrated in Figures 17 and 18.

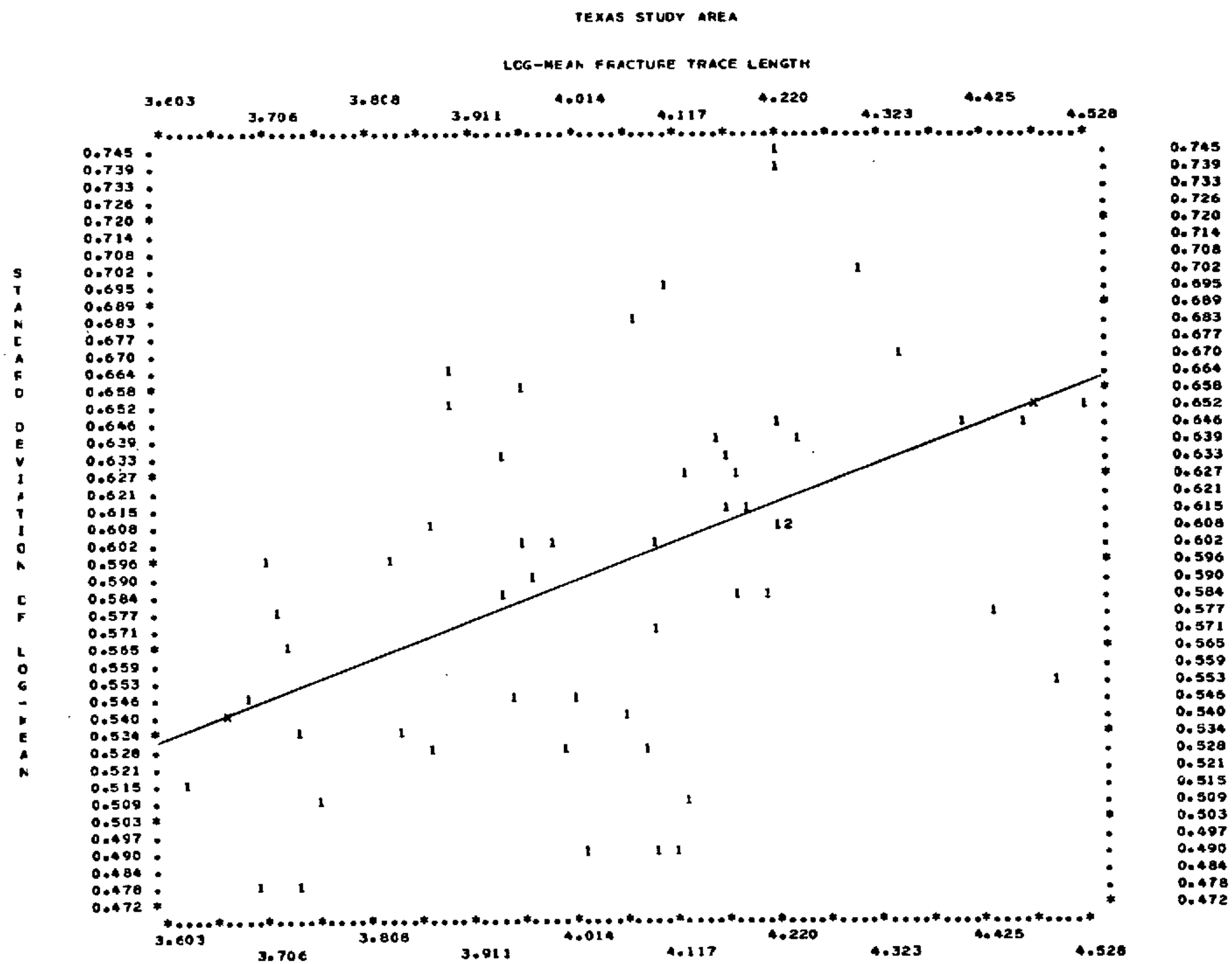

Figure 13. Regression Analysis Plot of Log-Mean Fracture Trace Length versus Standard Deviation for the Texas Data.

REPRODUCIBILITY OF THE
ORIGINAL PAGE IS POOR

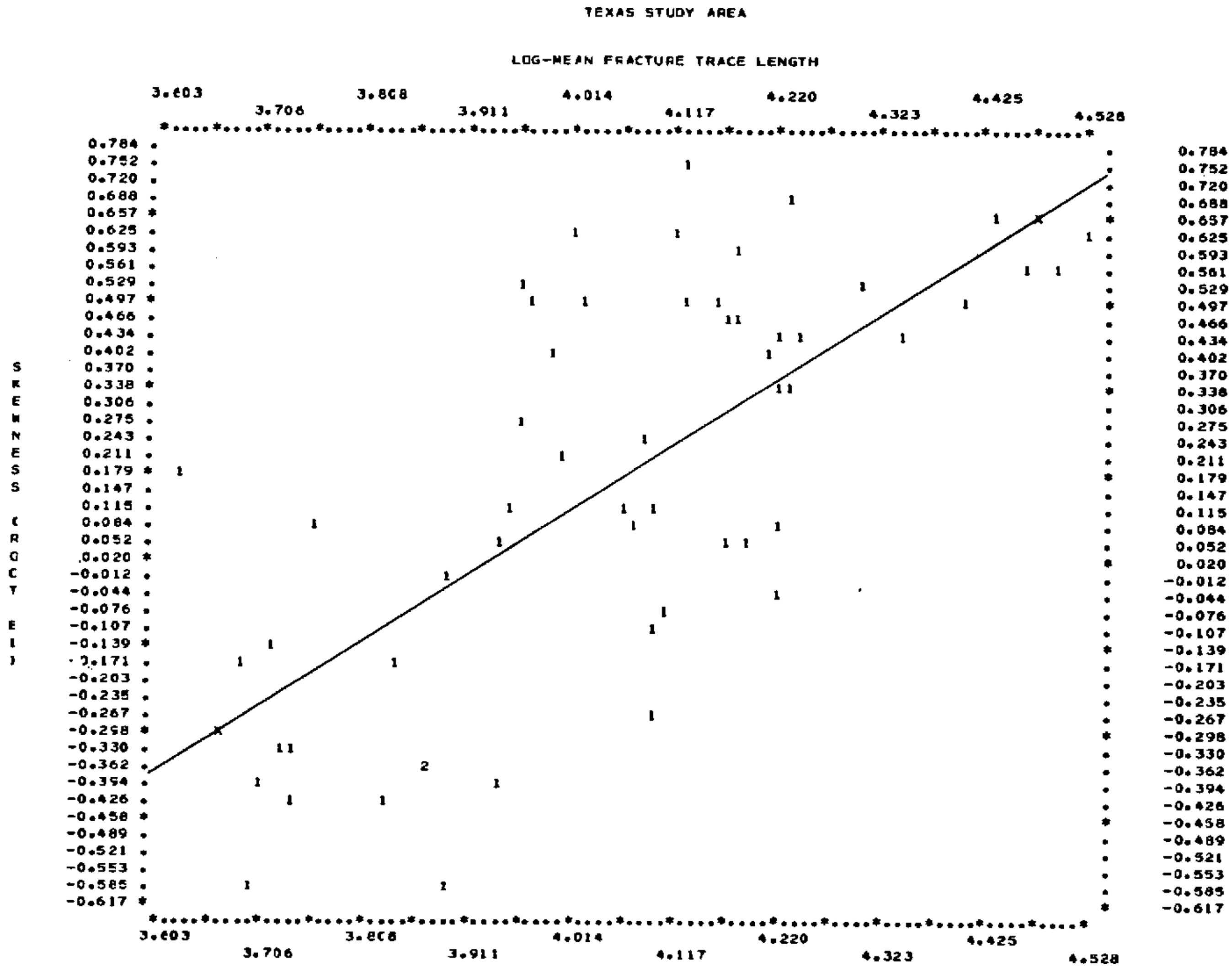

Figure 14. Regression Analysis Plot of Log-Mean Fracture Trace Length versus Skewness for the Texas Data.

REPRODUCIBILITY OF THE ORIGINAL PAGE IS POOR

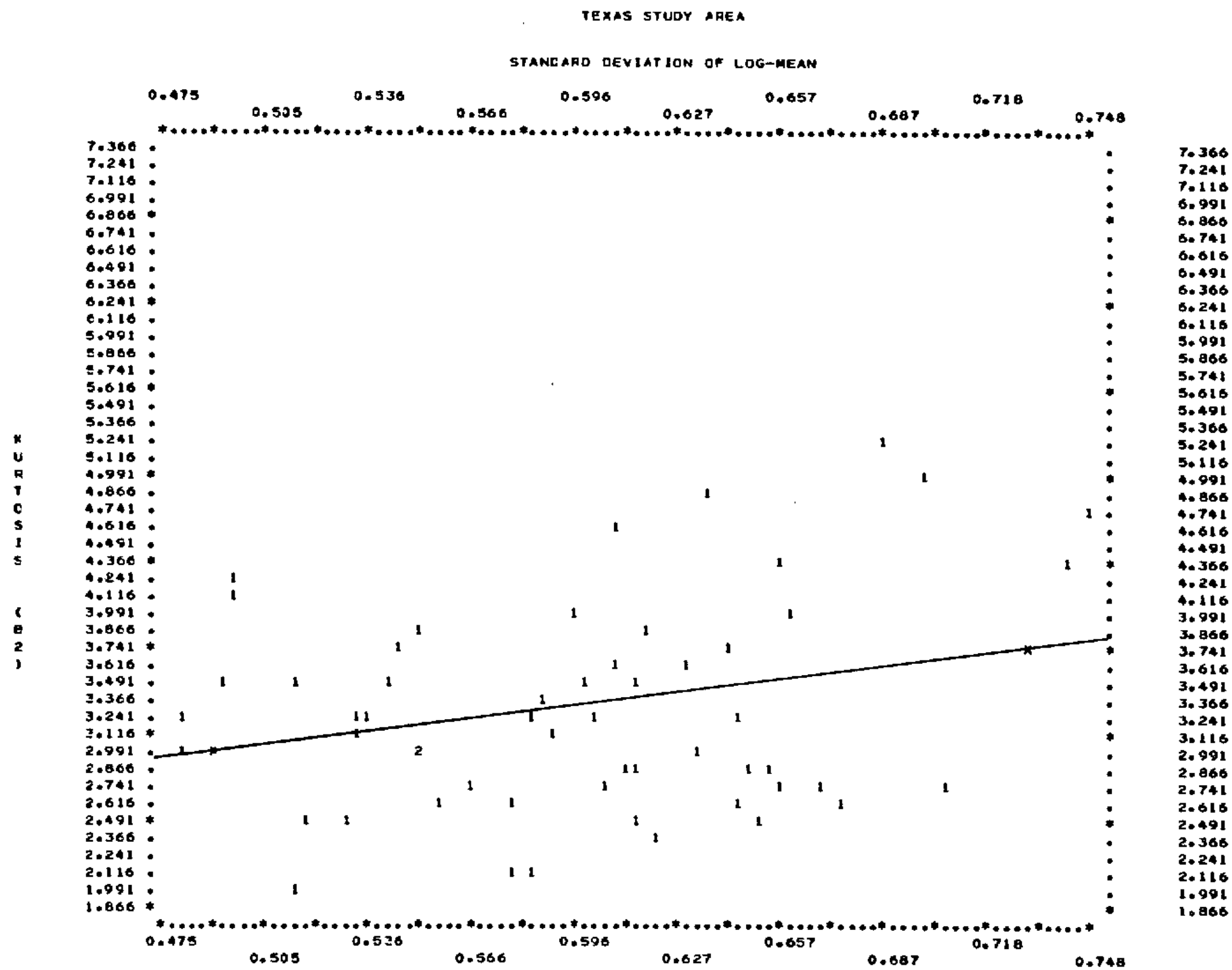

Figure 15. Regression Analysis Plot of Standard Deviation versus Kurtosis for the Texas Data.

REPRODUCIBILITY OF THE ORIGINAL PAGE IS POOR

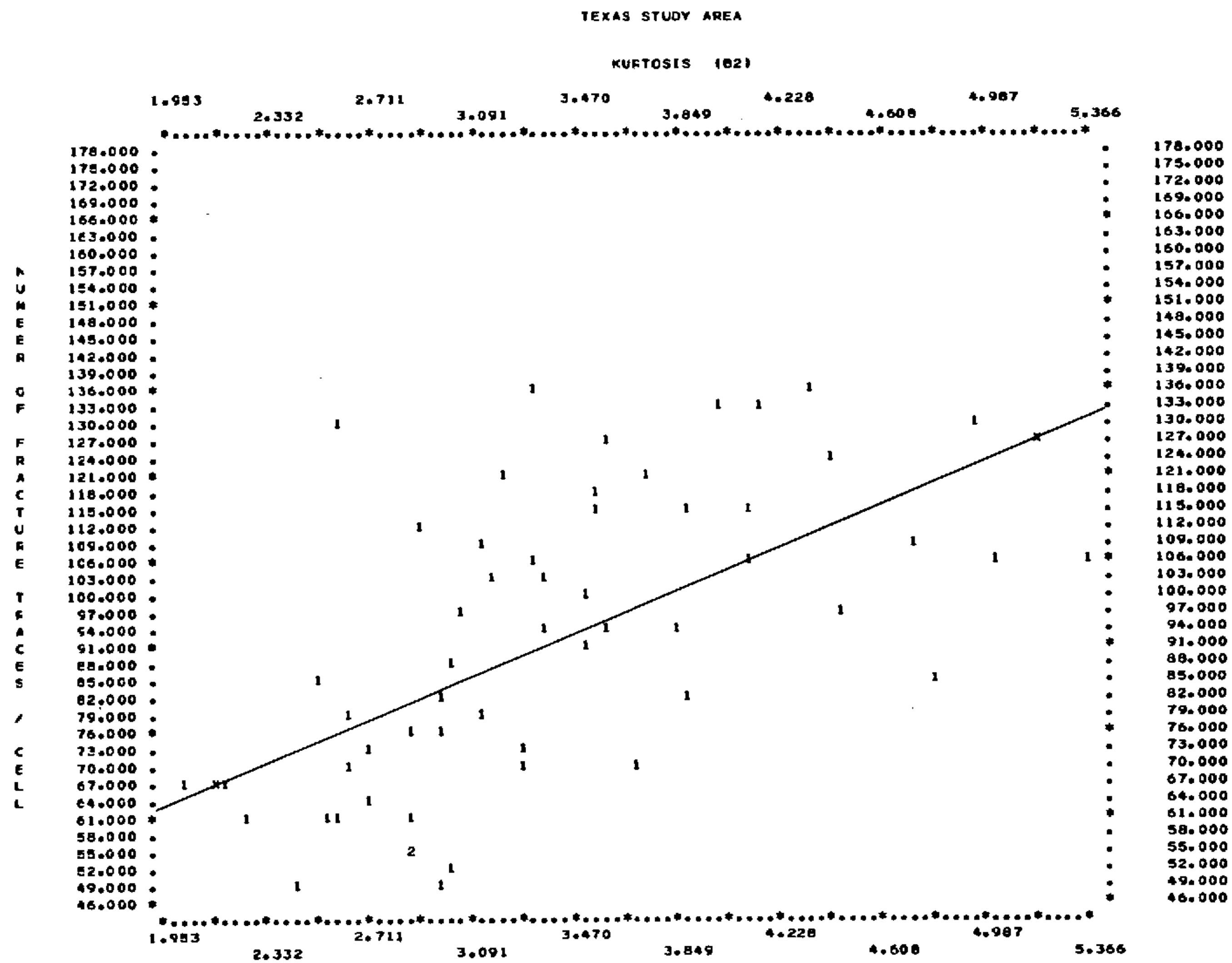

Figure 16. Regression Analysis Plot of Kurtosis versus Number of Fracture Traces per Unit Cell for the Texas Data.

REPRODUCIBILITY OF THE ORIGINAL PAGE IS POOR

KANSAS STUDY AREA

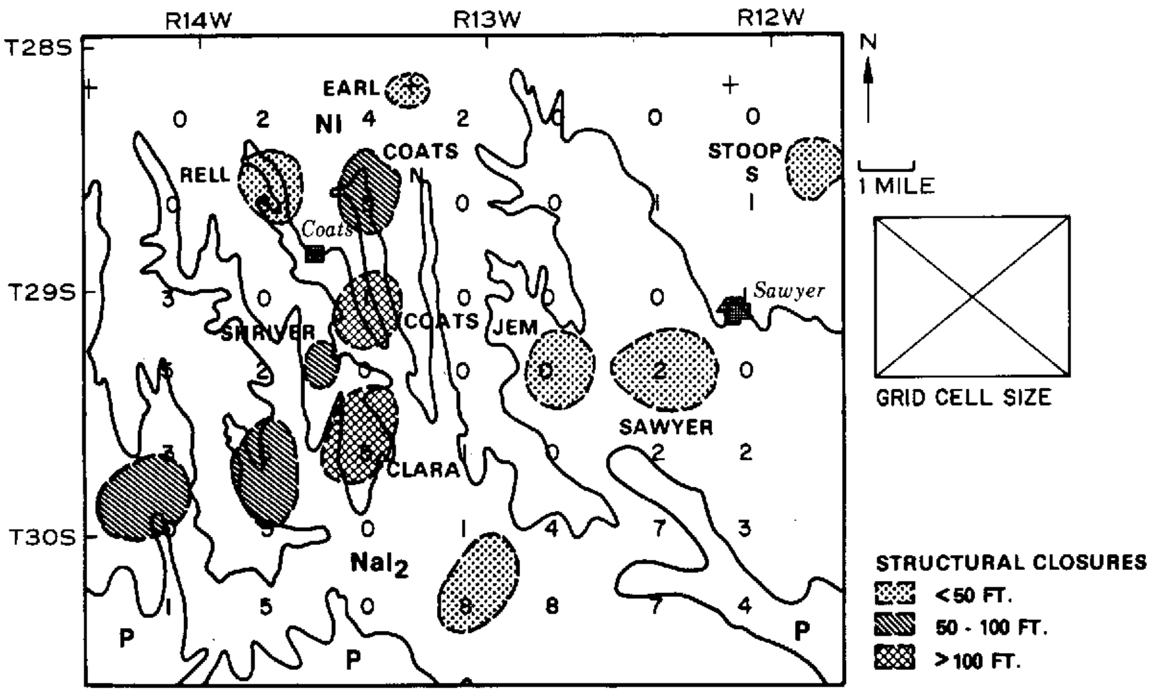

Figure 17. Results of Test for the Distribution of Fracture Trace Lengths to Log-Normality. Rank-values Are Associated With the Centerpoint of Each Grid Cell. Refer to Table 3 and Text for Key to Rank Values.

TEXAS STUDY AREA

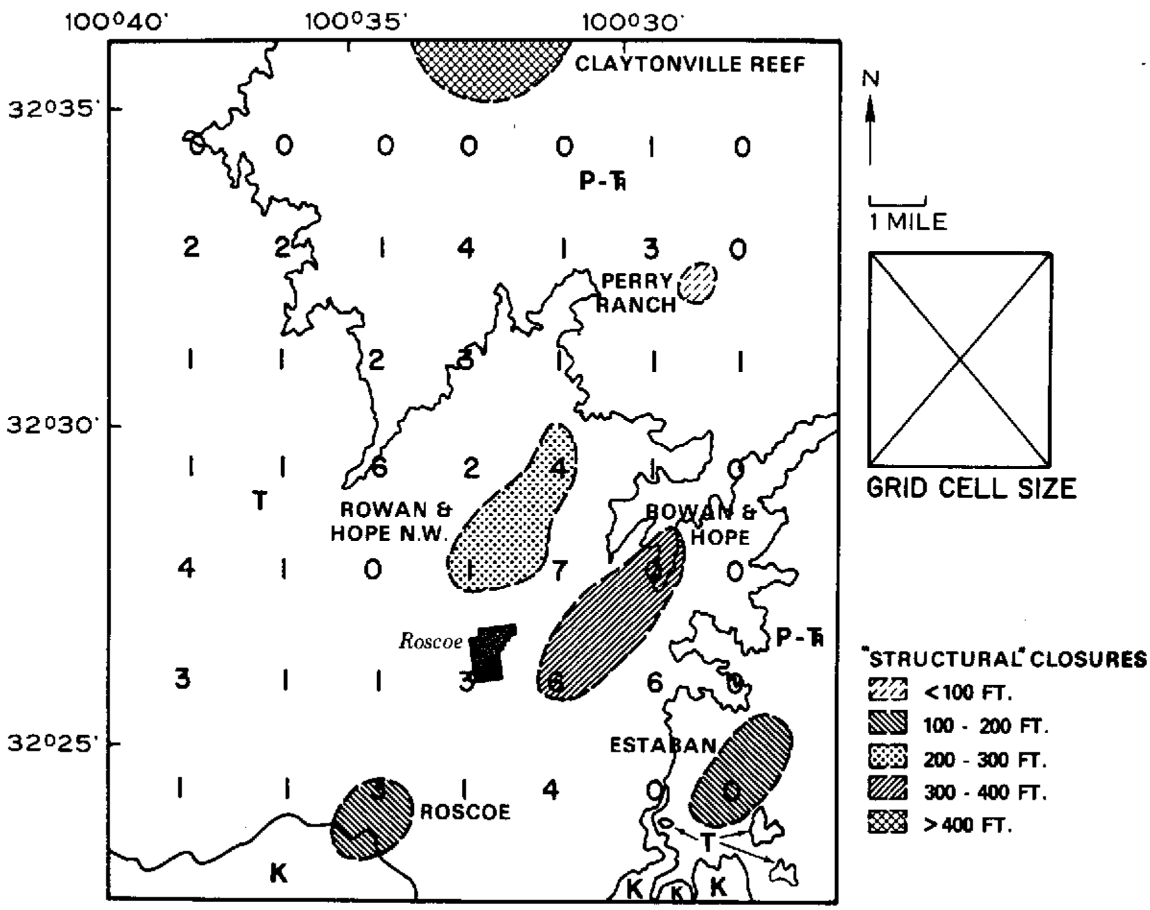

Figure 18. Results of Test for Distribution of Fracture Trace Lengths to Log-Normality. Rank-values Are Associated with the Center-point of Each Grid Cell. Refer to Table 3 and Text for Key to Rank Values.

Table 3

Rankings for Deviations from Log-Normality

Criterion	Level of Significance	Rank
Chi Square	0.05	2
	0.01	4
Skewness	0.05	1
	0.01	2
Kurtosis	0.05	1
	0.01	2

In many cases, significant deviations from log-normality occur over known structures. Analysis of fracture trace log-lengths in the Kansas study area indicates a consistent positive skewing (mode displaced towards smaller values with respect to the mean) in cells which rank four or higher; their respective kurtosis values are leptokurtic. Several factors may account for these variations. First, structural control may exist, possibly causing development of shorter fractures over structures due to enhancement of surface factors such as erosion along the fractures. Secondly, control may be due to changes in lithology. Analysis of fracture trace lengths does indicate a lithologic control and will be discussed shortly. Thus, mixing of two surface rock types within a grid cell may cause this type of discrepancy. However, it should be pointed out that similar mixing also takes place in the two Pleistocene aged formations in the eastern part of the study area, and these types of deviations do not exist in this area. Very high deviations in the southern portion of the Kansas area (ranked 7 and 8) may be due to the proximity to Permian outcrops and/or the influence of two fractures greater than one mile (1.6 km) in length that were inadvertently mapped (see Figure 7). Because these features were larger by a factor of two over all other fracture traces in the area, they cause highly significant deviations from log-normality. These same fractures were responsible for the high correlation between the skewness and kurtosis in the regression analysis plot (see Figure 12). Thirdly, biases due to operator fatigue or cultural land practices may occur. These hopefully were minimized with field checking, rest periods during mapping and cross checking with photographic coverage of earlier dates to eliminate these possible errors.

Significant deviations from log-normality (ranked four or higher) also occur over some of the known reefs in the west Texas study area. Skewness and kurtosis behave similarly to the anomalies in the Kansas area. The same three arguments stated in the previous paragraph may be employed. Cultural effects have been minimized by reference to earlier photographic coverage.

Because lithology shows little control in the northern part of the area where cells transgress lithologic boundaries, it is probably not a controlling factor in the anomalous eastern portion of the study area. The high value (a rank of 6 in row 4, column 3) in the central portion of the map area is due to the presence of a lineament. The fracture trace length distribution for this area is unlike those over the reefs; it is skewed positive and is nearly normal in its kurtosis. In some cases, the anomalous ranks do not directly overlie the structure, but lie on its flanks. Harris et al., (1960); Gol'braikh et al., (1968a) and Saunders (1969) indicate that increased fracture density may occur along the flanks of a structure, however, no mention has been made of changes in fracture length.

Further reduction of the grid cell size produced many cells with too small a population, and thus reliable statistics were not possible. Analysis of fracture trace length distributions in individual 10 degree azimuth classes in each grid cell also proved fruitless because of the small number of fracture traces in each cell.

ANALYSIS OF FRACTURE TRACE FREQUENCY

Trainer and Ellison (1967) define frequency as the number of fracture traces, irrespective of their length, which fall within a unit area under consideration. Trend surface analysis (O'Leary et al., 1966) was applied to the fracture trace frequency values generated by the VECLEN program for the 1/16th unit areas discussed above. This technique attempts to fit surfaces which represent polynomial equations of increasing order to map data. Increasing polynomial order represents increasing complexity of the surface, which thus more closely approximates the given data. It can be used in some instances to extract different components responsible for variations which may be present in the data. In most cases, first through sixth order surfaces were fitted to the data. Analysis of variance was applied to the output statistics of this technique to determine which surfaces were a significant improvement over their lower order neighbors (Krumbein and Graybill, 1965); the probability level used was based on $P = 0.005$. Only selected surfaces which achieved the prescribed level of significance and their residual plots will be discussed. Tables 4 and 5 summarize the data for each study area.

Figure 19 illustrates the second order surface for the Kansas data and accounts for 82% of the variations. It shows that fracture trace frequency is highest in the southeastern part of the map area near the Permian outcrops, and decreases northward toward the younger Pleistocene deposits and towards the map peripheries, where coverage is incomplete or control is lacking. This suggests that lithology may be a controlling factor for one of several reasons. 1) The

Table 4

Analysis of Variance of Trend Surfaces Data for Fracture Trace Frequency Kansas Study Area

Surface Order	Sum of Squares	Degrees of Freedom	Mean Square	F	Significance	Cumulative Percent Variation Explained	Percent Variation Improvement for Each Surface
1st	7238.8	2	3619.4	11.2	.005-.001	39.8	39.8
Dev. from 1st	10964.8	34	322.5				
2nd	7711.8	3	2570.6	24.5	<.001	82.1	42.3
Dev. from 2nd	3253.0	31	104.9				
3rd	781.4	4	195.4	2.1	.10-.25	86.4	4.3
Dev. from 3rd	2471.6	27	91.5				
4th	1963.1	5	392.6	17.0	.01-.025	97.2	10.8
Dev. from 4th	508.5	22	23.1				
5th	158.2	6	26.3	1.2	.25-.50	98.1	0.9
Dev. from 5th	350.3	16	21.9				
6th	238.1	7	34.0	2.72	.05-.10	99.4	1.3
Dev. from 6th	112.2	9	12.5				

Table 5

Analysis of Variance of Trend Surface Data for Fracture Trace Frequency Texas Study Area

Surface Order	Sum of Squares	Degrees of Freedom	Mean Square	F	Significance	Cumulative Percent Variation Explained	Percent Variation Improvement for Each Surface
1st	8142.2	2	4071.1	13.0	<.001	37.7	37.7
Dev. from 1st	13446.7	43	312.7				
2nd	6432.7	3	2144.2	12.2	<.001	67.5	29.8
Dev. from 2nd	7014.0	40	175.4				
3rd	1041.4	4	260.4	1.6	.10-.25	72.3	4.8
Dev. from 3rd	5972.6	36	165.9				
4th	3443.6	5	688.7	8.4	<.001	88.3	16.0
Dev. from 4th	2529.0	31	81.58				
5th	896.4	6	149.4	2.3	.05-.10	92.4	4.1
Dev. from 5th	1632.6	25	65.3				
6th	908.8	7	129.8	3.2	.01-.025	96.6	4.2
Dev. from 6th	723.8	18	40.2				

KANSAS STUDY AREA

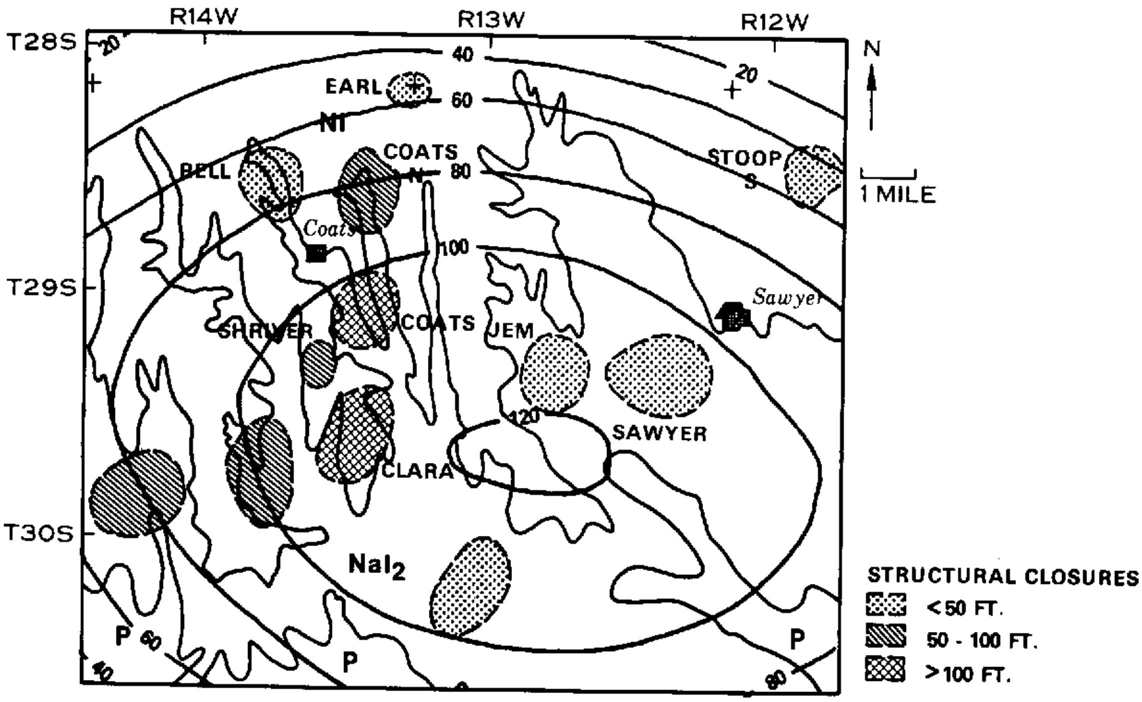

Figure 19. Second Order Trend Surface for Fracture Trace Frequency

unconsolidated Pleistocene sediments may have a masking effect, subduing the number of fractures propogated to the surface; 2) the younger sediments may have been subjected to lower stress levels, fewer periods of deformation and a shorter time for the propogation of the fractures; or 3) different rock types may have different mechanical properties. Because Pleistocene unconsolidated deposits do thicken northward, the first two factors are probably the most significant.

Analysis of the residuals* map (Figure 20) indicates a large positive residual (greater than the calculated model) in the southeast part of the map, underlain by outcropping Permian rocks, and may be explained by several factors. Harris et al. (1960) noted changes in jointing frequency due to contrasting lithologies over the Goose Egg Dome in Wyoming. Not only did they find a progressive decrease in frequency from siliceous limestone, calcareous quartz sandstone, soft sandstones to ductile shales, but also that fracture frequency was inversely proportional to strata thickness. In his study on joints in the Great Scar limestones in England, Doughty (1968) recorded changes between differing limestone types of similar age. Huntington (1969) found changes in fracture trace frequency due to contrasting lithology and suggests that observations be confined to like rock types. DeSitter (1964) recognized lithology and strata thickness, amongst others, as controls of rock fracturing intensity. Another factor which should be considered is the possible masking of the fractures due to the strong contrast in mechanical properties of the consolidated Permian deposits as opposed to the unconsolidated Pleistocene materials, which could act as a filter, either totally obliterating or subduing some fracture traces.

Another positive residual is associated with a series of structural closures in the vicinity of the town of Coats (Figure 20). Although the anomaly overlies two different map units, the mechanical contrast between these two unconsolidated Pleistocene deposits should be minimal. Excluding possible operator bias, the residual might reflect the subsurface Pennsylvanian structures. Residuals along the map peripheries are discounted due to lack of control. Gol'braikh et al. (1968a), Saunders (1969) and Dranovskii (1970) have suggested that the number of airphoto linears per unit area (frequency) is an indicator of structural culmination. Moreover, Dranovskii (1970) further states that in box-like uplifts, maximum fracturing occurs on the fold limbs, while in ridge-like uplifts it develops on the crest of the structure.

The second order surface for the Texas data accounts for 67% of the variation and is illustrated in Figure 21. It shows fewer fracture traces over the

* For any given observed data point on the map: residual = observed - expected value calculated for the coordinates of the observed data points.

KANSAS STUDY AREA

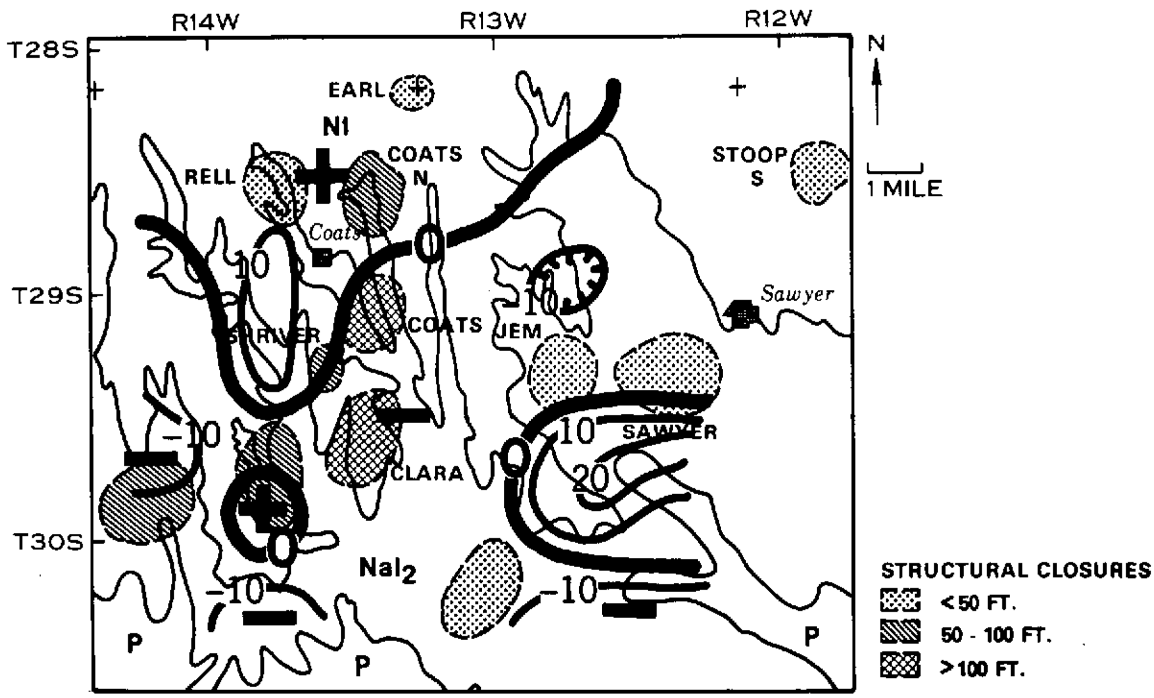

Figure 20. Map of Second Order Trend Surface Residuals for Fracture Trace Frequency

TEXAS STUDY AREA

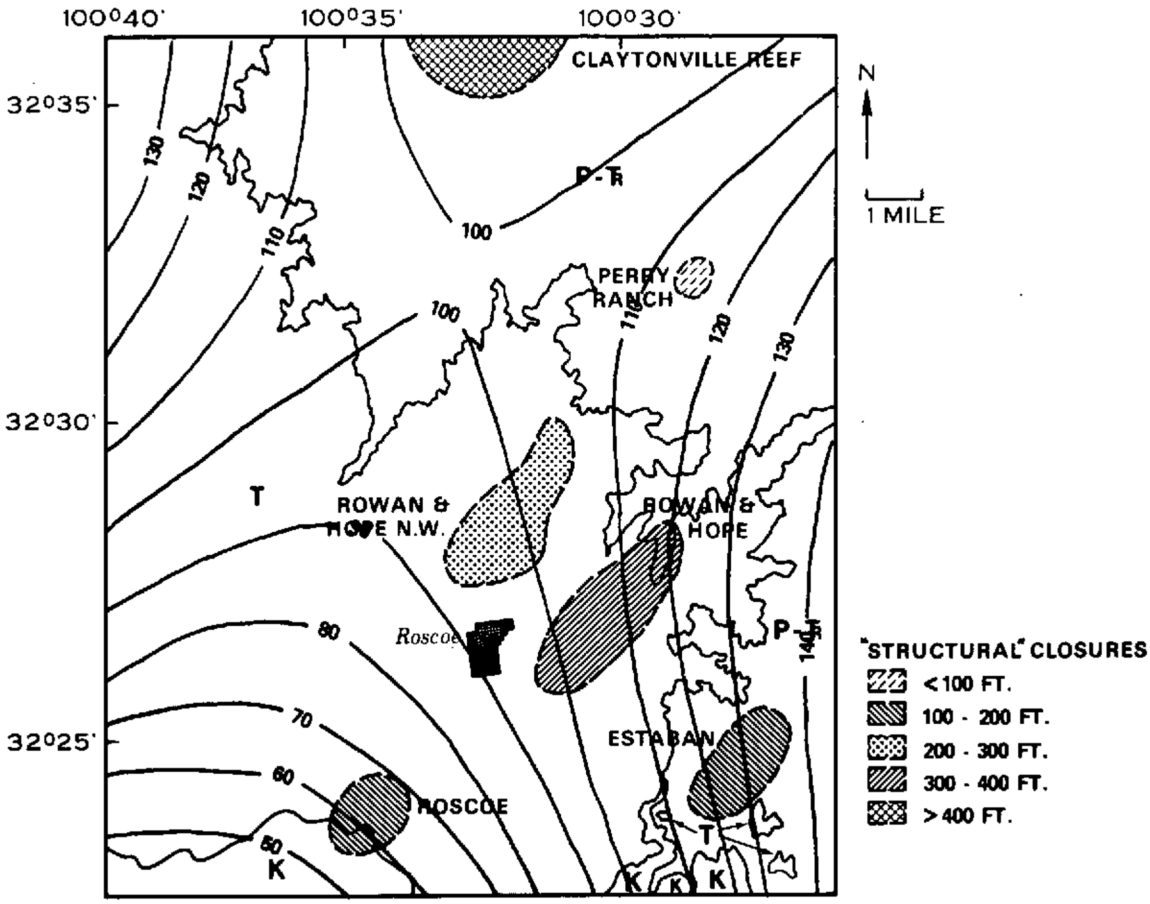

Figure 21. Second Order Trend Surface for Fracture Trace Frequency

Tertiary deposits and the immediately underlying Cretaceous limestones, whereas more fracture traces occur over the Permo-Triassic rocks. In conformity with the previously stated conclusions of Harris et al. (1960) and other workers, the same reasons may explain the lower frequency over the Cretaceous-Tertiary rocks. The Ogallala Formation forms a thin blanket, not exceeding 6 - 8 feet in thickness over the study area. In addition, inspection of several quarries in the Fredricksburg Group limestones revealed a large population of curved joint surfaces which usually terminated at bedding planes. These are non-systematic joints that are not associated with quarrying operations. The paucity of vertical systematic joints suggests that most stresses may have been taken up and diffused in the non-systematic joints, thereby precluding the formation of wide zones of weakness suitable for the development of fracture traces. Because the fourth order residual map more clearly illustrates the results, a discussion of the second order map residual is unnecessary.

Figure 22 shows the results of the fourth order fit and answers 89% of the variation. The model contours tend to parallel the north-south flightlines, which suggests an operator bias due to changes in accuity during mapping, however, higher frequencies again occur over the Permo-Triassic rocks. This inter-flightline variation was the predominating signal in the residual plot of the second order surface. It is therefore suggested that mapping of fracture traces either be done on a suitable scaled mosaic or that individual photographs or pairs should be picked randomly from the total available set so that this type of variation might be distributed more evenly.

Figure 23 contains the residuals map based on the fourth order surface. Although some alignment parallel to the north-south flightlines does occur, most has been removed by this surface. The large positive anomaly in the northern portion of the area is associated with the "saddle" in the trend surface (Figure 16) and is anomalous. The strong negative anomalies in the eastern portion of the map area appear to be associated with the flanks of three of the reef structures. This observation is further enhanced by the fact that they occur along several flightlines, thereby indicating a consistency between flightlines after removal of the inter-flightline variation.

In summary, the predominating portion of the variation in frequency of fracture traces is associated with differences in lithology. Lesser amounts of the variation are due to operator variability due to changes in perceptibility during fracture trace mapping. Another variation which may occur is associated with "structural closures." Basement uplift structures are accentuated by positive (high) fracture trace frequencies along their flanks, whereas "passive" structures such as reefs, may be associated with negative (low) fracture trace frequencies in these study areas.

TEXAS STUDY AREA

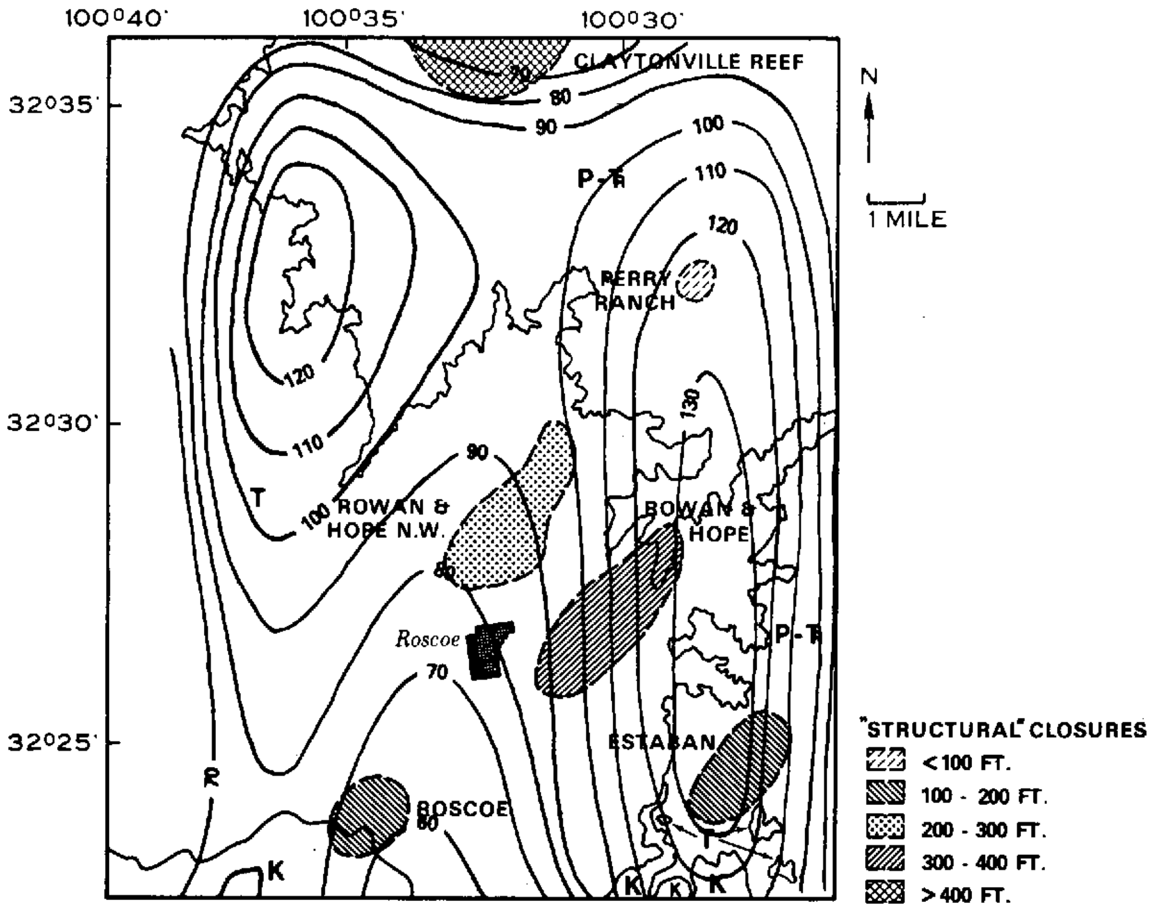

Figure 22. Fourth Order Trend Surface for Fracture Trace Frequency

TEXAS STUDY AREA

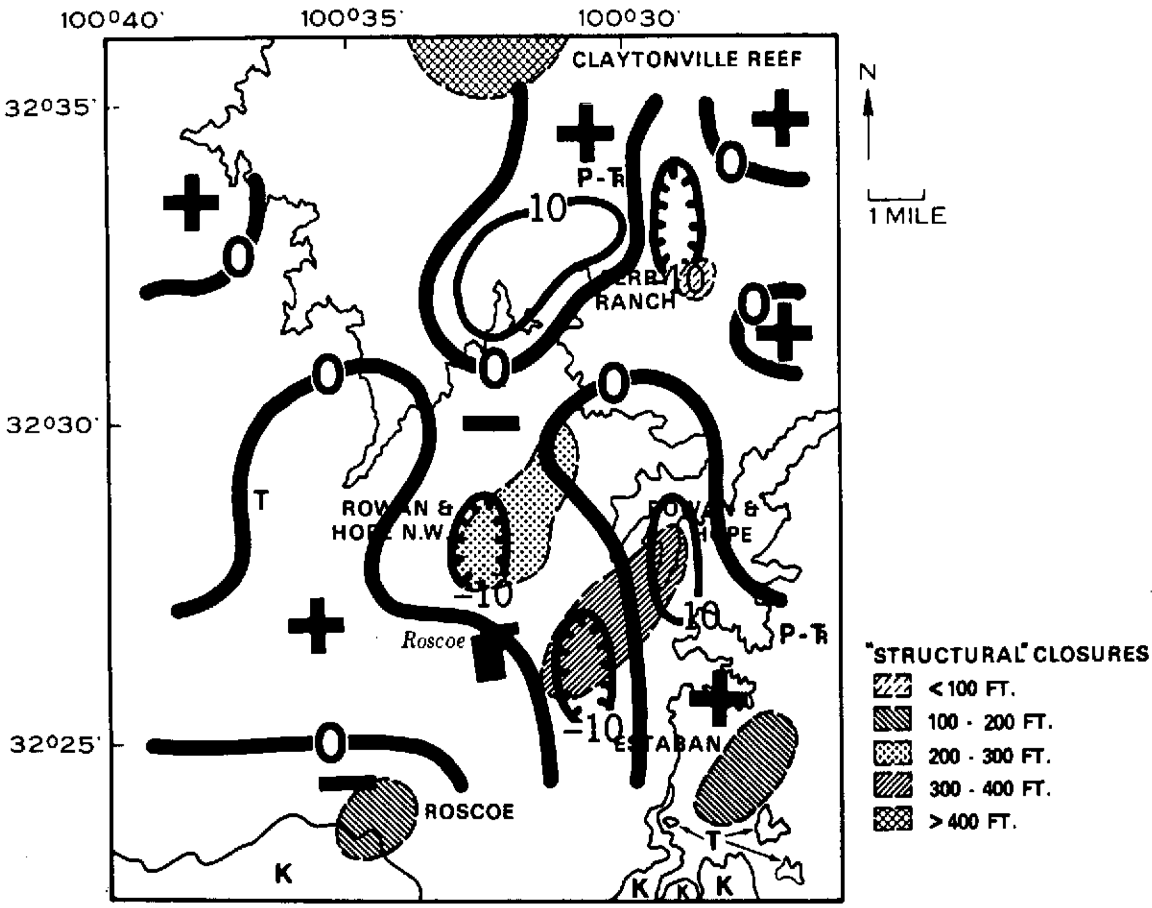

Figure 23. Map of Fourth Order Trend Surface Residuals for Fracture Trace Frequency

ANALYSIS OF LOG-MEAN FRACTURE TRACE LENGTHS

Log-mean fracture trace lengths generated for the 1/16th unit areas by the computer program VECLEN were also analyzed using trend surface analysis. Significance of improvement in the information level of each surface was tested as described earlier. Tables 6 and 7 summarize the results. Only the highest order surface showing the prescribed level of significance (less than 0.005) will be discussed.

Figure 24 illustrates the fifth order surface for the Kansas study area and accounts for 80% of the variation. The model shows longer fracture traces in the northern part of the study area, becoming progressively shorter towards the Permian outcrop area. This may be interpreted as a masking effect of the glacial overburden, causing the operator to overlook shorter fracture traces due to their less pronounced nature or their complete obliteration by the overburden. The model also shows a parallelism between some of the contours and geologic formation boundaries, as exemplified by the 4.1 contour, which further reinforces the lithologic control hypothesis. The parallelism of contours and their steep gradient in the western part of the area is due to lack of control in this area.

The corresponding residuals map (Figure 25) indicates a broad positive residual trending northwest in the central part of the area, and parallels the boundaries between the two mapped Pleistocene units. The positive bands in the northeast and southwest sectors also may be associated with the formational boundaries. A negative residual is present in the west-central portion of the map and coincides with the increased fracture trace frequency derived from the second order residual (Figure 20). These two factors may be inter-related; increased deformation may cause more intense fracturing (higher frequency) and because of surficial processes, greater erosion generates more linear first and second order streams, which manifest themselves as fracture traces.

The fifth order surface for the west Texas study area (Figure 26) indicates longer fracture traces over the Cretaceous-Tertiary deposits, with shorter fracture traces occurring in the Permo-Triassic rocks. The observed differences may be due to masking effects as discussed earlier for the Kansas area, however, Trainer and Ellison (1967) found that longer fractures traces occurred in the limestone units of the Shennandoah Valley. They suggested that this might be due to solution and coalescence of joint planes and zones of weakness, a process which has operated in this area as evidenced by the development of karst features.

Figure 27 illustrates the residuals map associated with the fifth order surface. No consistent pattern is found with respect to the reef structures. The dominant features include a negative residual trending northwest in the central part of

Table 6

Analysis of Variance of Trend Surface Data for Fracture Trace Log-Mean Length Kansas Study Area

Surface Order	Sum of Squares	Degrees of Freedom	Mean Squares	F	Significance	Cumulative Percent Variation Explained	Percent Variation Explained By Each Surface
1st	.0514	2	.0257	7.79	<.001	21.5	21.5
Dev. from 1st	.1872	56	.0033				
2nd	.0696	3	.0232	10.55	<.001	50.6	29.1
Dev. from 2nd	.1176	53	.0022				
3rd	.0167	4	.0042	2.00	.10-.25	57.7	7.1
Dev. from 3rd	.1009	49	.0021				
4th	.0230	5	.0046	3.56	.025-.05	67.4	9.7
Dev. from 4th	.0779	44	.0018				
5th	.0309	6	.0052	4.33	.005-.001	80.3	12.9
Dev. from 5th	.0470	38	.0012				
6th	.0204	7	.0029	3.22	.01-.025	88.9	8.6
Dev. from 6th	.0266	31	.0009				

Table 7

Analysis of Variance of Trend Surface Data for Fracture Trace Log-Mean Length Texas Study Area

Surface Order	Sum of Squares	Degrees of Freedom	Mean Squares	F	Significance	Cumulative Percent Variation Explained	Percent Variation Explained By Each Surface
1st	1.58	2	.790	29.26	<.001	48.8	48.8
Dev. from 1st	1.66	61	.027				
2nd	.71	3	.037	14.81	<.001	70.7	22.1
Dev. from 2nd	.95	58	.016				
3rd	.28	4	.070	5.83	<.001	79.2	8.3
Dev. from 3rd	.67	54	.012				
4th	.30	5	.060	7.50	<.001	88.6	9.4
Dev. from 4th	.37	49	.008				
5th	.14	6	.023	4.60	<.001	92.9	4.3
Dev. from 5th	.23	43	.005				
6th			NOT ANALYZED				
Dev. from 6th							

KANSAS STUDY AREA

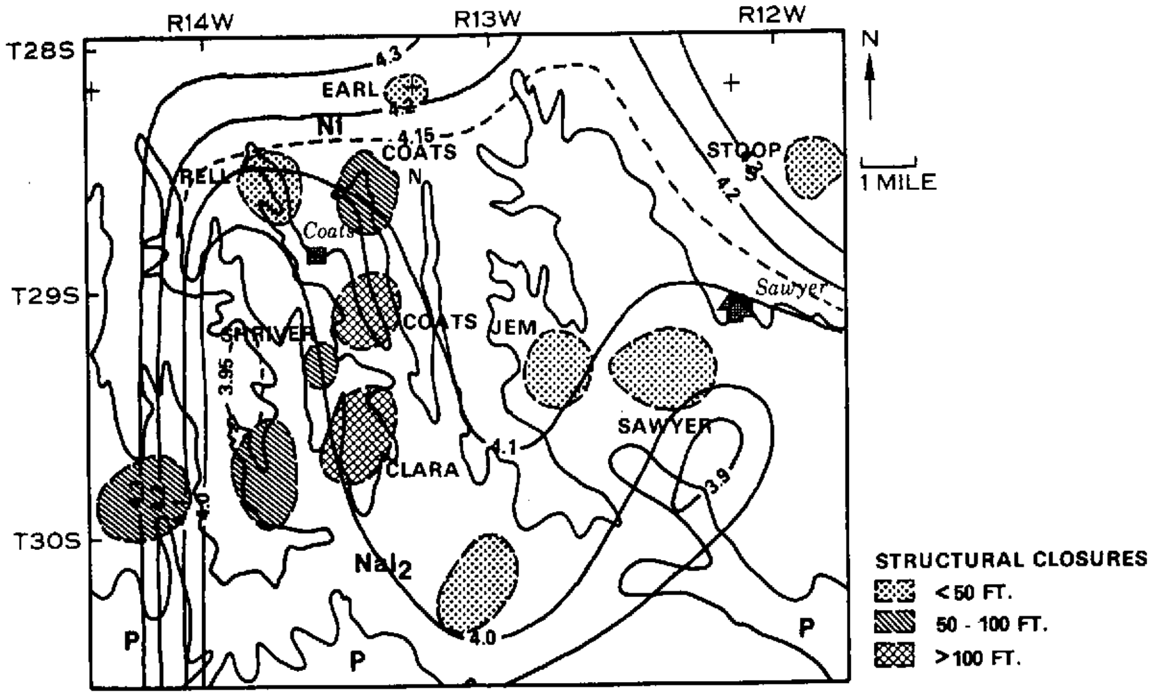

Figure 24. Fifth Order Trend Surface for Log-Mean Fracture Trace Length

KANSAS STUDY AREA

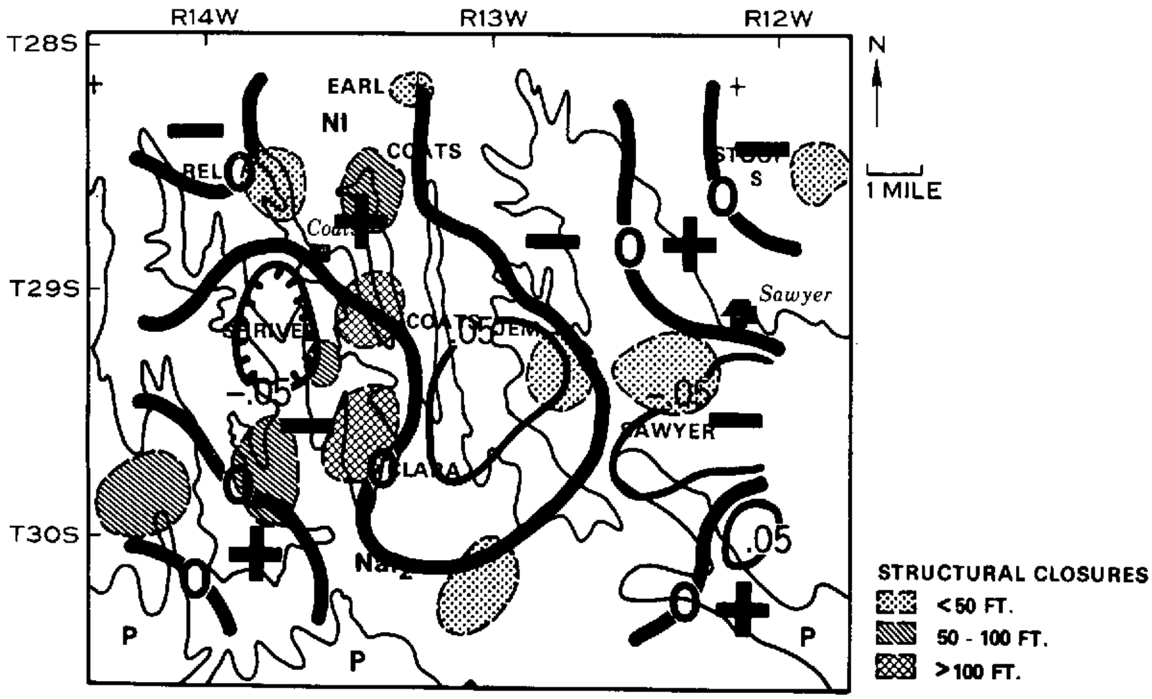

Figure 25. Map of Fifth Order Trend Surface Residuals for Log-Mean Fracture Trace Length

TEXAS STUDY AREA

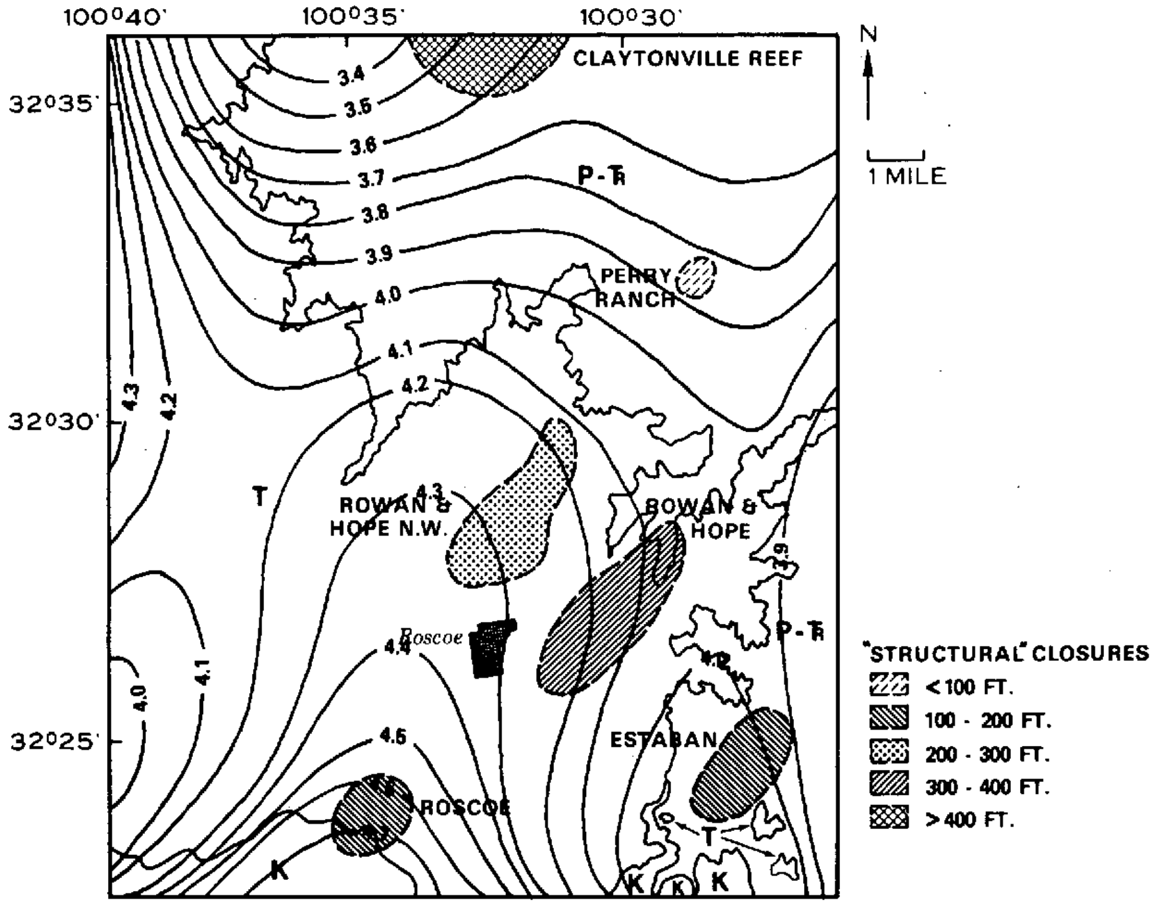

Figure 26. Fifth Order Trend Surface for Log-Mean Fracture Trace Length

TEXAS STUDY AREA

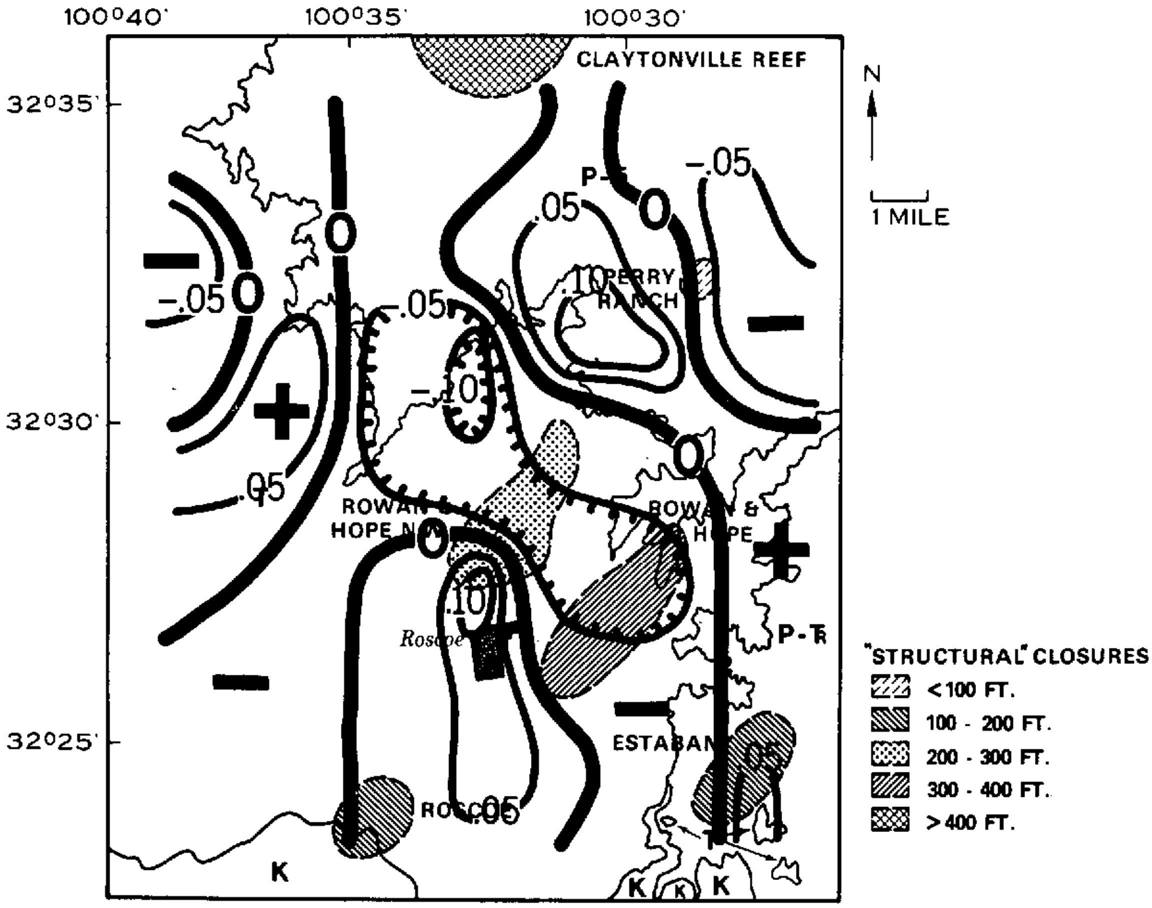

Figure 27. Map of Fifth Order Trend Surface Residuals for Log-Mean Fracture Trace Length

the map area. Its extension across several flightlines tends to bear out the reality of this feature. Examination of an aerial photographic mosaic reveals a lineament passing through the area in this direction which is most likely related to this anomaly. The same argument previously discussed concerning increased structural deformation, which produces a greater number of shorter fractures, may be invoked. Again, some variation is noted between flightlines and some of the positive anomalies in the south.

In summary, log-mean fracture trace lengths are predominantly controlled by the type of sedimentary material. Variations between flightlines may occur, but their effect is not as pronounced as in fracture trace frequency. Fracture traces may be shorter over basement uplift structures. This effect may not occur over passive structures, such as those formed by a draping of sediments over bedrock highs.

ANALYSIS OF ROSE DIAGRAMS

Several formats are available for displaying directional data. Three dimensional data, such as attitude of joint planes, can be efficiently portrayed on stereographic (Wulff) or equal area (Schmidt) nets. Statistical analysis of these data are cumbersome, but has been discussed by several works (Chayes, 1949; Fisher, 1953; Pincus, 1953). Two dimensional data, such as the strike of fracture traces, may be displayed as histograms or as rose diagrams (Podwysocki, 1974). Both these formats can be conveniently tested and may be generated by computers and will be used in this paper because of their suitability for visual comparison.

Several methods can be utilized to summarize the data for rose diagrams. Trainer and Ellison (1967) use the terms "frequency" and "density." Frequency as described earlier, refers to the number of fracture traces, irrespective of their length, while density refers to the total length of fracture traces. Each of these respective techniques has its disadvantages. Summarization using frequency eliminates a bias due to length. Thus, a fracture trace of 0.25 mile (0.4 km) is given as much weight as one 0.75 mile (1.2 km) long. However, due to the mapping technique employed in this paper, which breaks up fracture traces into components based on their continuous exposure, the shorter fracture traces are favored. Thus, density was chosen as the analysis criterion in this work in order to minimize this bias. In addition, the need for a standard unit to facilitate comparison has been noted elsewhere. Gol'braikh et al. (1968) suggest conversion of the units into percent values prior to plotting, so that the size of all roses will be standardized.

Joints were measured in several bedrock exposures in the west Texas study area. Their orientation frequencies were compared to the density of rose diagrams of fracture traces measured in grid cells approximately three miles square surrounding each of these localities. Data in 10 degree azimuth classes were analyzed using AZMAP and ROSE, computer programs written by Podwysocki (1974). In order to compare statistically the two dissimilar units of measurement, both sets of data were converted to percentages. A total of 69 systematic joints were measured in Cretaceous limestones of the Fredricksburg Group, exposed in a quarry near the central-western edge of the map area. Nearly all systematic joints were vertical, eliminating the need to use three-dimensional displays and making the measurements suitable for comparison with the fracture trace distribution. As discussed earlier, there also were many non-systematic joints. Permian exposures in the extreme central-eastern part were measured and consisted of a roadcut in a gypsiferous sandstone and a railroad cut in a massive sandstone. A total of 59 joints were measured and combined from these two adjacent cuts. All joints in these cuts were within 5 degrees of vertical. Figure 28 contains a graphical comparison of the two sets of patterns.

Neither set of rose diagrams show a good visual fit; a Chi Square test comparing the fracture trace and joint orientations for each locality indicates that the patterns were not similar based on a 0. 01 level of rejection. Neither could it be influenced that much by population size, because Gol'braikh et al. (1968a) indicated that 40 - 50 joint measurements were required to achieve statistical reliability. It should be noted that while there is conformity in direction in the Permian rocks there is a consistent angular displacement between the two patterns in the Cretaceous rocks. The former set may reflect fracture traces that are occupied by zones of joints sub-parallel to the direction of the fracture trace (Lattman, 1969, pers. comm.); the latter may represent a displacement of the second order joints from the direction of maximum shear stress. This phenomenon has been documented by Renner (1969) and may relate to a hierarchichal structural framework as postulated by Moody and Hill (1956) and discussed by Nemec (1970) and Gold et al. (1973). Because of the dissimilarity in the Cretaceous patterns and partial agreement in the Permian patterns, it might also be suggested that either the rocks have behaved differently when subjected to the same stresses or that the older units were subjected to an additional period of stress not experienced by the younger units.

These results are partly contrary to those of Lattman and Nickelsen (1958), Hough (1959), Boyer and McQueen (1964) and Alpay (1973), who generally found good agreement between fracture trace and joint directions in their investigations in sedimentary rocks dipping less than 5 degrees. Matzke (1961), Lattman and Matzke (1961, 1971) and Trainer and Ellison (1967), however, reported that fracture traces and joint directions do not totally

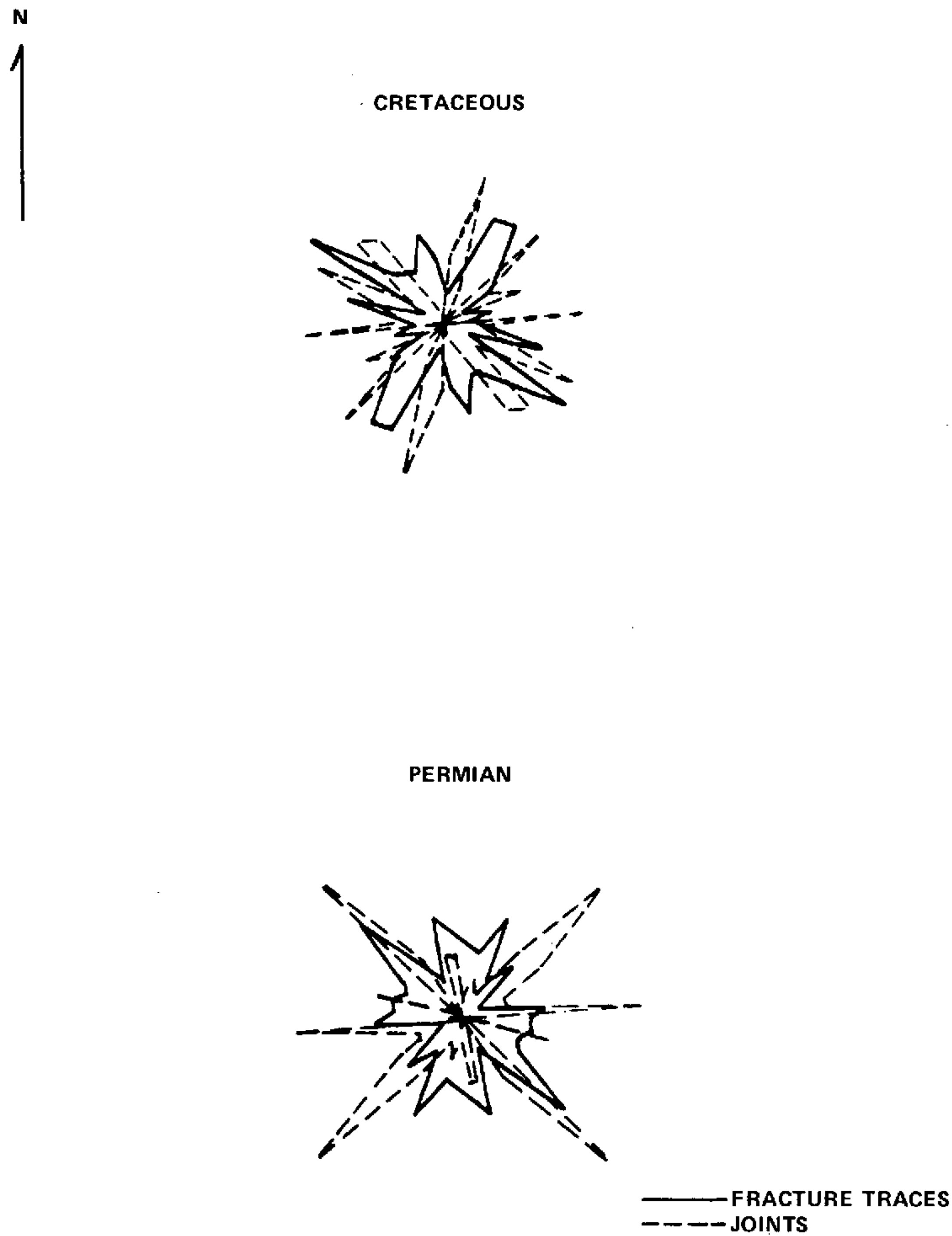

Figure 28. Comparison of Joint and Fracture Trace Rose Diagrams, Texas Study Area

coincide. Their observations were made in more deformed rocks (i. e. the Appalachian fold belt). Lattman and Matzke (1961) suggest that joint patterns in relatively stable cratonic areas are paralleled by fracture traces whereas, local structure in highly deformed materials impress their own local joint sets which may deviate from the regional trends.

Although orientation directions coincide for the Permian rocks, the length of the rays (degree of preferred orientation) is greater for the joints. This is probably due to the big difference in the size scale of the areas sampled (9 square miles (23 sq. km) versus 2 outcrops 1/2 mile apart).

ANALYSIS OF FRACTURE TRACE PATTERNS

Pattern recognition of preferred orientation in fracture analysis tends to be more difficult due to the large amount of data and its multivariate nature. Several approaches have been used to enhance patterns. Haman (1961, 1964) isolated and plotted all macrofractures (lineaments) and mesofractures (fracture traces) which fell within narrow azimuth ranges and used them in a qualitative fashion to discern faulting and to locate changes in regime of individual tectonic blocks. Maffi and Marchesini (1964) describe the use of optical and computer processing techniques to filter and isolate individual trends. Gol'braikh et al. (1968a) also isolated regional structures by plotting their megajoint densities for narrow azimuth ranges, and showed the applicability of Permyakov's (1949) "rule of the parallelogram" to determine regional trends by analysis of the rose diagram modes. Little has been published on a method for the comparison of several rose diagrams. Chudinskii (Mirkin, 1973, pers. comm.) suggests that rose diagrams of small subsets of the total area should be compared against the grand rose diagram for the whole territory. A variation of the Chi Square criterion could then be used to compare the subset against the composite rose diagram. Those which proved to vary significantly from the composite diagram were zones of "tectonic complications." Lattman (1969, pers. comm.) suggested a similar technique, but instead of comparing a subset against the composite rose diagram, the subset was compared against all of its adjacent neighbors. Significant variations between neighboring diagrams would then indicate structural complexities.

The fracture trace data compiled by the TRANSFORM program was processed by AZMAP (Podwysocki, 1974), which classified the fracture traces into direction categories within each unit cell (1/16th of the total study area). As described previously in the analysis of fracture trace frequency and lengths, a 1/2 cell sliding average increment also was used. An azimuth class interval of 10 degrees was utilized during the classification.

Several classification techniques could be used in AZMAP. The first, entitled "Part" analyzed only that portion of the fracture trace length which lies within the cell. "Mid" considered the whole fracture trace within the cell if its midpoint fell within the cell. A comparison of the two techniques showed that there was no significant difference if the results of the two classification techniques were compared against each other for each of the 49* grid cells of each area, using the Chi Square test and a rejection level of 0.05.

Punched card output of the summary length of fracture traces per azimuth class per grid cell were processed by a computer program ROSE (Podwysocki, 1974), which produced rose diagrams (see Figures 29 and 30). The punched card output from AZMAP also was utilized in a multivariate analysis computer program CLUS (Rubin and Friedman, 1967). Each rose diagram consisted of 18 variables or measurements (the sum total length of fracture traces within each of the 10 degree azimuth classes). A total of 49 grid cells (objects) were generated by AZMAP for each study area and these were treated as 49 samples.

Multivariate techniques have been shown by Dahlberg and Griffiths (1967) to be an effective method for determining the relationships between objects with interacting properties. The Rubin and Friedman program is appropriate for determining the relationships between samples because the procedures allow classification on the basis of a number of groups determined by the user. A determination of the optimum grouping is made on the basis of several computer generated criteria for each classification.

The inverse of the Wilk's lambda criterion, log $(\max |T| / |W|)$, is used as an informal indicator of the best number of groups (Friedman and Rubin, 1967), where:

- W is the pooled within-group matrix of the cross products of deviations,
- T is the matrix of cross products of deviations for the total sample,
- B is the matrix of between-group cross products of deviations of groups from the grand means weighted by group size (Cooley and Lohnes, 1962),

and

$$T = B + W.$$

*A total of 15 cells occupying the easternmost and southernmost areas was eliminated due to the low fracture trace frequency caused by incomplete photo coverage.

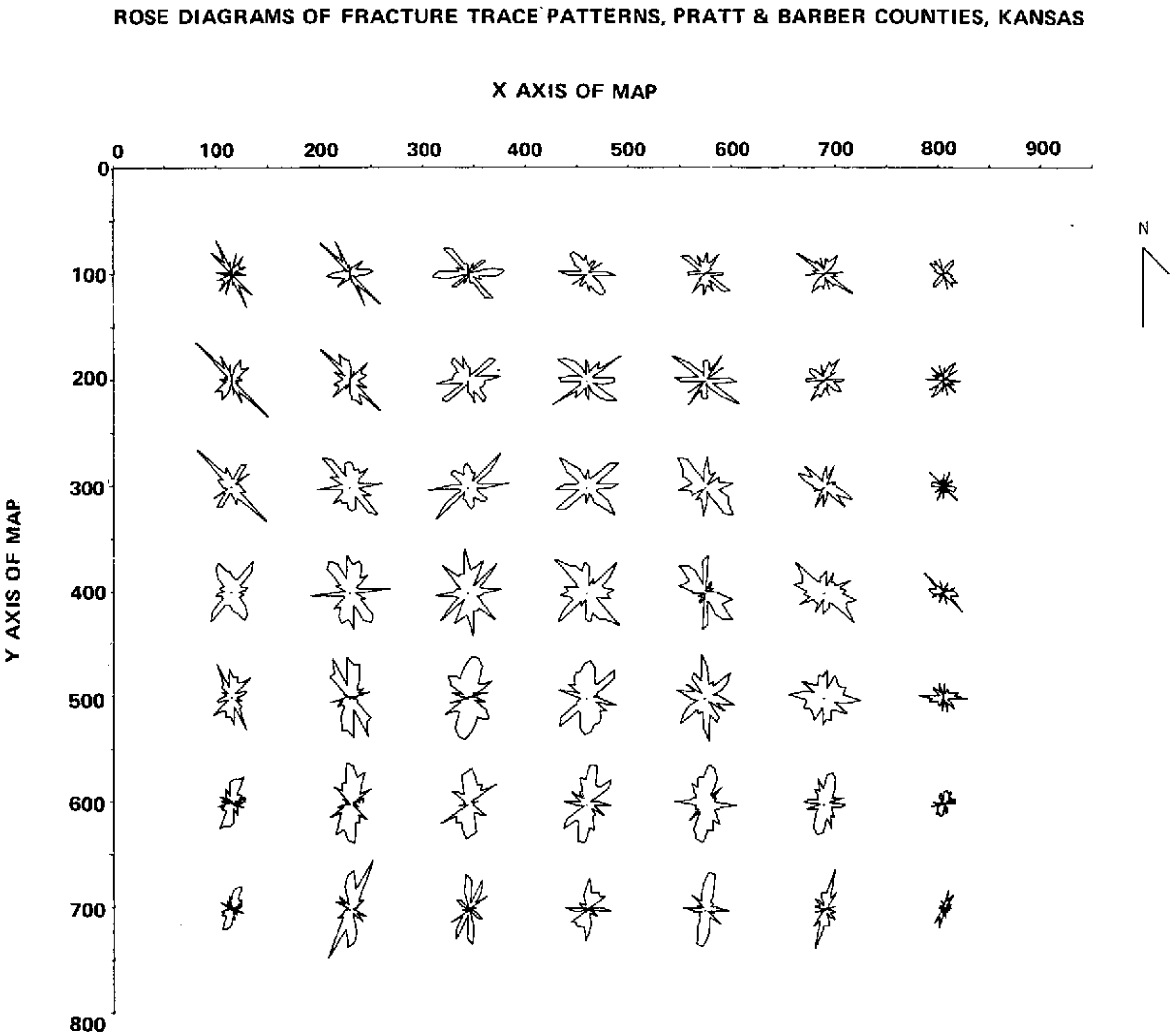

Figure 29. Rose Diagram Plot of Fracture Trace Patterns for the Kansas Study Area

ROSE DIAGRAMS OF FRACTURE TRACE PATTERNS, NOLAN & FISHER COUNTIES, TEXAS.

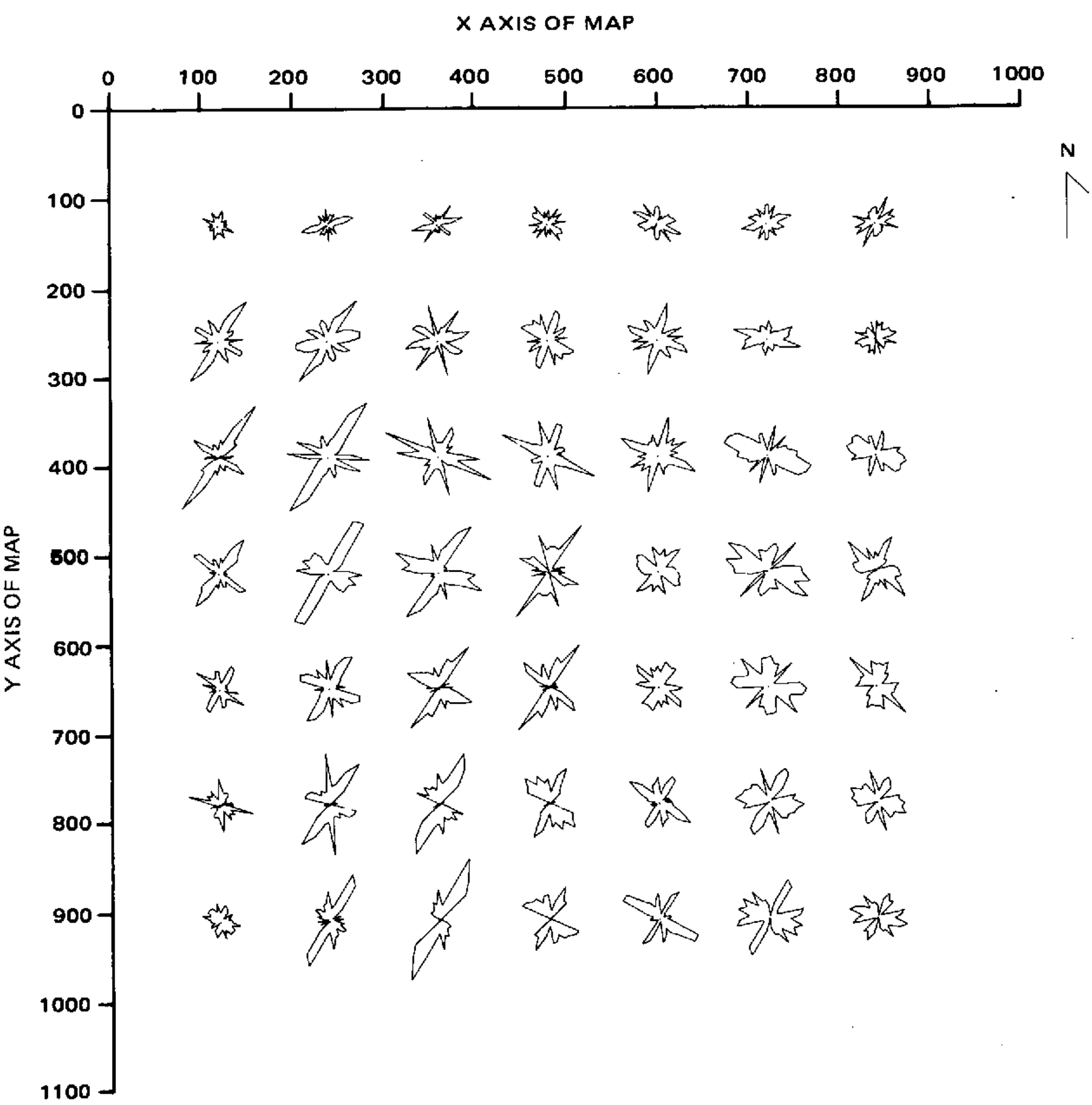

Figure 30. Rose Diagram Plot of Fracture Trace Patterns for the Texas Study Area

The best partition may also be determined by use of the total generalized distance, the Mahalanobis D^2 criterion, where D^2 is defined as the sum of the distances between multivariate means of all possible pairs of groups, in terms of standardized measurements.

Using principle components, a plot of the eigenvalues of the total correlation matrix indicates a gradual decrease in the amount of variation explained by each additional component (Figure 31). It was arbitrarily decided to choose the 8 component level as the cutoff. A total of 85% of the variation is explained by the 8 components in the Kansas data and 82% is explained in the west Texas data.

The two sets of data were processed by the program CLUS, using 2 through 11 groups. Figure 32 illustrates the plot of the two criteria using the log (max $|T| / |W|$)* algorithm for the Kansas data using 8 components. An inflection at the three group level in both criteria is interpreted as significant. The six group level also indicates a major inflection of the D^2* criterion. An additional run on the data using six components produced exactly the same classification for the 6 group level, but showed a more marked increase in the value of both criteria. Figure 33 illustrates the three group classification, which in a crude fashion, tends to outline the geology. Group 2 mainly occupies the northern part of the area of exposed Illinoian deposits, group three occupies the area underlain by the Kansan and Permian deposits and group 1 covers areas occupied by a mixture of groups 2 and 3. The six group level (Figure 34) contains some isolated members of groups 3 and 5 within the central part of the map. These overlie the Coats Anticline, which has a structural closure of approximately 250 feet (76 m) and may thus have affected the overlying fracture pattern. Examination of the rose diagram patterns in Figure 29 reveals a pronounced enhancement of the northeast ray directly over the structure (row 3, column 3), which may be associated with the northeast trending fault in the basement rocks underlying this structure (Cole, 1962).

Figure 35 illustrates the plot of the two indicator criteria for the west Texas data. No pronounced peaks were noted, although a change in slope for both criteria occurs at the two and seven group level. The two group classification (Figure 36) seems to be related to geologic materials exposed on the surface. Group 1 tends to overlie areas of Permo-Triassic rocks whereas group 2 occupies areas of Cretaceous-Tertiary deposits. The 7 group level (Figure 37) shows no obvious relation to any of the reef structures. The classification is again partly related to lithology; groups 1, 2, and 3 overlie Cretaceous-Tertiary deposits, whereas groups 4, 5, and 7 overlie the transition between the two

*Based on the grouping of log (max $|T|/|W|$).

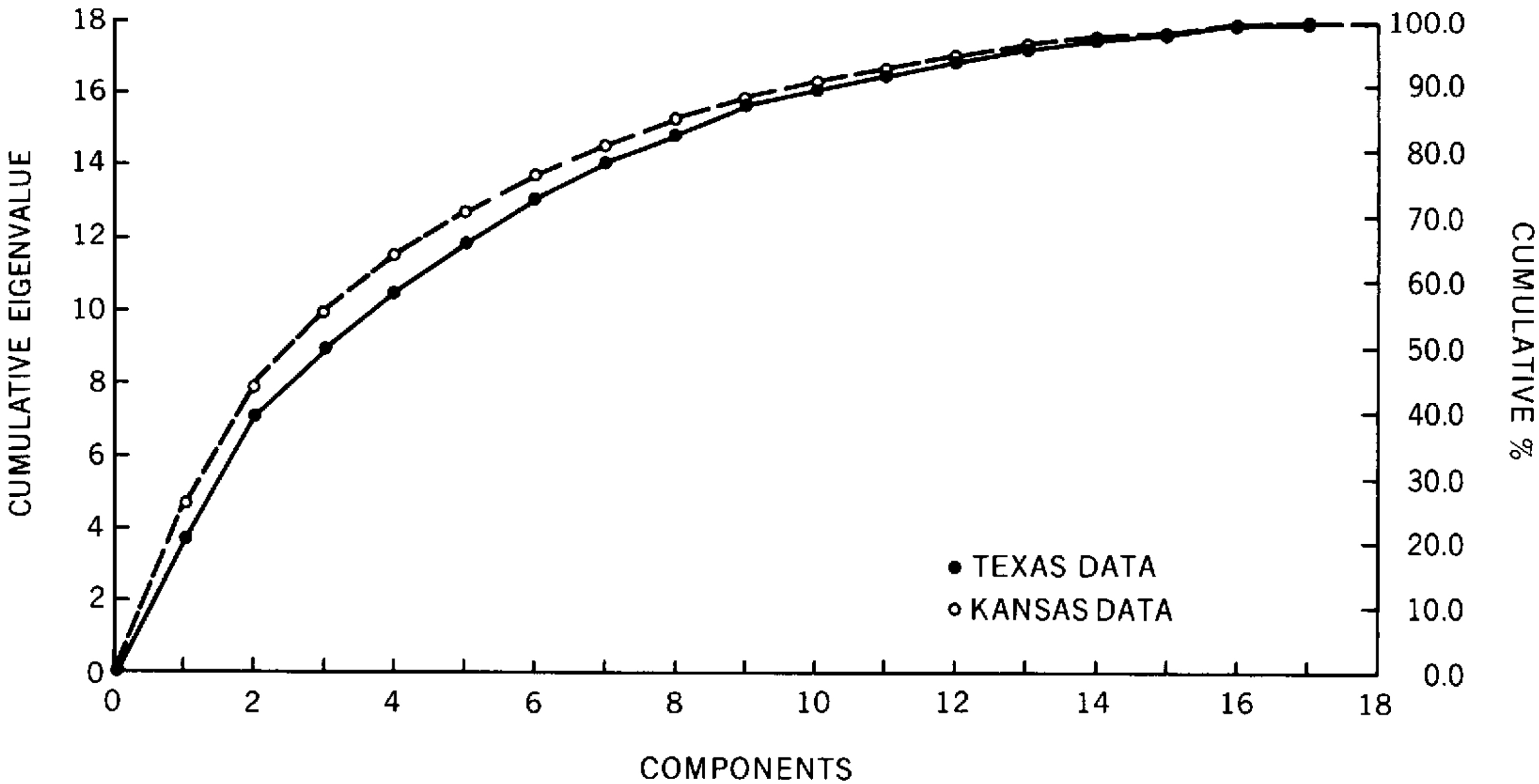

Figure 31. Plot of Eigenvalues versus Principal Components for Both Study Areas

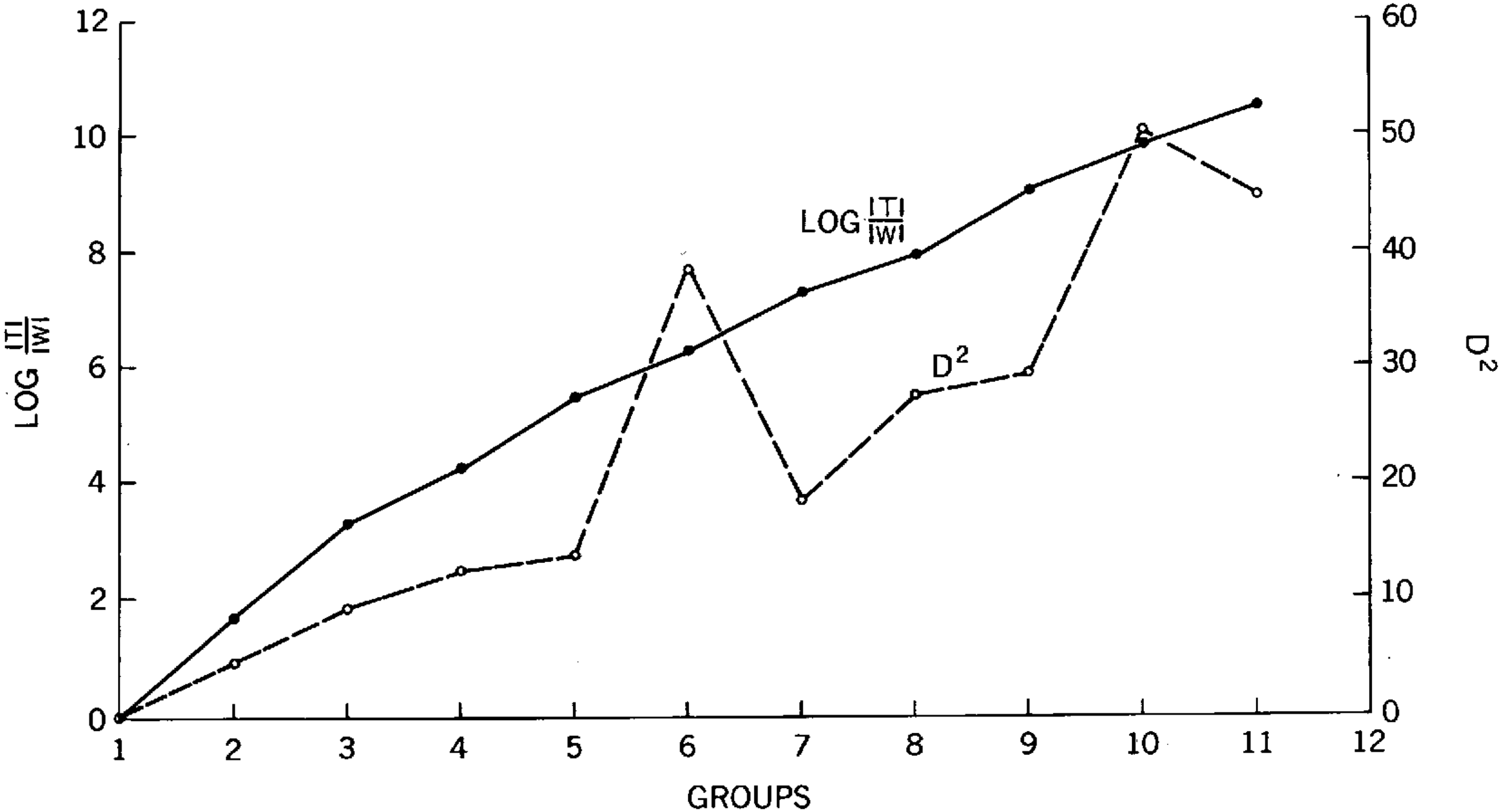

Figure 32. Plot of CLUS Classification Criteria for the Kansas Data Using 8 Components, Log (|T| / |W|) Maximized

KANSAS STUDY AREA

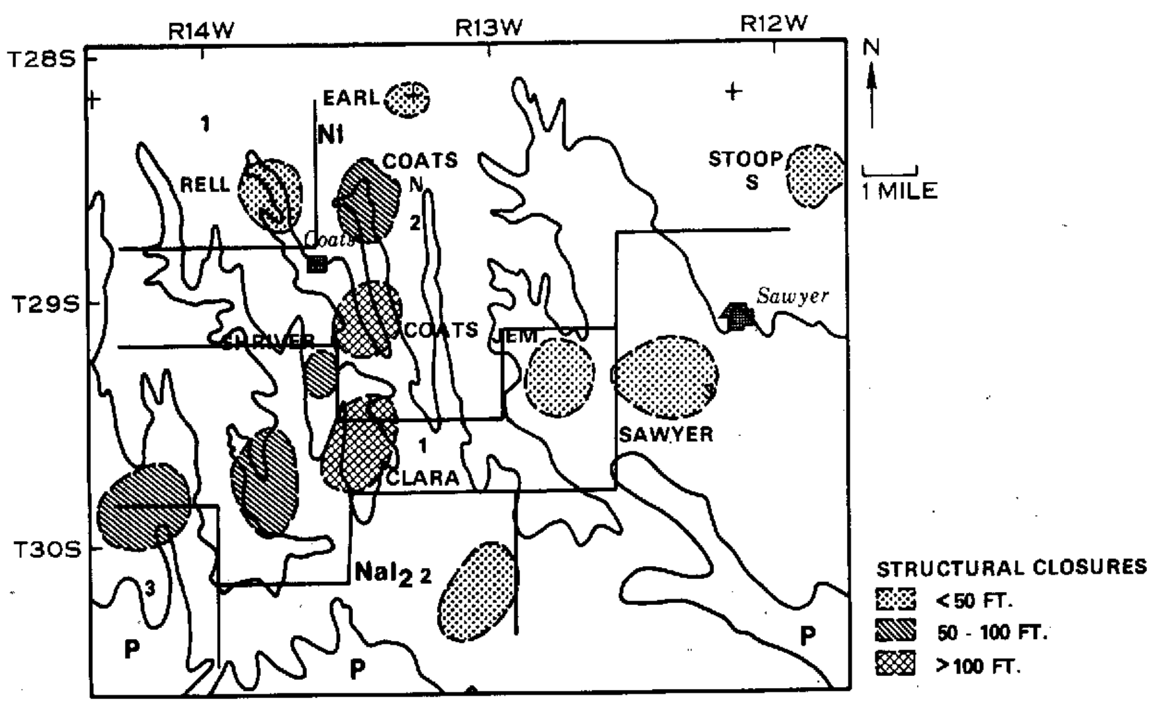

Figure 33. Results of the 3 Group Classification of Rose Diagrams

KANSAS STUDY AREA

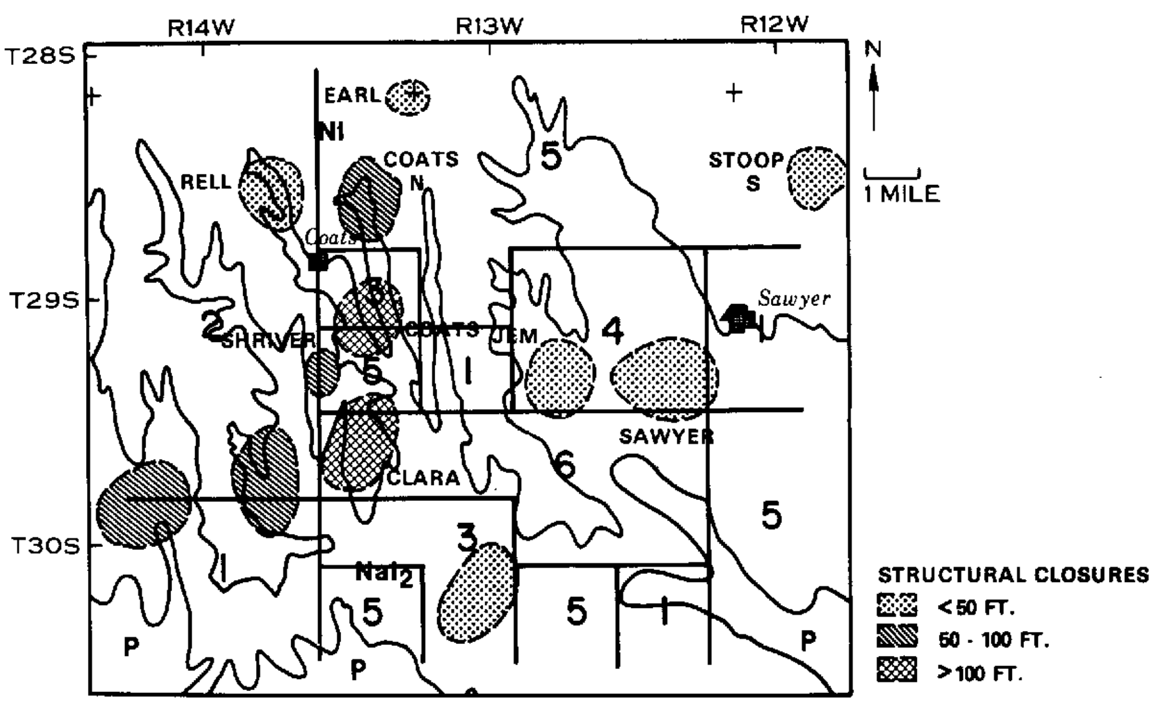

Figure 34. Results of the 6 Group Classification of Rose Diagrams

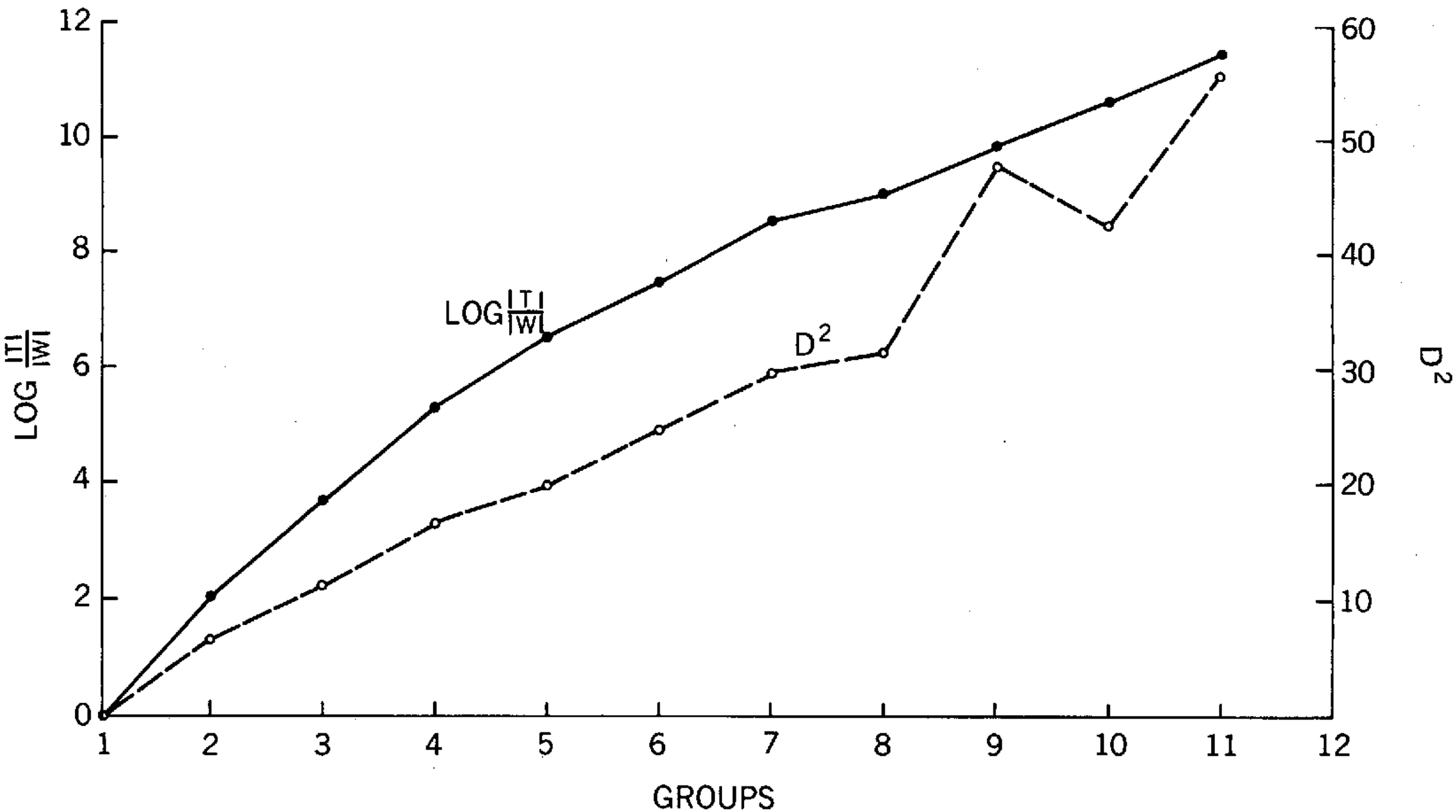

Figure 35. Plot of CLUS Classification Criteria for the Texas Data Using 8 Components, Log (|T| /|W|) Maximized

TEXAS STUDY AREA

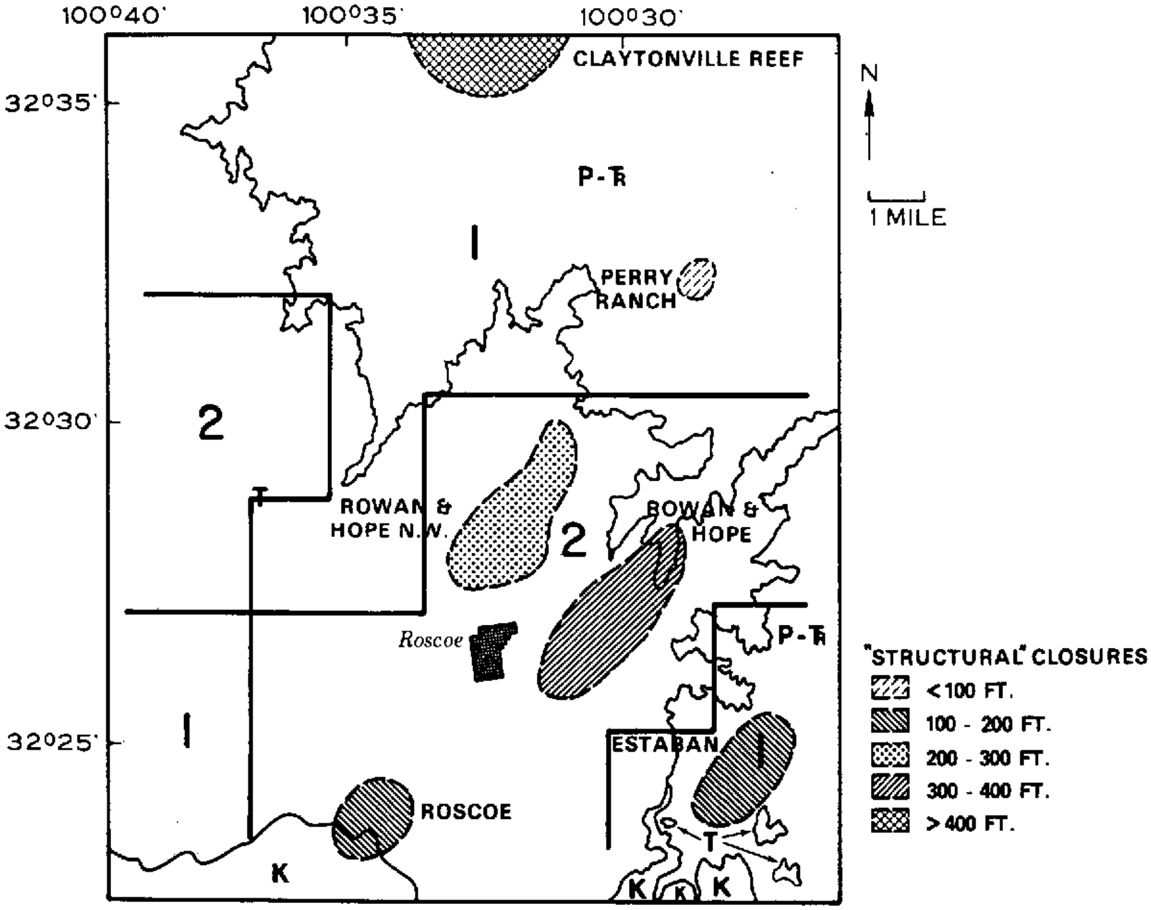

Figure 36. Results of the 2 Group Classification of Rose Diagrams

TEXAS STUDY AREA

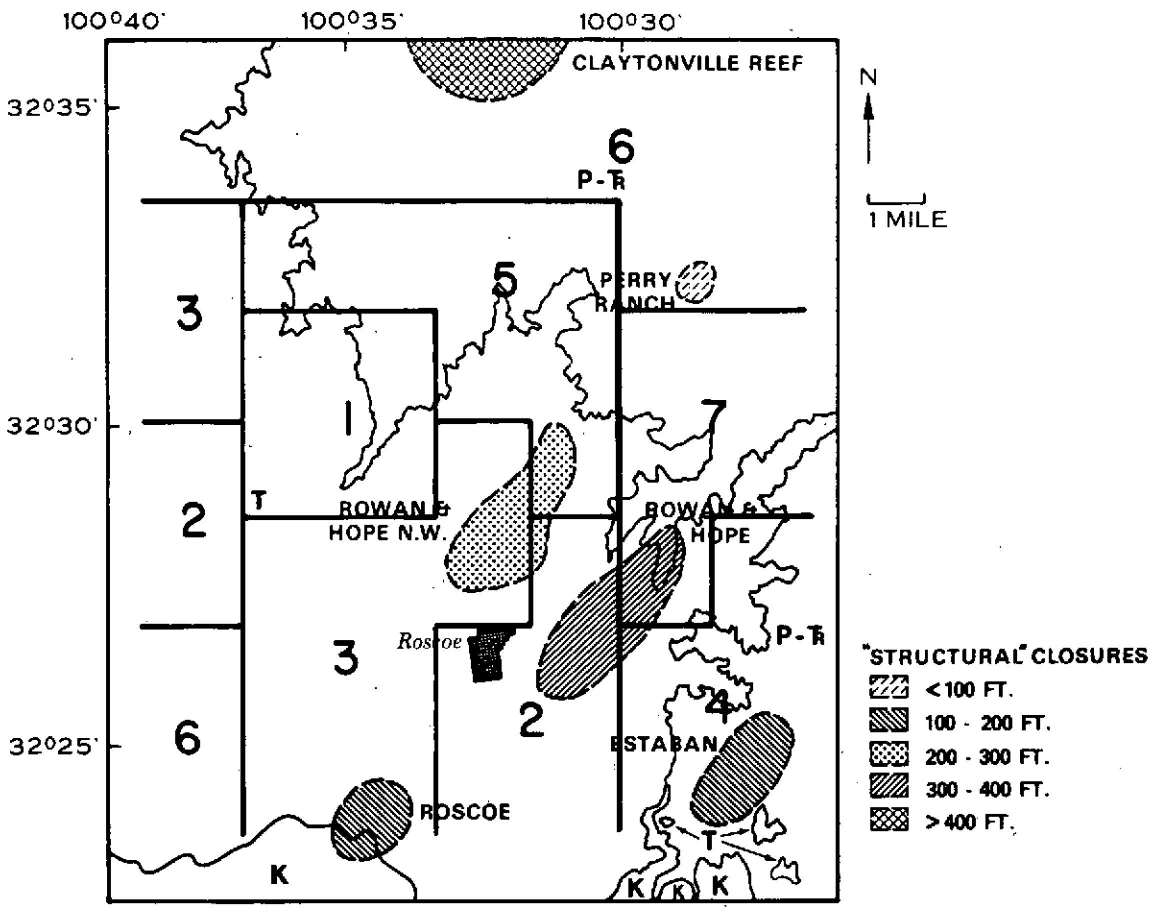

Figure 37. Results of the 7 Group Classification of Rose Diagrams

major map units. Group 6 occupies mainly Permo-Triassic rocks. The misclassification of the cells in the southwestern part is probably due to the small sample size in this area due to incomplete coverage, producing rose diagrams without any preferred rays.

In summary, classification of the rose diagrams using a multivariate classification scheme produces groupings which are predominantly controlled by surface lithologic factors if classification is limited to a small number of groups. Active structures (i.e. basement uplift anticlines) may be recognizable because their fracture patterns may differ from their immediate neighbors and may be isolated by classifications at higher group levels. Passive (reef) "structures" do not create fracture patterns which can readily be isolated from their surrounding neighbors by this technique.

CONCLUSIONS

Detailed quantitative analysis of fracture trace patterns can be routinely performed using repetitive techniques and computer algorithms. Cultural features can affect the ability to map fracture traces. Fracture trace lengths tend to be log-normally distributed. Deviations from log-normality tend to be associated with structural closures in both study areas, suggesting that fracture pattern may be disturbed over the structures.

Trend surface analysis may allow extraction of several levels of information that may be present in a set of data. Examination of fracture traces by trend surface analysis indicates that lithology mainly controlled the frequency and log-mean fracture trace length. Frequency was also affected by an operator bias, which caused alignment of some of the model contours with flightline paths in at least one of the study areas. Higher order surfaces extracted the majority of these variations. Residuals in the frequency analysis isolated areas of increased fracture frequency in the Kansas area that appeared to be associated with either bedrock exposures or with structural culminations. In the west Texas area, strong negative residuals appear to be related to reef structures. The increase in frequency in the active structure (anticline) and the scarcity in the passive structure (reef) suggests either different mechanisms for propagation of fractures through these two types of structural discontinuities or different stress fields produced above the structures. Analysis of residuals for log-mean fracture trace length indicates that in at least one instance, fracture traces may be shorter over active structures in the Kansas study area. The west Texas residuals map shows some alignment parallel to flightline paths; however, a strong negative anomaly (shorter lengths) may be associated with a through-going lineament in the area. Both areas show a shortening of fracture traces in areas underlain by tectonic structures (anticlines, lineaments), possibly due to increased fracturing and subsequent erosion of the fractures.

Fracture traces and joints measured in an area underlain by Permian rocks (sandstones) coincide in orientation, but there may be large differences in the length of the frequency rays. In an area of Cretaceous rocks (limestone), the apparent displacement in orientation between joints and fracture traces may represent a possible second order shear relationship between the fracture trace and jointing directions.

Analysis of rose diagrams using a multivariate statistical approach shows that the basic source of variation is due to differences in surface lithologies, and that a lesser amount may be due to deformational effects in an active structure, thus changing the fracture pattern. For example, in the Kansas area, an anticlinal structure, with a normal fault at depth, was isolated from its surrounding neighbors, whereas in the west Texas area, the predominant effect was lithology even in the larger group classifications.

ACKNOWLEDGEMENTS

I wish to thank Dr. Laurence Lattman, University of Cincinnati, for the initial encouragement and suggestions in the early stages of this study. My deep-felt appreciation is extended to the faculty of the Geosciences Department, The Pennsylvania State University, particularly to Drs. D. P. Gold and J. C. Griffiths, for their critical review of the paper and Dr. M. E. Bell, Earth and Mineral Sciences Experiment Station, for computer support for the project. Field work was partially supported by a Grant-in-Aid from the Geosciences Department and a Research Fellowship from the Chevron Oil Corporation.

My thanks also go to Mr. Norman Sawyer and his staff, Soil Conservation Service, Pratt, Kansas, for his permission to utilize early sets of aerial photography and to Mr. Michael Brown and his staff, Soil Conservation Service, Sweetwater, Texas, whose efforts opened many locked gates in the Texas study area. Gratitude is also extended to the Sunray-DX Corporation and Geo-Map Company, Dallas, Texas and Chevron Oil Corporation, Denver, Colorado, for the use of proprietary information on subsurface geology.

FUTURE WORK

Similar areas should be studied to determine if a valid exploration technique has been developed. Additional work also should be carried out to determine if lithologic control may be extracted from fracture trace orientations summarized as rose diagrams. Conversion to percent rose diagrams may achieve this end.

REFERENCES

Abilene Geological Society, 1960, The stratigraphic distribution of hydrocarbon production from 12 counties in the Abilene area.

Alpay, O. A., 1973, Application of aerial photographic interpretation to the study of reservoir natural fracture systems; Jour. Petroleum Technol., V. 25, No. 1, p. 37-45.

Barton, D. C., 1933, Surface fracture system of south Texas; Bull. Amer. Assoc. Petrol. Geol., V. 19, No. 10, p. 1194-1212.

Beene, D. L., 1967, Oil and gas fields in Kansas; Kansas Geol. Surv. Map M-3.

Benedict, L. G. and Thompson, R. R., 1973, The use of geological information to describe coal-mine roof conditions; paper presented at Annual Meeting, Amer. Chem. Soc., Chicago, Ill.

Blanchet, P. H., 1957, Development of fracture analysis as an exploration method; Bull. Amer. Assoc. Petrol. Geol., V. 41, No. 8, p. 1748-1759.

Boyer, R. E. and McQueen, J. E., 1964, Comparison of mapped rock fractures and airphoto linears; Photogrammetric Engineering, V. 30, No. 4, p. 630-635.

Brock, B. B., 1957, World patterns and lineaments; Trans. Geol. Soc. South Africa, V. 60, p. 127-175.

Chayes, F., 1949, Statistical analysis of three dimensional fabric diagrams in Structural Petrology of Deformed Rocks (Fairbairn, W. H., editor), Addison-Wesley Press, Cambridge, Mass., 344 p.

Cole, V. B., 1962, Configuration of the top of the Precambrian rocks in Kansas; Oil and Gas Inv. 27, Kansas Geol. Surv.

Conselman, F. B., 1959, Permian Basin east shelf has variety of prospects; World Oil, V. 148, No. 7, p. 124-217, 147.

Cooley, W. W. and Lohnes, P. P., 1962, Multivariate procedures for the behavior sciences; John Wiley and Sons, New York, 211 p.

Curtis, G. R., 1956, Coats Field; in Kansas Oil and Gas Fields, V. 1, South Central Kansas, Kansas Geol. Soc. p. 19-24.

Dahlberg, E. C. and Griffiths, J. C., 1967, Multivariate analysis of a sedimentary rock for evaluating effects of sedimentation; Amer. Jour. Sci., V. 265, p. 833-842.

DeSitter, L. U., 1964, Structural Geology, 2nd ed.; McGraw-Hill, New York, 587 p.

Doughty, P. S., 1968, Joint densities and their relation to lithology in the Great Scar Limestone; Proc. Yorkshire Geol. Soc., V. 36, Pt. 4, No. 27, p. 479-512.

Dranovskii, Ya. A., 1970, Morphological-structural analysis of the Lower Anadyr Depression; Geomorphology, No. 3, p. 234-240.

Fisher, R. A., 1953, Dispersion on a sphere; Proc. Royal Soc. (London), Ser. A, V. 217, p. 295-305.

Gol'braikh, I. G., Zabaluyev, V. V., Lastochkin, A. N., Mirkin, G. R., and Reinin, I. V., 1968a, Morfostrukturnye metody izucheniya tektoniki zakrytykh platformennykh neftegazonosnykh oblastei (Morphostructural methods for the study of tectonics in covered platform oil and gas bearing regions), NEDRA, 151 p.

Gol'braikh, I. G., Zabaluyev, V. V. and Mirkin, G. R., 1968b, Tectonic analysis of megajointing: a promising method of investigating covered territories; Internat. Geol. Rev., V. 8, No. 9, pp. 1009-1016.

Gold, D. P., Alexander, S. S., and Parizek, R. R., 1974, Application of remote sensing to natural resources and environmental problems in Pennsylvania; Earth and Mineral Sciences Bull., The Pennsylvania State Univ., V. 43, No. 7, p. 49-53.

Gold, D. P., Parizek, R. R. and Alexander, S. S., 1973, Analysis and application of ERTS-1 data for regional geological mapping; Symposium on Significant Results Obtained from the Earth Resources Technology Satellite-1; NASA SP-327, V. 1, p. 231-245.

Griffiths, J. C., 1967, Scientific method in analysis of sediments; McGraw-Hill, New York, 508 p.

Griffiths, J. C. and Ondrick, C. W., 1968, Sampling a geological population; Computer Contrib. 30, Kansas Geol. Surv., 53 p.

Gross, W. H., 1951, A statistical study of topographic linears and bedrock structures; Proc. Geol. Assoc. Canada, V. 4, p. 77-87.

Haman, P. J., 1961, Lineament analysis on aerial photographs as exemplified in the North Sturgeon Lake Area, Alberta; West Canadian Research Publ. of Geology and Related Sciences, Ser. 2, No. 1, 23 p.

Haman, P. J., 1964, Geomechanics applied to fracture analysis on aerial photographs; West Canadian Research Publ. of Geology and Related Sciences, Ser. 2, No. 2, 84 p.

Harris, J. F., Taylor, G. L. and Walper, J. L., 1960, Relation of deformational fractures in sedimentary rocks to regional and local structure; Bull. Amer. Assoc. Petrol. Geol., V. 44, No. 12, p. 1853-1873.

Hobbs, W. B., 1911, Repeating patterns in the relief and in the structure of the land; Bull. Geol. Soc. Amer., V. 22, p. 123-176.

Hope, A. C., Jr., 1956, Subsurface geology of the Claytonville area, Fisher County, Texas; M. S. Thesis, Texas A & M College, 32 p.

Hough, V. N. D., 1959, Joint orientations of the Appalachian Plateau in southwestern Pennsylvania; M. S. Thesis, The Pennsylvania State Univ., 82 p.

Huntington, J. F., 1969, Methods and applications of fracture trace analysis in the quantification of structural geology; Geological Magazine, V. 106, No. 5, p. 430-451.

Jewett, J. M., 1964, Geologic map of Kansas; Kansas Geol. Surv.

Keim, J. W., 1962, Study of photogeologic fracture traces over the Bisbee Quadrangle, Arizona; M. S. Thesis, The Pennsylvania State Univ., 42 p.

Krumbein, W.C., 1938, Size frequency distribution of sediments and the normal phi scale; Jour. Sedimen. Petrol., V. 8, No. 1, p. 84-90.

Krumbein, W. C. and Graybill, F. A., 1965, An introduction to statistical models in geology; McGraw-Hill, New York, 475 p.

Kutina, J., 1969, Hydrothermal ore deposits in the western United States, a new concept of structural control of distribution; Science, V. 165, No. 3898, p. 1113-1119.

Lattman, L. H., 1958, Technique of mapping geologic fracture traces and lineaments on aerial photographs; Photogrammetric Engineering, V. 24, No. 4, p. 568-576.

Lattman, L. H. and Matzke, R. H., 1961, Geologic significance of fracture traces; Photogrammetric Engineering, V. 27, No. 3, p. 435-438.

Lattman, L. H. and Matzke, R. H., 1971, Fracture traces and joints in central Pennsylvania; Bull. Amer. Assoc. Petrol. Geol., V. 55, No. 10, p. 1878-1881.

Lattman, L. H. and Nickelsen, R. P., 1958, Photogeologic fracture trace mapping in the Appalachian Plateau; Bull. Amer. Assoc. Petrol. Geol., V. 42, No. 9, p. 2238-2245.

Lattman, L. H. and Parizek, R. R., 1964, Relationship between fracture traces and the occurrence of groundwater in carbonate rocks; Jour. Hydrology, V. 2, No. 1, p. 73-91.

Layton, D. W. and Berry, D. W., 1973, Geology and groundwater resources of Pratt County, south central Kansas; Bull. 205, Kansas Geol. Surv., 33 p.

Lloyd, A. M. and Thompson, W. C., 1929, Areal map showing outcrops on the east side of the Permian Basin; Texas Bur. Econ. Geol.

Maffi, C. and Marchesini, E., 1964, Semi-automated equipment for statistical analysis of airphoto linears; Photogrammetric Engineering, V. 30, No. 1, p. 139-141.

Matzke, R. H., 1961, Fracture trace and joint patterns of western Centre County, Pennsylvania; M. S. Thesis, The Pennsylvania State Univ., 39 p.

Merriam, D. F., 1963, The geologic history of Kansas; Bull. 162, Kansas Geol. Surv., 317 p.

Mollard, J. R., 1957, Aerial mosaics reveal fracture patterns on surface materials in southern Saskatchewan and Manitoba; Oil in Canada, August 5, 1957, p. 26-50.

Moody, J. D. and Hill, M. J., 1956, Wrench fault tectonics; Bull. Geol. Soc. Amer., V. 67, No. 9, p. 1207-1246.

Nemec, V., 1970, The law of regular structural pattern: Its application with special regard to mathematical geology; paper presented at Internat. Colloq. on Geostatistics, Lawrence, Kansas.

O'Leary, M., Lippert, R. H., and Spitz, O. T., 1966, FORTRAN IV and map program for computation and plotting of trend surfaces for degrees 1 through 6; Computer Contrib. 3, Kansas Geol. Surv., 48 p.

Parizek, R. R., 1971, Prevention of coal mine drainage formation by well dewatering; Special Research Report SR-82, Coal Research Section, The Pennsylvania State Univ., 73 p.

Parizek, R. R. and Voight, V., 1970, Question 37: on remote sensing investigations for dam and reservoir construction in karst terrains; Trans. 10th Internat. Congress on Large Dams, Montreal, Canada, V. 6, p. 538-546.

Permyakov, Ye. N., 1949, Tektonicheskaya treshchinovatost' Russkoi platformy (Tectonic jointing on the Russian Platform); MOIP, Nov. Ser. Vyp. 12/16.

Permyakov, Ye. N., 1954, Osnovnye metodike ispol'zovaniya treshchinovatosti gornykh porod dlya izucheniya tektoniki platformennykh oblastei (Principle methods for the utilization of bedrock joints for the study of platform region tectonics); Trudy Moskv. Fil., VNIGRI, Vyp. 2.

Pincus. H. J., 1953, The analysis of aggregates of orientation data in the earth sciences; Jour. Geol., V. 61, No. 6, p. 482-509.

Plafker, G., 1964, Oriented lakes and lineaments of northeastern Bolivia; Bull. Geol. Soc. Amer., V. 75, No. 6, p. 503-522.

Podwysocki, M. H., 1974, FORTRAN IV programs for summarization and analysis of fracture trace and lineament patterns; NASA - Goddard Space Flight Center Document X-644-74-3, 44 p.

Podwysocki, M. H. and Gold, D. P., 1974, The surface geometry of inherited joint and fracture trace patterns resulting from active and passive deformation, NASA - Goddard Space Flight Center Document X-923-74-222 (in press).

Renner, J. G. A., 1969, The structural significance of lineaments in the eastern Monsech Area, province of Lerida, Spain; Publ. of the Internat. Inst. for Aerial Surv. and Earth Sci. (ITC), Ser. B, No. 45, 29 p.

Rich, J. L., 1928, Jointing in limestone as seen from the air; Bull. Amer. Assoc. Petrol. Geol., V. 12, No. 8, p. 861-862.

Rubin, J. and Friedman, H. P., 1967, A cluster analysis and taxonomy system for grouping and classifying data; IBM Corp., New York, 221 p.

Saunders, D. F., 1969, Airborne sensing as an oil reconnaissance tool; in Unconventional Methods in Exploration for Petroleum and Natural Gas (Heroy, W. B., editor), Southern Methodist Univ., p. 105-125.

Shamburger, V. M., Jr., 1967, Groundwater resources of Mitchell and western Nolan Counties, Texas, Rpt. 50, Texas Water Develop. Board, 175 p.

Shul'ts, S. S., 1969, Nekotorye voprosy planetarnoi treshchinovatosti i svyazannykh s neyu yavlenii (Some aspects of planetary jointing and related phenomena); Vestnik Leningrad. Univ., No. 1, p. 86-99.

Siddiqui, S. H. and Parizek, R. R., 1971, Hydrogeologic factors influencing well yields in folded and faulted carbonate rocks in central Pennsylvania; Water Resources Research, V. 7, No. 5, p. 1295-1312.

Siegal, S., 1956, Nonparametric statistics for the behavioral sciences; McGraw-Hill, New York, 312 p.

Trainer, F. W., 1967, Measurement of the abundance of fracture traces on aerial photographs; U. S. Geol. Surv. Prof. Paper 575-C, p. C184-C188.

Trainer, F. W. and Ellison, R. L., 1967, Fracture traces in the Shenandoah Valley; Photogrammetric Engineering, V. 33, No. 2, p. 190-199.

Vance, W. R. and Johnson, E. D., 1929, Geologic map of Fisher County, Texas; Texas Bur. Econ. Geol.

Van Siclen, D. C., 1958, Depositional topography - examples and theory; Bull. Amer. Assoc. Petrol. Geol., V. 52, No. 8, p. 1897-1913.

Williams, C. D., 1968, Pre-Permian geology of the Pratt Anticline area in south central Kansas; M. S. Thesis, Wichita State Univ., 116 p.

Wise, D. U., 1968, Regional and sub-continental sized fracture systems detectable by topographic shadow techniques; in Conf. on Research in Tectonics (Kink Bands & Brittle Deformation) (Baer, A. J. & Norris, D. K., eds.), Geol. Surv. Canada Paper 68-52, p. 175-199.

APPENDIX A

SOURCE LISTING OF FORTRAN IV COMPUTER PROGRAM "VECLEN"

REPRODUCIBILITY OF THE
ORIGINAL PAGE IS P...

```
C                    ******************************
C                      VECTOR    LENGTH    PROGRAM
C                    ******************************
C
C        THE PROGRAM WAS WRITTEN BY MELVIN PODWYSOCKI OF THE GEOSCIENCES
C        DEPT., THE PENNSYLVANIA STATE UNIVERSITY, APRIL, 1972 FOR THE
C        IBM 360/67 COMPUTER, AND WAS MODIFIED IN APRIL, 1974, FOR USE
C        ON OTHER COMPUTERS HAVING THE EQUIVALENT OF 120K BYTES STORAGE.
C
C      PROGRAM SUMMARIZES VECTOR DATA AS FREQUENCY-LENGTH DISTRIBUTIONS.
C      OPERATOR SPECIFIES CLASS LENGTH, SIZE OF MAXIMUM CLASS AND DETER-
C      MINES THE DIMENSIONS OF THE AREA (GRID CELL) IN WHICH THE DATA
C      ARE SUMMARIZED. A VECTOR IS COUNTED IN A GRID CELL IF ITS MID-
C      POINT FALLS IN THE CELL. NO CONSIDERATION IS GIVEN TO VECTOR AZI-
C      MUTH. PROVISION IS MADE FOR A LOG BASE 2 TRANSFORMATION IF DESI-
C      RED TO ATTEMPT NORMALIZATION OF THE DATA. A TEST FOR NORMALITY IS
C      MADE BY COMPARING A THEORETICAL DISTRIBUTION USING THE CALCULATED
C      MEAN AND STANDARD DEVIATION OF THE OBSERVED POPULATION AGAINST
C      THE DISTRIBUTION OF THE OBSERVED POPULATION UTILIZING THE CHI
C      SQUARE CRITERION. EXAMPLES OF PROGRAM OUTPUT AND APPLICATIONS ARE
C      GIVEN IN. PODWYSOCKI, M.H., 1974, "ANALYSIS OF FRACTURE TRACE
C      PATTERNS IN AREAS OF FLAT-LYING SEDIMENTARY ROCKS FOR THE DETEC-
C      TION OF BURIED GEOLOGIC STRUCTURE"; NASA - GODDARD SPACE FLIGHT
C      CENTER DOCUMENT X-923-74-200. DATA ARE READ FROM CARDS GENERATED
C      BY VECTOR TRANSFORM PROGRAM (SEE PODWYSOCKI, M.H., 1974, "FORTRAN
C      IV PROGRAMS FOR SUMMARIZATION AND ANALYSIS OF FRACTURE TRACE AND
C      LINEAMENT PATTERNS"; NASA - GSFC DOCUMENT X-644-74-3).
C      CONTROL & TITLE CARDS ARE READ FROM CARD READER WHILE DATA CARDS
C      MAY BE READ FROM ANY UNIT DECLARED BY 'ITAPE2' ON CONTROL CARD 4.
C
C      ALL NUMERIC INPUT DATA IS RIGHT JUSTIFIED; "I" INDICATES INTEGER
C      FORMAT, "F" INDICATES FLOATING POINT FORMAT, "A" INDICATES CHA-
C      RACTER FORMAT, "#" PRECEEDING NUMBERS INDICATES COLUMNS USED FOR
C      EACH PARAMETER. TO SPECIFY NONUSE OF AN OPTION, PUNCH 0
C
C ********CONTROL CARDS 1 THRU 3------TITLE CARDS
C     TITLE WILL BE PRINTED AT THE TOP OF EACH GRID CELL SUMMARIZED
C        (20A4,#1-80). NOTE: 3 CARDS MUST BE USED; IF ALL 3 ARE NOT USED
C        , BLANK CARDS MUST BE INSERTED IN THEIR PLACE.
C ********CONTROL CARD 4------OPTIONS CARD
C     XINC=INCREMENT OF X-AXIS TRAVERSE IN MM. (I4,#1-4)
C     YINC=INCREMENT OF Y-AXIS TRAVERSE IN MM. (I4,#5-8)
C     XSTART=STARTING POINT FOR X-AXIS TRAVERSE IN MM. (I4,#9-12)
C     YSTART=STARTING POINT FOR Y-AXIS TRAVERSE IN MM. (I4,#13-16)
C     XSTOP=END OF X-AXIS TRAVERSE IN MM. (I4,#17-20)
C     YSTOP=END OF Y-AXIS TRAVERSE IN MM. (I4,#21-24)
C        NOTE: PROGRAM SUCCESSIVELY SCANS DATA IN MAP GRID CELLS 'XCELL'
C        BY 'YCELL' IN SIZE, INCREMENTING BY 'XINC' UNTIL 'XMAX' >
C        'XSTOP', WHEN 'YINC' IS INCREMENTED.  PROGRAM TERMINATES WHEN
C        'YMAX' > 'YSTOP'. NONE OF THE ABOVE 6 VALUES CAN BE NEGATIVE.
C     AMPSCL=MAP SCALE ENTERED AS MILES/MM. (F5.4,#25-29)
C        NOTE: WHEN VECTORS ARE MEASURED ON A 1:24000 SCALE MAP AND OUT-
C        PUT IS DESIRED IN MILES,'AMPSCL'=.0149 (I.E. 1 MM.=.0149 MILES)
C     DHINC=NUMERICAL VALUE OF EACH 'X' INCREMENT OF FREQUENCY-LENGTH
C        HISTOGRAM (I.E. EACH 'X'= 2 VECTORS) (F5.2,#30-34)
C     SCINC=FREQUENCY CLASS INTERVAL; DEPENDENT ON  DATA TREATMENT
C        (SEE 'NTRAN' BELOW). (F5.2,#35-39)
C     SCLMAX=UPPER CLASS LIMIT OF LAST FREQUENCY-LENGTH CLASS (SEE
C        'NTRAN' BELOW). (F5.2,#40-44)
C     NHIST--PUNCH 1 FOR FREQUENCY-LENGTH HISTOGRAM IN PRINTED OUTPUT
```

REPRODUCIBILITY OF THE
ORIGINAL PAGE IS POOR

```
C        (I1,#45)                                                       VLN00605
C     NPUNCH--PUNCH 1 IF FREQUENCY-LENGTH DISTRIBUTION IS DESIRED       VLN00615
C        ON CARDS (I1,#46)                                              VLN00625
C     NSTAT--PUNCH 1 IF FREQUENCY MCMENTS (I.E. MEAN, STANDARD DEVIATIONVLN00635
C        , SKEWNESS, ETC.) ARE DESIRED ON CARDS (I1,#47)                VLN00645
C     XCELL=CELL SIZE (IN MM.) IN X DIRECTION (I4,#48-51)               VLN00655
C     YCELL=CELL SIZE (IN MM.) IN Y DIRECTION (I4,#52-55)               VLN00665
C     NFOLD--PUNCH 1 TO FOLD TAILS OF FREQUENCY-LENGTH DISTRIBUTION TO  VLN00675
C        SATISFY REQUIREMENTS FOR CHI SQUARE TEST. TAILS ARE FOLDED WHENVLN00685
C        EXPECTED FREQUENCY OF A CLASS IS < 0.95  (I1,#56)              VLN00695
C     ITAPE2=LOGICAL UNIT FOR READING DATA CARDS GENERATED BY "TRANS-   VLN00705
C        FORM" PROGRAM (I2,#57-58)                                      VLN00715
C     NTRAN--SELECTS DATA TREATMENT (I2,#59-60)                         VLN00725
C        PUNCH 1 IF DATA IS TO BE TREATED IN A LINEAR FASHION (I.E.     VLN00735
C        INTERVAL IN MILES  AS SPECIFIED IN 'AMPSCL'). NOTE: 'NFOLD' CANVLN00745
C        NOT BE 1 IF THIS OPTION IS CHOSEN                              VLN00755
C        PUNCH -1 IF DATA IS TO BE CONVERTED TO LOG BASE 2 BY THE FOR-  VLN00765
C        MULA:  Z = (1/LOG10(2))*LOG10(X)+6. WHERE X = VECTOR LENGTH    VLN00775
C        IN MILES. NOTE: FOLD OPTION MAY BE USED.                       VLN00785
C        'SCLMAX' AND 'SCINC' ARE GOVERNED BY 'NTRAN'. FREQUENCY-LENGTH VLN00795
C        CLASSES BEGIN WITH A MINIMUM VALUE OF 0 AND INCREMENT BY 'SCINCVLN00805
C        ' UNTIL 'SCLMAX' IS REACHED. IF A LINEAR SCALE IS USED, 'SCLMAXVLN00815
C        ' IS > THE LARGEST VECTOR LENGTH IN MILES. IF DATA IS TRANSFOR-VLN00825
C        MED TO LOGARITHMS.. 'SCLMAX' IS DETERMINED BY THE CONVERSION OFVLN00835
C        THE LARGEST VECTOR LENGTH BY THE ABOVE FORMULA. 'SCINC' MUST BEVLN00845
C        CHOSEN APPROPRIATELY FOR EACH CASE.                            VLN00855
C *******DATA CARDS------                                                VLN00865
C     VECTOR DATA INPUT FROM VECTOR TRANSFORM PROGRAM                   VLN00875
C                                                                       VLN00885
      DIMENSION TITLE(60),VECLEN(2000),XMID(2000),YMID(2000),Z(2000),SCMVLN00895
     1IN(40),SCMAX(40),FNUM(40),ZI(40),AREA(40),DIFF(40),FREQEX(40),CHISVLN00905
     2Q(40),D(40),FD(40),FD2(40),FD3(40),FD4(40),FD5(40)                VLN00915
      DIMENSION FFRQX(40), FFNUM(40),FCHISQ(40)                         VLN00925
      DATA IHX/1HX/,AC/3.32193/,IREAD/5/,IPRINT/6/,IPUNCH/7/,A1/.0997926VLN00935
     18D0/,A2/.0443201400/,A3/.0096992000/,A4/-.00009862D0/,A5/.00058155VLN00945
     2D0/                                                               VLN00955
      INTEGER XINC,YINC,XSTART,YSTART,YMIN,XMIN,XSTOP,YSTOP,XMAX,YMAX,XCVLN00965
     1ELL,YCELL,BOMB                                                    VLN00975
C                                                                       VLN00985
C     READ CONTROL CARDS                                                VLN00995
C                                                                       VLN01005
      BOMB=0                                                            VLN01015
      READ(IREAD,5) (TITLE(L),L=1,60)                                   VLN01025
      READ(IREAD,10) XINC,YINC,XSTART,YSTART,XSTOP,YSTOP,AMPSCL,DHINC,  VLN01035
     1SCINC,SCLMAX,NHIST,NPUNCH,NSTAT,XCELL,YCELL,NFOLD,ITAPE2,NTRAN    VLN01045
      IF(XINC.LT.0.OR.YINC.LT.0.OR.XSTART.LT.0.OR.YSTART.LT.0.OR.XSTOP. VLN01055
     1LT.0.OR.YSTOP.LT.0.OR.XCELL.LT.0.OR.YCELL.LT.0.OR.NFOLD.EQ.1.AND  VLN01065
     2.NTRAN.GT.0) BOMB=1                                               VLN01075
   11 IF(BOMB) 18,18,13                                                 VLN01085
   13 WRITE(IPRINT,15) XINC,YINC,XSTART,YSTART,XSTOP,YSTOP,XCELL,YCELL  VLN01095
     1,NFOLD,NTRAN                                                      VLN01105
      GO TO 800                                                         VLN01115
C                                                                       VLN01125
C     READ DATA CARDS FROM LOGICAL UNIT 'ITAPE2'                        VLN01135
C                                                                       VLN01145
   18 DO 25 I=1,5000                                                    VLN01155
      READ(ITAPE2,20,END=30) VECLEN(I),XMID(I),YMID(I)                  VLN01165
      IF(I-2000) 25,25,22                                               VLN01175
   22 WRITE(IPRINT,24)                                                  VLN01185
      GO TO 800                                                         VLN01195
   25 NUM =I                                                            VLN01205
```

```
   30 DO 35 M=1,NUM                                                     VLN01215
      Z(M)=VECLEN(M)*AMPSCL                                             VLN01225
      IF(NTRAN) 32,13,35                                                VLN01235
   32 Z(M)=(ALOG10(Z(M))*AC)+6.                                         VLN01245
   35 CONTINUE                                                          VLN01255
      NCLASS=SCLMAX/SCINC+0.5                                           VLN01265
      IF(NCLASS-40) 39,39,36                                            VLN01275
   36 WRITE(IPRINT,38) SCLMAX,SCINC                                     VLN01285
      GO TO 800                                                         VLN01295
   39 DO 70 N=1, NCLASS                                                 VLN01305
      IF(N-1) 40,40,50                                                  VLN01315
   40 SCMIN(N)=0.                                                       VLN01325
      GO TO 60                                                          VLN01335
   50 SCMIN(N)=SCMAX(N-1)                                               VLN01345
   60 SCMAX(N)=SCMIN(N)+SCINC                                           VLN01355
   70 CONTINUE                                                          VLN01365
C                                                                       VLN01375
C     SCAN AND SUMMARIZE VECTORS IN EACH GRID CELL                      VLN01385
C                                                                       VLN01395
      DO 700 YMIN=YSTART,YSTOP,YINC                                     VLN01405
      IF(YMIN.GE.YSTOP) GO TO 800                                       VLN01415
      DO 700 XMIN=XSTART,XSTOP,XINC                                     VLN01425
      IF(XMIN.GE.XSTOP) GO TO 700                                       VLN01435
      DO 80 L=1,NCLASS                                                  VLN01445
      AREA(L)=0.                                                        VLN01455
      CHISQ(L)=0.                                                       VLN01465
      D(L)=0.                                                           VLN01475
      DIFF(L)=0.                                                        VLN01485
      FD(L)=0.                                                          VLN01495
      FD2(L)=0.                                                         VLN01505
      FD3(L)=0.                                                         VLN01515
      FD4(L)=0.                                                         VLN01525
      FD5(L)=0.                                                         VLN01535
      FCHISQ(L)=0.                                                      VLN01545
      FFROX(L)=0.                                                       VLN01555
      FFNUM(L)=0.                                                       VLN01565
      FNUM(L)=0.                                                        VLN01575
      FREQEX(L)=0.                                                      VLN01585
      ZI(L)=0.                                                          VLN01595
   80 CONTINUE                                                          VLN01605
      TFNUM=0.                                                          VLN01615
      XMAX=XMIN+XCELL                                                   VLN01625
      YMAX=YMIN+YCELL                                                   VLN01635
      DO 140 I=1,NUM                                                    VLN01645
      IF(XMID(I).GE.XMIN.AND.XMID(I).LT.XMAX.AND.YMID(I).GE.YMIN.AND.YMIVLN01655
     1D(I).LT.YMAX) GO TO 100                                           VLN01665
      GO TO 140                                                         VLN01675
  100 IAC=I                                                             VLN01685
      DO 120 J=1,NCLASS                                                 VLN01695
      IF(Z(IAC).GE.SCMIN(1).AND.Z(IAC).LT.SCMAX(NCLASS)) GO TO 105      VLN01705
      WRITE(IPRINT,102) IAC,Z(IAC),SCMIN(1),SCMAX(NCLASS)               VLN01715
      GO TO 800                                                         VLN01725
  105 IF(Z(IAC).GE.SCMIN(J).AND.Z(IAC).LT.SCMAX(J)) GO TO 110           VLN01735
      GO TO 120                                                         VLN01745
  110 NTYPE=J                                                           VLN01755
      GO TO 130                                                         VLN01765
  120 CONTINUE                                                          VLN01775
  130 FNUM(NTYPE)=FNUM(NTYPE)+1.                                        VLN01785
  140 CONTINUE                                                          VLN01795
      DO 150 N=1,NCLASS                                                 VLN01805
      TFNUM=TFNUM+FNUM(N)                                               VLN01815
```

REPRODUCIBILITY OF THE
ORIGINAL PAGE IS POOR

```
  150 CONTINUE
      NC=(SCLMAX-0.)/SCINC+0.5
C
C     ELIMINATION OF LOWER EMPTY CLASSES
C
      DO 161 JK=1,NCLASS
      IF(FNUM  (JK)) 161,161,162
  161 CONTINUE
  162 JKL=JK
C
C     ELIMINATION OF EMPTY UPPER CLASSES
C
      DO 163 JK=1,NCLASS
      KH=(NCLASS-JK)+1
      IF( FNUM (KH)) 163,163,164
  163 CONTINUE
  164 JKH=KH
C
C     CALCULATE STATISTICAL MOMENTS FOR EACH GRID CELL
C
      MAXCLS=1
      DO 166 M=JKL,JKH
      IF(FNUM(MAXCLS)-FNUM(M)) 165,165,166
  165 MAXCLS=M
  166 CONTINUE
      CLSMDP=(SCMIN(MAXCLS)+SCMAX(MAXCLS))/2
      DO 170 MS=JKL,JKH
      D(MS)=((SCMIN(MS)+SCMAX(MS))/2-CLSMDP)/SCINC
  170 CONTINUE
      SD=0.
      SD2=0.
      SD3=0.
      SD4=0.
      SD5=0.
      DO 175 I=JKL,JKH
      FD(I)=FNUM(I)*D(I)
      SD=SD+FD(I)
      FD2(I)=FNUM(I)*(D(I)**2)
      SD2=SD2+FD2(I)
      FD3(I)=FNUM(I)*(D(I)**3)
      SD3=SD3+FD3(I)
      FD4(I)=FNUM(I)*(D(I)**4)
      SD4=SD4+FD4(I)
      FD5(I)=FNUM(I)*((D(I)-1.)**4)
      SD5=SD5+FD5(I)
  175 CONTINUE
      GCK=SD4-(4.*SD3)+(6.*SD2)-(4.*SD)+TFNUM
      AMOM1=SD /TFNUM
      AMOM2=SD2/TFNUM
      AMOM3=SD3/TFNUM
      AMOM4=SD4/TFNUM
      TMOM1=AMOM1*SCINC
      TMOM2=(SCINC**2)*(AMOM2-((AMOM1)**2))
      TMOM3=(SCINC**3)*(AMOM3-(3.*AMOM2*AMOM1)+(2.*(AMOM1**3)))
      PT4A=(AMOM4-(4.*AMOM3*AMOM1)+(6.*(AMOM1**2)*AMOM2))
      PT4B=PT4A-(3.*(AMOM1**4))
      TMOM4=(SCINC**4)*(PT4B)
      XBAR=CLSMDP+TMOM1
      VAR=TMOM2
      STDV=SQRT(VAR)
      RTB1=(TMOM3/((SQRT(VAR))**3))
```

```
      B2  =(TMOM4/(TMCM2**2))
C
C     CALCULATE CHI SQUARE CONTRIBUTION & EXPECTED FREQUENCIES FOR EACH
C     CLASS ASSUMING A NORMAL DISTRIBUTION WITH A XBAR & STDV OF THE
C     OBSERVED POPULATION
C
      NDF=(JKH-JKL)-2
      DO 200 J=JKL,JKH
      ZI(J)=(SCMAX(J)-XBAR)/STDV
  200 CONTINUE
      TDIFF=0.
      TFRQEX=0.
      TCHISQ=0.
      IJK=0
      IKC=JKL-1
      AREA(IKC)=0.
      DO 290 I=JKL,JKH
      IIV=I-1
      IF(ZI(I))210,220,220
  210 AVT=-ZI(I)
      GO TO 230
  220 AVT=ZI(I)
  230 AREA(I)=1.+AVT*(A1+AVT*(A2+AVT*(A3+AVT*(A4+AVT*A5))))
      AREA(I)=0.5/(AREA(I)**8)
      IF(ZI(I))240,250,250
  240 DIFF(I)=AREA(I)-AREA(IIV)
      GO TO 280
  250 IJK=IJK+1
      IF(IJK-1) 260,260,270
  260 DIFF(I)=1.-AREA(I)-AREA(IIV)
      GO TO 280
  270 DIFF(I)=AREA(IIV)-AREA(I)
  280 TDIFF=TDIFF+DIFF(I)
      FREQEX(I)=DIFF(I)*TFNUM
      TFRQEX=TFRQEX+FREQEX(I)
      CHISQ(I)=((   FNUM(I)-FREQEX(I))**2)/FREQEX(I)
      TCHISQ=TCHISQ+CHISQ(I)
  290 CONTINUE
      CHIPRB=PRBCHI(TCHISQ,NDF)
      NFLAG=0
      MFLAG=0
      IF(NFOLD)495,495,300
C
C     FOLD LOWER TAIL OF DISTRIBUTION IF REQUIRED
C
  300 DO 302 MP=JKL,JKH
      FCHISQ(MP)=CHISQ(MP)
      FFROX(MP)=FREQEX(MP)
      FFNUM(MP)=FNUM(MP)
  302 CONTINUE
      DO 310 LL=JKL,MAXCLS
      IF(FFROX(LL)-0.95) 305,310,310
  305 FFROX(LL+1)=FFROX(LL)+FFROX(LL+1)
      FFNUM(LL+1)=FFNUM(LL)+FFNUM(LL+1)
      FCHISQ(LL)=0.
      JKL1=LL+1
      NFLAG=1
  310 CONTINUE
      JKQ=(JKH-MAXCLS)+1
C
C     FOLD UPPER TAIL OF DISTRIBUTION IF REQUIRED
```

REPRODUCIBILITY OF THE
ORIGINAL PAGE IS POOR

```
C
      DO 320 LH=1,JKQ
      KHH=(JKH-LH)+1
      IF(FFRQX(KHH)-0.95) 315,320,320
  315 FFRQX(KHH-1)=FFRQX(KHH-1)+FFRQX(KHH)
      FFNUM(KHH-1)=FFNUM(KHH-1)+FFNUM(KHH)
      FCHISQ(KHH)=0.
      JKH1=KHH-1
      MFLAG=1
  320 CONTINUE
      IF(NFLAG) 325,325,330
  325 J2=JKL
      GO TO 335
  330 J2=JKL1
  335 IF(MFLAG) 340,340,345
  340 J3=JKH
      GO TO 350
  345 J3=JKH1
  350 TFFRQX=0.
      TFCHSQ=0.
      DO 355 JI=J2,J3
      TFFRQX=TFFRQX+FFRQX(JI)
      FCHISQ(JI)=((FFNUM(JI)-FFRQX(JI))**2)/FFRQX(JI)
      TFCHSQ=TFCHSQ+FCHISQ(JI)
  355 CONTINUE
      NFDF=(J3-J2)-2
      FCHPRB=PRBCHI(TFCHSQ,NFDF)
C
C     OUTPUT
C
  495 WRITE(IPRINT,500) (TITLE(L),L=1,60)
      NROW=(YMIN+YINC)/YINC
      NCOL=(XMIN+XINC)/XINC
      WRITE(IPRINT,510) NROW,NCOL,XMIN,XMAX,YMIN,YMAX
      WRITE(IPRINT,520)
      NXERR=0
      DO 630 IJ=JKL,JKH
      WRITE(IPRINT,530) IJ,SCMIN(IJ),SCMAX(IJ),FREQEX(IJ),CHISQ(IJ),
     1FNUM(IJ)
      IF(NFOLD.EQ.1.AND.NFLAG.EQ.1.AND.J2.EQ.IJ) WRITE(IPRINT,532)
     1FFRQX(IJ),FCHISQ(IJ),FFNUM(IJ)
      IF(NFOLD.EQ.1.AND.MFLAG.EQ.1.AND.J3.EQ.IJ) WRITE(IPRINT,532)
     1FFRQX(IJ),FCHISQ(IJ),FFNUM(IJ)
      IF(NPUNCH-1) 560,540,560
  540 WRITE(IPUNCH,550)NROW,NCOL,IJ,SCMIN(IJ),SCMAX(IJ),   FNUM(IJ)
  560 IF (NHIST-1) 630,570,630
  570 NUMX=  FNUM(IJ)/DHINC
      IF(NUMX) 600,580,600
  580 WRITE(IPRINT,590)
      GO TO 630
  600 IF(NUMX-70) 620,620,610
  610 NUMX=70
      NXERR=1
  620 WRITE(IPRINT,625) (IHX,IUKA=1,NUMX)
  630 CONTINUE
      WRITE(IPRINT,640) TFRQEX,TCHISQ, TFNUM,DHINC
      IF(NFOLD.EQ.1.AND.NFLAG.EQ.1.OR.MFLAG.EQ.1) WRITE (IPRINT,645)
     1TFCHSQ
      IF(NXERR.EQ.1) WRITE(IPRINT,650)
      WRITE(IPRINT,652) NDF,CHIPRB
      IF(NFOLD.EQ.1.AND.NFLAG.EQ.1.OR.MFLAG.EQ.1) WRITE (IPRINT,654)
```

```
     1NFDF,FCHPRB                                                         VLN03655
      WRITE(IPRINT,655)      MAXCLS,CLSMDP,FNUM(MAXCLS)                   VLN03665
      WRITE (IPRINT,660) XBAR,VAR,STDV,RTB1,B2                            VLN03675
      IF(NSTAT.EQ.1) WRITE(IPUNCH,665) NROW,NCOL,XMIN,XMAX,YMIN,YMAX,     VLN03685
     1XBAR,STDV,RTB1,B2                                                   VLN03695
      IF(GCK-SD5.GT.10.) WRITE(IPRINT,670) GCK,SD5                        VLN03705
  700 CONTINUE                                                            VLN03715
    5 FORMAT(20A4)                                                        VLN03725
   10 FORMAT(6I4,F5.4,3F5.2,3I1,2I4,I1,2I2)                               VLN03735
   15 FORMAT('1','ONE OR MORE OF THE FOLLOWING DO NOT CONFORM TO PROGRAMVLN03745
     1 LIMITATIONS',/' ',4X,'XINC',4X,'YINC',2X,'XSTART',2X,'YSTART'      VLN03755
     2,3X,'XSTOP',3X,'YSTOP',3X,'XCELL',3X,'YCELL',3X,'NFOLD',3X,         VLN03765
     3'NTRAN',/' ',10I8,/'0',30X,'JOB ABORTED')                           VLN03775
   20 FORMAT(T25,F6.1,T56,2F7.1)                                          VLN03785
   24 FORMAT('1','MORE THAN 2000 VECTORS IN DATA SET',/'0',30X,'JOB ABORVLN03795
     1TED')                                                               VLN03805
   38 FORMAT('1','NUMBER OF FREQUENCY-LENGTH CLASSES EXCEEDS PROGRAM LIMVLN03815
     1IT OF 40 WHERE: SCLMAX/SCINC=NCLASS'/,' ',T69,F6.2,'/',F5.2,' =     VLN03825
     2',I5,//'0',30X,'JOB ABORTED')                                       VLN03835
  102 FORMAT('1','VECTOR #',I6,' LENGTH OF',F11.5,' EXCEEDS CLASS LIMITSVLN03845
     1 OF',2F12.5,/'0',30X,'JOB ABORTED')                                 VLN03855
  500 FORMAT('1',3(T30,20A4,//))                                          VLN03865
  510 FORMAT('0','ROW',I4,' ,COLUMN',I4,T30,'(',I5   ,' < X < ',I5   ,' ; VLN03875
     1',I5   ,' < Y < ',I5   ,')')                                        VLN03885
  520 FORMAT('0',T9,'LOWER',2X,'UPPER',T42,'CHI',/,T9,'CLASS',2X,'CLASS'VLN03895
     1,5X,'EXPECTED',7X,'SQUARE',5X,'OBSERVED',/,T2,'CLASS',2X,'LIMIT',2VLN03905
     2X,'LIMIT',5X,'FREQUENCY',5X,'CONTRIB.',4X,'FREQUENCY',9X,'OBSERVEDVLN03915
     3 FRECUENCY HISTOGRAM',//)                                           VLN03925
  530 FORMAT(' ',2X,I2,2X,F5.2,2X,F5.2,F7.2,8X,F8.2, 9X,F4.0)             VLN03935
  532 FORMAT('+',T27,'(',F5.2,')',T43,'(',F6.2,')',T56,'(',F3.0,')')      VLN03945
  550 FORMAT(3I5,2F10.2,F12.2)                                            VLN03955
  590 FORMAT('+',T61,'>')                                                 VLN03965
  625 FORMAT('+',T61,'>',70A1)                                            VLN03975
  640 FORMAT(' ',T20,7('-'),T36,7('-'),T53,'----',/,T10,'TOTALS',T19,F8.VLN03985
     12,T35,F6.2,T50,F6.0,T70,'EACH "X" = ',F10.2,' VECTOR(S)')           VLN03995
  645 FORMAT(' ',T34,'(',F8.2,')')                                        VLN04005
  650 FORMAT('0',T70,'ONE OR MORE FREQUENCY CLASSES EXCEED HISTOGRAM LIMVLN04015
     1ITS')                                                               VLN04025
  652 FORMAT('0','DEGREES OF FREEDOM (NON-FOLDED) = ',I4,';  CHI SQUARE VLN04035
     1PROBABILITY = ',E10.4)                                              VLN04045
  654 FORMAT('0','DEGREES OF FREEDOM (FOLDED) = ',I4,';  CHI SQUARE PROBVLN04055
     1ABILITY = ',E10.4)                                                  VLN04065
  655 FORMAT('0',T50,'MODAL STATISTICS',/T50,16('-'),//,T20,'CLASS',T40,VLN04075
     1'MIDPOINT',T60,'OBS.FREQUENCY',//,T21,I2,T40,F7.3,T64,F6.2)         VLN04085
  660 FORMAT('0',T50,'STATISTICAL MOMENTS',/,T50,19('-'),//T20,'AVERAGE'VLN04095
     1,T40,'VARIANCE',T60,'STANDARD DEVIATION',T85,'ROOT B1 ',T105,'   BVLN04105
     22    ',//,T20,F8.3,T40,F8.3,T65,F8.3,T85,F8.3,T105,F8.3)            VLN04115
  665 FORMAT(6I4,4F8.3)                                                   VLN04125
  670 FORMAT('0','GRAM-CHARLIER CHECK = ',F15.4,' ;SUM = ',F15.4)         VLN04135
  800 STOP                                                                VLN04145
      END                                                                 VLN04155
C                                                                         CHI 0005
      FUNCTION PRBCHI (CHISQ,IDF)                                         CHI 0015
C                                                                         CHI 0025
C     WRITTEN BY H.D. KNOBLE & F.YATES BORDEN, THE PENNSYLVANIA STATE     CHI 0035
C     UNIVERSITY, 1966                                                    CHI 0045
C     THIS FUNCTION COMPUTES BY THE APPROXIMATIONS ON PAGE 941 OF         CHI 0055
C     "HANDBOOK OF MATHEMATICAL FUNCTIONS",U.S. DEPT. OF COMMERCE,1964.   CHI 0065
C     GIVEN A VALUE OF CHI-SQUARE AND ITS DEGREES OF FREEDOM, FUNCTION    CHI 0075
C     PRBCHI COMPUTES THE PROBABILITY OF A GREATER VALUE OF CHI-SQUARE.   CHI 0085
C     THE Z(ARGUMENT) FUNCTION IS COMPUTED BY FORMULA 26.2.1, P. 931.     CHI 0095
```

REPRODUCIBILITY OF THE
ORIGINAL PAGE IS POOR

```
C
      INTEGER TEST
C     ALL REAL*8 ARGUMENTS CHANGED TO DOUBLE PRECISION BY M.PODWYSOCKI.
      DOUBLE PRECISION DSQRT,DEXP,ARG,SCHISQ,XPLEVL
      DOUBLE PRECISION Q,R,S,T,L,V,V9,PROB,S2PI,Z005,APPROX
      DATA S2PI/2.5066282D00/
C
      Q(ARG)=(DEXP(-ARG*ARG*0.5)/2.5066282D00)*(T*(0.3193815D00+T*
     1(-0.3565638D00+T*(1.781478D00+T*(-1.821256D00+(1.330274D00*T))))))
      XPL=2.57623596D00
      PRBCHI=0.0
      IF(CHISQ.LT.0.0)  RETURN
      IF(IDF.LE.0) RETURN
  100 SCHISQ=CHISQ
      S=1.0
      V=IDF
      V9=2.0/FLOAT(9*IDF)
      U=-SCHISQ*0.5
      SCHISQ=DSQRT(SCHISQ)
      IF (DABS(U).LT.174.6) GO TO 110
C
C     174.6 IS THE LARGEST ARGUMENT THAT EXP WILL TAKE.
C
      PROB=0.0
      GO TO 240
C
C   CHECK FOR DEGREES OF FREEDOM GREATER THAN 100 OR GREATER THAN 30
C
  110 IF (IDF.GT.100) GO TO 200
      IF (IDF.GT.30) GO TO 170
C
C   DEGREES OF FREEDOM LESS THAN OR EQUAL TO 30
C
      PROB=0.0
      TEST=MOD(IDF,2)
      IF (TEST.NE.0) GO TO 140
C
C   EVEN DEGREES OF FREEDOM  **  LESS THAN OR EQUAL TO 30  ** FORMULA
C   26.4.5, PAGE 941
C
      IRANGE=(IDF-2)/2
      IF (IRANGE.EQ.0) GO TO 130
      DO 120  I=1,IRANGE
      IR=I+I
      S=S*IR
  120 PROB=PROB+SCHISQ**IR/S
  130 PROB=DEXP(U)*(1.0+PROB)
      GO TO 230
C
C   ODD DEGREES OF FREEDOM  **  LESS THAN OR EQUAL TO 29  ** FORMULA
C   26.4.4, PAGE 941
C
  140 IRANGE=(IDF-1)/2
      IF (IRANGE.EQ.0) GO TO 160
      DO 150  I=1,IRANGE
      IR=I+I-1
      S=S*IR
  150 PROB=PROB+SCHISQ**IR/S
  160 T=1.0/(1.0+0.2316419D00*SCHISQ)
      PROB=2.0*(Q(SCHISQ))+2.0*(DEXP(U)/S2PI)*PROB
      GO TO 230
```

REPRODUCIBILITY OF THE
ORIGINAL PAGE IS POOR

```
C
C    ********** GREATER THAN 30 DEGREES OF FREEDOM **********
C    AN APPROXIMATE VALUE OF CHISQ IS FIRST COMPUTED THEN COMPARED WITH
C    THE GIVEN CHISQ. IF THE APPROX. VALUE IS GREATER THAN THE GIVEN
C    VALUE, Q(CHISQ.IDF) IS RETURNED AS .995.
C    ***********************************************************************
C    FOR GREATER THAN 30 AND LESS THAN OR EQUAL TO 100 DEGREES OF FREEDOM
C    THE APPROX. VALUE OF CHISQ AT THE .995 LEVEL IS COMPUTED BY FORMULA
C    26.4.17, PAGE 941.  THE SIGN OF X(P) IN THE FORMULA WAS CHANGED
C    FROM + TO - TO ALLOW COMPUTATION OF CHISQ AT THE .995 LEVEL RATHER
C    THAN THE .005 LEVEL AS IS THE CASE WHEN THE SIGN IS +.
C
  170 APROX=((1.0-V9-XPL*DSQRT(V9))**3)*V
      IF (APROX.LE.CHISQ) GO TO 180
      GO TC 210
  180 V=((CHISQ/V)**0.33333333D00-(1.0-V9))/DSQRT(V9)
  190 T=1.0/(1.0+0.2316419D00*V)
      PROB=Q(V)
      GO TO 230
C
C    GREATER THAN 100 DEGREES OF FREEDOM.    THE APPROX. VALUE OF CHISQ
C    IS COMPUTED BY FORMULA 26.4.16, PAGE 941.  THE SIGN OF X(P) WAS
C    CHANGED FOR THE SAME REASON AS ABOVE.
C
  200 APROX=((-XPL+DSQRT(V+V-1.0))**2)*0.5
C
      IF (APROX.LE.CHISQ) GO TO 220
  210 PROB=+0.995
      GO TO 240
  220 V=DSQRT(2.0D0*CHISC)-DSQRT(2.0*V-1.0)
      GO TO 190
  230 IF (PROB.GT.0.955) GO TO 210
  240 PRBCHI=PROB
      RETURN
      END
```